THE UNIVERSITY of EDINBURGH

Edinburgh Research Explorer

Biosensors and Point-of-Care Devices for Bacterial Detection: Rapid Diagnostics Informing Antibiotic Therapy

Citation for published version:
Gopal, A, Yan, L, Kashif, S, Munshi, T, Roy, VAL, Voelcker, NH & Chen, M 2021, 'Biosensors and Point-of-Care Devices for Bacterial Detection: Rapid Diagnostics Informing Antibiotic Therapy', *Advanced Healthcare Materials*. https://doi.org/10.1002/adhm.202101546

Digital Object Identifier (DOI):
10.1002/adhm.202101546

Link:
Link to publication record in Edinburgh Research Explorer

Document Version:
Peer reviewed version

Published In:
Advanced Healthcare Materials

General rights
Copyright for the publications made accessible via the Edinburgh Research Explorer is retained by the author(s) and / or other copyright owners and it is a condition of accessing these publications that users recognise and abide by the legal requirements associated with these rights.

Take down policy
The University of Edinburgh has made every reasonable effort to ensure that Edinburgh Research Explorer content complies with UK legislation. If you believe that the public display of this file breaches copyright please contact openaccess@ed.ac.uk providing details, and we will remove access to the work immediately and investigate your claim.

Download date: 01. Dec. 2022

Biosensors and Point-of-Care Devices for Bacterial Detection: Rapid Diagnostics Informing Antibiotic Therapy

Ashna Gopal, Li Yan, Saima Kashif, Tasnim Munshi, Roy AL Vellaisamy, Nicolas H Voelcker, Xianfeng Chen

A. Gopal, S. Kashif, Dr. X. Chen

School of Engineering, Institute for Bioengineering, The University of Edinburgh, King's Buildings, Mayfield Road, Edinburgh, EH9 3JL, UK

E-mail: xianfeng.chen@oxon.org; Michael.Chen@ed.ac.uk

Dr. L. Yan

College of Health Science and Environmental Engineering, Shenzhen Technology University, Shenzhen, 518118, China

Dr. T. Munshi

School of Chemistry, University of Lincoln, Brayford Pool, Lincoln, Lincolnshire, LN6 7TS, UK

Prof. R.A.L. Vellaisamy

James Watt School of Engineering, University of Glasgow, G12 8QQ, UK

Prof. N.H. Voelcker

Drug Delivery, Disposition and Dynamics, Monash Institute of Pharmaceutical Sciences

Monash University, Parkville, Victoria, Australia

Melbourne Centre for Nanofabrication, Victorian Node of the Australian National Fabrication Facility

151 Wellington Road, Clayton, Victoria, 3168, Australia

Commonwealth Scientific and Industrial Research Organisation (CSIRO), Clayton, Victoria, 3168, Australia

E-mail: Nicolas.Voelcker@monash.edu

Abstract

With an exponential rise in antimicrobial resistance and stagnant antibiotic development pipeline, there is, more than ever, a crucial need to optimise current infection therapy approaches. One of the most important stage in this process requires rapid and effective identification of pathogenic bacteria responsible for diseases. Current gold standard techniques of bacterial detection include culture methods, polymerase chain reactions, and immunoassays. However, their use is fraught with downsides with high turnaround time and low accuracy being the most prominent. This imposes great limitations on their eventual application as point-of-care devices. Over time, innovative detection techniques have been proposed and developed to curb these drawbacks. In this review, we provide a systematic summary of a range of biosensing platforms with a strong focus on technologies conferring

high detection sensitivity and specificity. We performed a thorough analysis and highlighted the benefits and drawbacks of each type of biosensor, discussed the factors influencing their potential as point-of-care devices, and provided our insights for their translation from proof-of-concept systems into commercial medical devices.

Keywords: Biosensors; rapid diagnostics; point-of-care; antibiotic therapy; bacteria detection

1. Introduction

Today, the threat posed by antimicrobial resistance to worldwide public health has led to more and more serious health problems and is predicted to kill at least 10 million people worldwide annually by 2050.[1] Antibiotics form part of a wider spectrum of antimicrobial agents and are currently the main line of defence against bacterial infections. However, in recent times, bacteria have become increasingly resistant to antibiotics. This is due to incorrect dosing and unnecessary prescriptions in healthcare settings enabling bacterial cells to adopt mechanisms to circumvent the therapeutic effect provided by these antibiotics.[2] In addition to antibiotic resistance, the development of antibiotics with new targeting mechanisms has been very slow; in 2019, the World Health Organisation (WHO) reported only 6 out of 32 antibiotics currently in clinical development which can be classified as 'innovative'.[3] However, these antibiotics are still far from being available in the clinic as they require more rigorous and extensive *in vitro* and *in vivo* testing and subsequent approval for effectiveness and biosafety by regulatory bodies.

With an exponential rise in antibiotic resistance and the lack of novel and highly effective antimicrobial agents to treat infectious diseases, the detection and identification of bacteria is essential for the optimisation of treatment regimens used by clinicians. Pathogen-directed therapy would ensure that specific infection-related bacteria are targeted by the right antibiotic/antimicrobial in the right patient, thereby leading to a more optimised recovery and avoiding the emergence of antimicrobial resistance.[4] This approach requires early identification of the infection-causing bacterial species. For a long time, traditional laboratory-based techniques such as bacterial culture,

polymerase chain reactions (PCRs), gene sequencing identification, and immunoassays have been used and have since become the current gold standard procedure in healthcare settings owing to their fairly high sensitivity and specificity.[5] Figure 1A summarises the most common bacterial detection platforms currently available.

In recent times, there has been a shift towards the design and use of novel detection techniques to circumvent some of the limitations associated with current techniques. Thus, to satisfy this need, biosensors have been extensively explored as detection platforms for pathogenic bacteria for rapid and accurate diagnosis of infectious diseases. These are highly versatile devices that can be used to exploit a range of physical, chemical and biological measurements to recognise the presence of specific microorganisms or biomarkers.[6] Biochemical signals are produced by interaction of bacteria with a target sensing element (the bioreceptor), which are then converted into measurable physically detectable signals by a transducing element.[7] Thus, the 3 main components are the bacterial sample to be analysed, sensing/transducing element, and the electronic system that amplifies and produce an output signal for display as detailed in Figure 1B.[8, 9] Based on this principle, several biosensing devices have been developed and are now commercially available. The first biosensor was invented by Clark in 1962 and the first commercial biosensor for medical applications designed by Yellow Spring Instruments in 1975 was a glucose sensor which is currently used to detect the onset of diabetes in patients.[10, 11] Since then, there has been a progressive growth in the use of biosensors for diagnosis of several medical conditions. This is further evidenced in the recent market analysis published by Grand View Research where the biosensors market was estimated at $19.6 billion in 2019.[12] Driven by the need for quick, simple and low-cost sorting and identification of bacteria in blood/urine samples from patients, biosensors for bacterial detection have gained momentum in the past decade.[13] This rise in the popularity of biosensors as reliable and innovative bacterial detection platforms since 2000 was further confirmed through a publication search using the key words (‘sensor’ or ‘sensors’ or ‘biosensor’ or ‘biosensors’ or ‘sensing’ or ‘biosensing’) and (‘bacteria’ or ‘bacterial’ or ‘microbial’) in Web of Science (Figure 2). These devices have been successfully shown

to effectively detect bacterial species using impedance, voltammetric and amperometric, optical, colourimetric, and mechanical measurements. There is currently growing interest in the research community to optimise the sensitivity – the minimum amount of analyte that can be detected – and the specificity of these biosensors.[14, 15]

In this review, we initially provide an overview of some current laboratory-based bacterial identification methods) and outline their benefits and downsides as well as the rising need to shift to alternative and more optimised detection platforms. Then, we systematically review different types of bacterial sensing devices and design developments over the last decade) aimed at improving their sensitivity and limit of detection (LOD). Their associated benefits and drawbacks are then detailed. Next, the current situation in point-of-care (POC) diagnostic systems is extensively discussed and the factors influencing the potential translation of bacterial biosensing platforms in the current research pipeline into clinical use are evaluated. Finally, we provide our insights of the future development of biosensors and POC devices for bacterial detection.

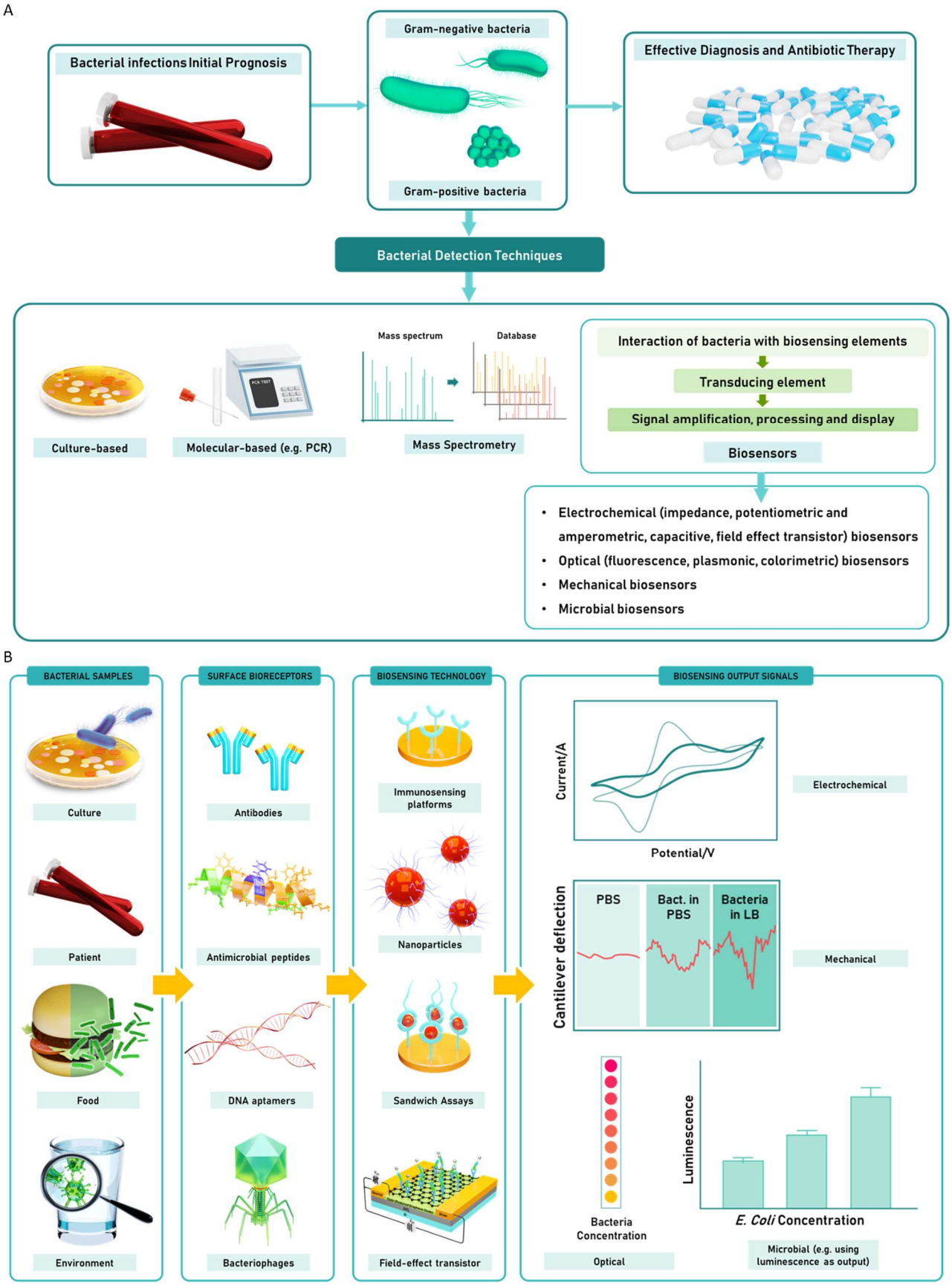

Figure 1: A. Common techniques currently available for bacterial detection; B. Components of a biosensing platform.

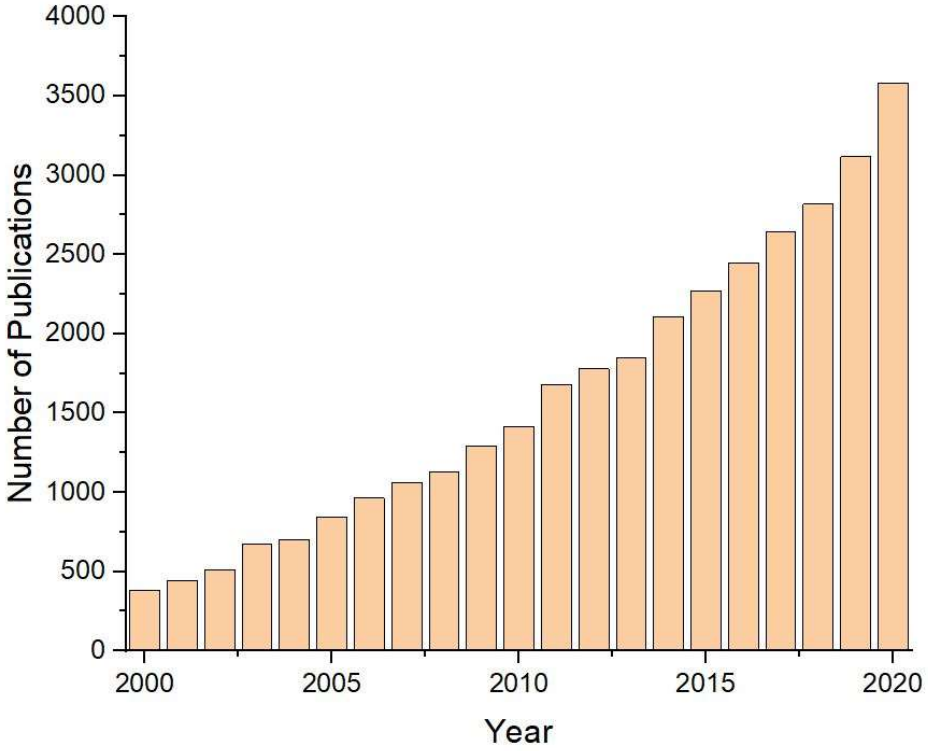

Figure 2: Number of annual publications on biosensors for bacterial detection available on Web of Science.

2. Traditional Bacterial Detection Methods

2.1. Culture of Bacterial Samples

Bacterial culture is the most prevalent detection technique used in bacterial identification. It essentially involves collecting samples from patients and then allowing any potential bacteria recovered to be enriched to grow in nutrient media under standard culture conditions. The number of viable colonies obtained after amplification of the sample can be then counted to determine the amount of bacteria present in the original inoculum in terms of colony-forming unit (CFU) per mL.[16, 17] This method can also indicate the presence of the suspected bacterial species by using specific nutrient media. Culture methods are generally very sensitive and can detect anywhere from 2000 CFU/mL down to 1- 10 CFU/mL but, usually yield results after a few days.[18, 19]

2.2. Polymerase Chain Reactions (PCRs)

Quantitative Polymerase Chain Reactions (qPCRs) are molecular methods aimed at targeting DNA sequences characteristic of the targeted bacteria and then amplifying these into multiple copies for

subsequent detection.[20] In addition to single DNA sequence amplification, multiplexed qPCR has been introduced as an improvement to conventional qPCR whereby multiple DNA sequences specific to different types of bacterial species can be simultaneously analysed. This was demonstrated in the publication by Kim *et al*. with five different bacteria, namely, *Escherichia coli* O157:H7, *Salmonella*, *Staphylococcus aureus*, *Listeria monocytogenes* (*L. monocytogenes*), and *Vibrio parahaemolyticus* (*V. parahaemolyticus*).[21] Furthermore, multiplexed qPCR is able to distinguish between different subtypes of a particular bacterial species as exemplified by the publications by Alvarez *et al*. and Vidal *et al*.[22] Detection limits for qPCRs typically range between 10^3 – 10^4 CFU/mL, with results being available in less than 24 h.[23]

2.3. Immunology-Based Assays

Most immunology-based molecular methods rely on highly specific antigen-antibody interactions.[24] Among these, the enzyme-linked immunosorbent assay (ELISA) is the most commonly used. In a typical analysis, an antigen is used to coat the surface of a solid microplate which is then complexed with a complementary antibody having a reporter enzyme on its surface. Upon incubation with a relevant substrate, a measurable signal can be detected.[24] Out of the four types of ELISA assays, the sandwich assay has been found to be highly suited for bacterial detection where the target antigen is not directly bound to the solid surface. Instead, it is trapped between an antibody already attached to the surface followed by the usual attachment of the complementary antibody-reporter enzyme complex. This technique has been shown to have typical LOD of 10^4 – 10^5 CFU/mL with sample analysis and processing taking up a few days.[25]

2.4. Discussion

From a survey of literature, it is evident that culture-based, PCR and ELISA techniques are currently indispensable in clinics and thus far, have provided fairly accurate results in relation to the presence of pathogenic bacteria in patients and the subsequent diagnosis of bacterial infections.[26] Culture-based techniques are universal and the culture incubation conditions can be easily and cheaply

tailored for the detection of either specific bacteria or different bacterial species at the same time through the use of non-selective media.[27, 28] Despite its reliability and accuracy with an ability to detect down to a few single cells, the effective use of culture methods is hindered by some major drawbacks, for instance, their time-consuming nature. In most cases, the appearance of viable colonies may take several days up to a week after sampling as evidenced by the reported 12 – 24 h for *Salmonella*, 2 – 4 days for *E. Coli*, 4 h to 4 days for *V. parahaemolyticus*, and 7 days for *L. monocytogenes*.[29, 30] In cases, where the bacterial concentrations are low, enrichment steps could take an additional 8 – 24 h as mentioned by Wang and Salazar.[17, 23] Another case in point is the ability of these bacteria to switch to a dormant state under normal culture conditions, thereby hampering the growth monitoring, as well as bacterial identification process.[16, 31] Furthermore, this method is unsuitable in cases where antibiotics have been already administered to patients or where bacterial strains are resistant to further culturing.[27] Finally, it is standard procedure to use large sample volumes to maximise the probability of acquiring a high initial amount of the desired bacterial strain for further culture.[32] A case in point is the publication by Opota *et al.* where they reported drawing ~20 - 40 mL of blood from patients for the detection of bacteria that can cause bloodstream infections, thereby causing patient discomfort and reluctance to treatment.[18]

Compared to culture-based methods, qPCR techniques, on the other hand, afford a simpler and more rapid sample analysis. Thus, qPCR tests require no prior culturing and are able to circumvent the limitations of conventional culture by detecting both bacteria from antibiotic-treated patients and culture-resistant bacteria.[27] Moreover, only a small amount of the original sample is enough to produce reliable results, thus making this technique ideal in cases where patient sample volumes collected are low.[16] In terms of sensitivity, even though culture is better, some publications, for instance, Batt reported the ability of some qPCR tests to detect down to a single bacterial cell.[33] However, a major drawback of qPCR-based bacterial detection is its high specificity which implies that only the targeted bacteria can be detected at any one time.[27] The assay has to be configured to the bacterial species of interest every time; in cases where multiple bacterial types need identification,

multiple qPCR assays have to be carried out, thereby increasing the turnaround time. Furthermore, qPCR testing is labour extensive, as trained laboratory workers have to carry out the assays using specialised equipment and specific reagents which further augment the operating and training costs. Finally, the qPCR technique can sometimes lead to false positives which often arise from the sample processing and nucleic acid amplification steps.[34]

With regards to sandwich-based ELISA methods, they can also detect bacteria in small sample volumes with high reproducibility. These techniques also use reagents which can last for a long time while being radiation-free and producing non-toxic wastes.[24] Unlike qPCR, relatively simple equipment is used during this assay, thereby lowering the operating costs. The ELISA methods offer very high specificity owing to the antigen-antibody binding but fairly low sensitivity in comparison to culture and qPCR methods. Yet, ELISA assays require multistep initial sample processing such as preparation of standard solutions, antibody incubation, washing, blocking before the actual assay can be carried out, which results in turnover times similar or even worse than cell culture techniques.[24]

In general, there are a range of advantages associated with the three methods described. Out of these, cell culture and qPCR techniques were found to possess superior detection sensitivity while ELISA provided the best selectivity. Yet, the application of each of these techniques is plagued by the above-discussed drawbacks such as long processing hours, need for initial sample enrichment, multistep sample preparation steps before analysis, expensive equipment, and the need for trained personnel, hence thwarting their efficacy as diagnostic tools.[35] Simplifying the laboratory workflow while reducing the costs and complexity of operation and use remains the ultimate goal of healthcare professionals in the diagnosis of bacterial infections. Aside from the above described culture and molecular-based methods, mass spectrometry, nucleic acid amplification, and biosensing have been widely reported as potential alternatives (Figure 1A).[15] Focusing on biosensing platforms for bacterial detection, Section 3 below explores advances in the design of different types of biosensors developed over the last 5 years and highlights design improvements aimed at improving their detection sensitivity. We first describe the fundamental principles underlying each biosensor

technology. Then, we provide representative examples which are presented in order of increasing sensitivity before finally discussing the different benefits and limitations associated with each type of biosensor described.

3. Biosensor Platforms for Bacterial Detection

3.1. Electrochemical Biosensors

Electrochemical biosensors are devices that primarily use electrodes to record electrochemical changes occurring when the analyte of interest interacts with the sensing element; the electrodes then converts these changes into measurable electrical signals.[36] The intensity of the electrical signal generated can be used as a direct measure of the analyte concentration as reported by Ronkainen and colleagues.[37] In general, electrochemical sensing makes use of different types of electrical signals, for instance, impedance, conductance, capacitance, voltage, and current to indicate the presence of bacteria as detailed in the following subsections. Electrochemical sensors receive significant attention in the field of biosensing because of their high sensitivity, rapid detection speeds and cost-effective detection methods such as voltammetric cyclic voltammetry (CV), differential pulse voltammetry (DPV), electrical impedance spectroscopy (EIS) and so on. However, the repeatability, stability of the substrates used, linearity, and the limit of quantification need to be considered.

3.1.1. Impedance-Based Biosensors

Impedance-based or impedimetric biosensors figure among electrochemical sensing platforms that use the application of an alternating current (AC) to generate an effective resistance, which is frequency dependent.[35] Impedimetric sensors can be broadly classified as being faradaic/non faradaic in the presence or absence of a redox mediator probe as further explained by Karbelkar and coworkers. EIS is the most common impedance measurement and transduction technique used in bacterial biosensing whereby a small amplitude sinusoidal current or potential disturbance is applied over a spectrum of frequencies or impedance phase angle changes.[38] As described by Labib *et al*., EIS can provide information on the resistive and capacitive properties of the targeted analyte by

monitoring the rate at which the redox responsive element move to the electrode upon the application of specific frequencies.[39] EIS results are often represented by Nyquist plots which show the variation of the imaginary impedance with the real impedance; the amplitude of the peak is found to increase as the concentration of the redox element binding to the electrode surface is increased.[40] For bacterial detection, these sensors make use of the inherent electrical properties of bacterial cells. Bacterial cells are known to contain highly conductive proteins and molecules. Furthermore, the lipid bilayer consists of hydrophilic head groups facing the external aqueous environment and hydrophobic tails which face inwards towards each other. This gives rise to an insulating membrane; the embedded proteins and ion channels within the membrane act as resistors, thereby giving rise to 'parallel ion channels'.[16] Hence, their attachment to an electrode surface produces an increase in measured impedance as the electrode area in contact with the redox-responsive molecules in the sample solution is reduced. Any changes in resistance in response to the interactions with specific biorecognition elements in the design can be then detected and electrically amplified to yield an EIS signal. Thus, the concentration of bacteria can be directly correlated to the signal generated for diagnostic purposes.

Impedance immunosensors are systems incorporating bacteria-recognising moieties and are deemed highly beneficial and effective for diagnostic applications where increased specificity is required. As detailed in the very recent publication by Russo *et al.*, immobilising specific antibodies or antimicrobial peptides on the surface of an electrode, conductive polymer, nanoporous membrane or hydrogel surface allows easy attachment and detection of the targeted bacterial species.[41] Two very common hospital and community-acquired bacteria, namely Gram-positive *Staphylococcus Aureus* (*S. Aureus*) and Gram-negative *Escherichia Coli* (*E. Coli*) have been widely studied as they are the leading cause of healthcare-associated infectious diseases such as pneumonia, urinary tract infections, bacteremia, and sepsis.[42] A simple impedimetric immunosensor was reported by Tan *et al*. whereby an alumina nanoporous membrane was functionalised with *E.Coli*-recognising antibodies by covalent bonding as shown in Figure 3A. This system was then integrated with a polydimethylsiloxane (PDMS) microfluidic device and sandwiched between two platinum wire

electrodes (Figure 3B).[43] Anti-*S. Aureus*, instead of *E. Coli* antibodies, were then grafted on a similar alumina surface, used to detect the presence of *S. Aureus*, hence showing the versatility of the system and multiple bacterial detection ability of this device. As illustrated in Figure 3B, the targeted bacteria were trapped in the upper compartment by the complementary antibody. This was further confirmed by fluorescence microscopy observation of FITC (fluorescein isothiocyanate) labelled antibodies which were bound to the bacterial surface, but not in contact with the antibodies on the nanoporous membrane. Capture of these bacteria hindered the current flow through the nanopores and subsequently produced an increase in the amplitude of impedance which was recorded using an electrochemical analyser VersaSTAT3. Their analyses revealed a sensitivity of up to 100 CFU/mL and showed highly specific binding of the two types of bacterial species to their respective antibodies.[43] After analysing the impedance spectra obtained over a frequency range of 1 – 100 kHz, operating the biosensor system at a frequency of 100 Hz was found to provide the optimal sensitivity of the impedance change readings in response to bacterial capture. The efficiency of using nanoporous alumina membranes was also demonstrated in the publication by Joung *et al*. The membrane was coated with hyaluronic acid which served as an intermediate and electrical signal enhancer as well as *E. Coli* specific antibodies for specific capture of the bacteria.[44] Their results showed sensitivities similar to the paper by Tan *et al*. While nanoporous membranes are highly useful in bacterial detection, interdigitated array microelectrodes (IDAM) have also gained momentum in this application. Biotin labelled antibodies were functionalised on a silicon surface laden with gold interdigitated array microelectrodes to detect the presence of *Salmonella Typhimurium* (*S. Typhi*) – bacteria playing a major role in inflammation of the gut (gastroenteritis) – as shown in Figure 3C. As expected, a similar LOD of 100 CFU/mL was observed.[45] Aside from antibodies, antibiotics have also been used in impedimetric immunosensing, for instance, in the design by Singh and coworkers, vancomycin, which usually binds to only Gram-Positive bacteria, was functionalised on the surface of tungsten oxide (WO_3) interdigitated gold electrodes immobilised on a silicon substrate.[46] This

device demonstrated similar LOD as with the use of antibodies, hence confirming the benefits of immunosensing in bacterial detection.

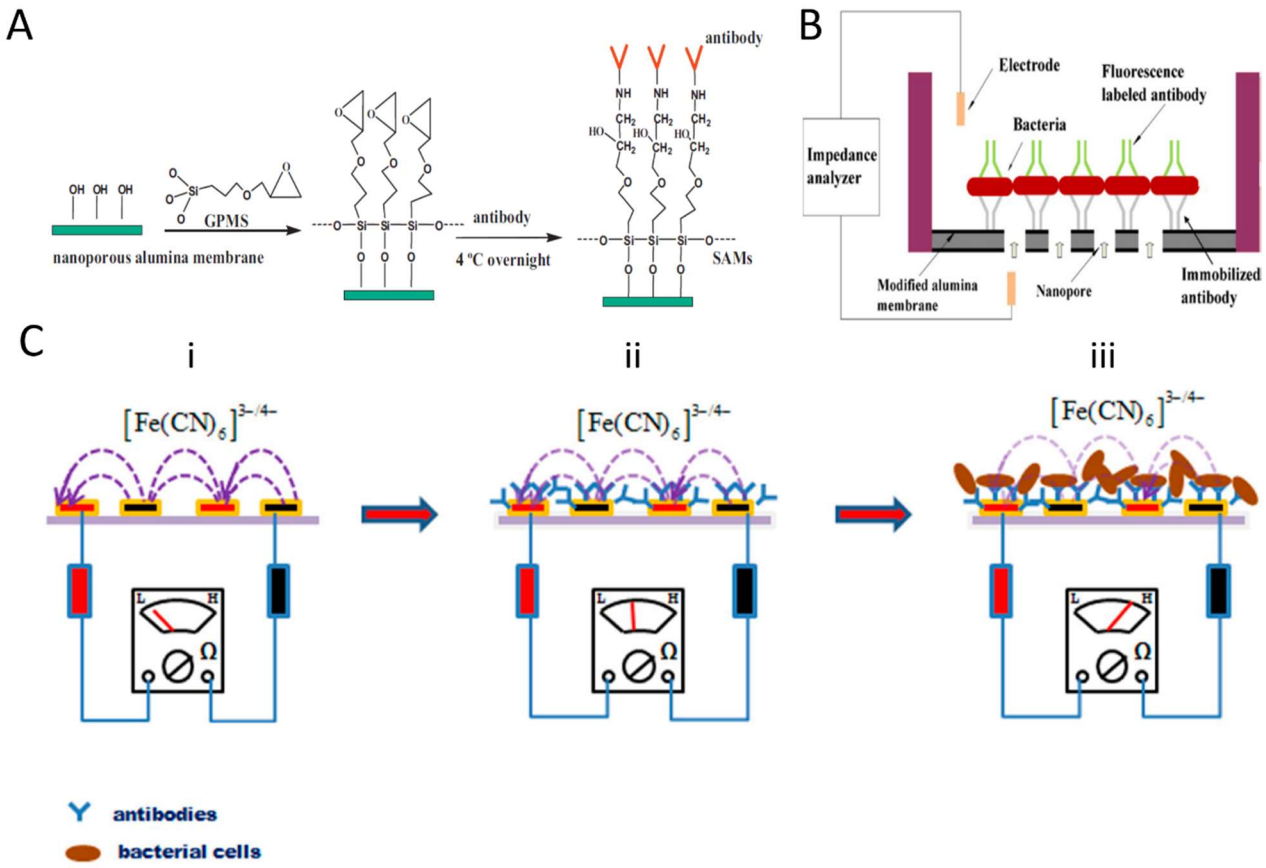

Figure 3: A. Schematic showing the functionalisation process of the alumina nanoporous membrane; B. Impedimetric biosensor system designed for *E. Coli* and *S. Aureus* detection.[43] (Reproduced from reference [43] with permission. Copyright 2011 Elsevier); C. Design of immunosensor (i) bare IDAM (ii) IDAM functionalised with antibodies (iii) bacterial cells captured on IDAM by Wen *et al.*[45] (Reproduced from reference [45] with permission. Copyright 2017 MDPI).

Gold nanomaterials are commonly used in the bacteria detection because of their biocompatibility, optical and electronic properties, and relatively simple production and modification, Pal *et al*., for example, designed an antibody-conjugated gold nanoparticle system for binding to *S. typhi* and *E. Coli*.[13, 47] A high precision resonant circuit or LCR circuit meter comprising an inductor (L), capacitor (C) and a resistor (R) interfaced with interdigitated platinum microelectrodes on glass substrates was used.[47] A polydimethylsiloxane (PDMS) slab with a 20 µL capacity hole was immobilised on the surface of the interdigitated electrodes and the hole was loaded with 10 µL of a bacterial sample and sealed before measurements. The changes in the impedance originating from gold nanoparticle-tagged bacteria binding were then recorded and amplified. The measured

impedance was found to increase with the bacterial concentration. This behaviour was attributed to the increasingly abundant cytoplasmic ionic content of the bacterial cells, which gave rise to a very high internal conductivity in comparison to the conductivity of the exterior background buffer. Hence, the cells were able to thwart the current flow, thereby leading to a rise in impedance. After optimisation of the experimental parameters such as incubation time, applied frequency, antibody concentration and cell concentration, the system proposed was able to achieve a low LOD of 100 CFU/mL.[47] The high sensitivity was the result of using a high AC electric field generated by the micron-gap interdigitated electrodes which improved the signal near the edges of the electrodes. This ensured that small changes in impedance upon bacterial binding are picked up and amplified.

In addition, bacteria-targeting moieties can also be decorated on the surface of nanomaterials. The benefits of magnetic nanomaterials was explored in an integrated anodic aluminium oxide (AAO) nanochannel chip system (called INCE), inspired from biological ion channels, which was recently designed by Zhu *et al*.. A layer of gold was deposited on both sides of the chip to act as electrodes of the electrochemical cell, which is in this case, the nanochannel.[49] The bacteria *S. Typhi* were captured by magnetic nanoparticles (MNPs) modified with *S. typhi*-specific antibodies. Owing to the large size of the bacteria-MNP-Ab composites, they were unable to pass through the pores of the nanochannels and thus, accumulated on the surface of the INCE; this allowed their effective separation from both free MNP-Ab and unbound bacteria. The resulting hindrance of electron transfer was used to yield an EIS signal. A detection limit of 50 CFU/mL was obtained with this system and its good detection performance was attributed to the electrochemical activity of the nanoporous surface as well as the bacterial filtration ability of the INCE.[49] Further taking advantage of such nanomaterial-based biosensing platforms, a hybrid three-dimensional (3D) gold nano-micro islands/graphene nanosheets electrode surface was integrated with a microfluidic platform for the label free capture and plasmonic-assisted impedimetric detection of three different bacteria. The capture ability was dictated by the nano-rough protrusions on the nano-micro islands as well as the spatial orientation of the hierarchical structures of the 3D nano-micro islands.[50] These also facilitated the attachment of graphene to the

nano-micro islands by electrical interactions which further enhanced the electrical conductivity and plasmonic properties of the system.[51] Capture efficiencies of up to 95% was reported at an *E. Coli* concentration of 100 CFU/mL. Upon bacterial capture, there was a rise in steric hindrance and reduction in surface area, thereby considerably decreasing electron transfer to the surface. The subsequent decrease in current and increase in impedance was found to be dependent on the number of captured bacteria on the surface which was subsequently quantified using EIS under simulated sunlight. Contact angle measurements revealed a signal dependence on the size, morphology, and shape of bacterial cells. The selectivity of the system was confirmed by the different Nyquist plots obtained for each of three different bacterial species, namely *E. Coli*, *Pseudomonas putida (P. Putida)*, and *Staphylococcus epidermidis (S. Epidermidis)*. In addition, in the presence of light, a lower internal resistance was observed owing to the additional photo-charges generated; this led to a subsequent rise in conductivity and improved sensitivity. Thus, an LOD of 20 CFU/mL was reported for this system.[52] As evidenced by these two studies, the use of nanomaterials played an important part in the effective separation and accumulation of the targeted bacteria from the rest of the sample, which greatly improved the sensitivity of the sensing platforms.

Unique structural and multi-layered design of detection platforms are often used to increase the sensitivity of biosensor, which could reach detection limits of around 10 CFU/mL or even lower. One example is the multifunctional nano-decorated porous electrode sensor designed by Wu and colleagues. Prickly zinc-doped copper oxide (Zn-CuO) NPs and graphene oxide (GO) nanosheets (Zn-CuO@GO) were formed by growing the metal ions *in situ* on the nanosheets using a sonochemical conditions, giving rise to the prickly structures.[53] These were then deposited on a commercial porous nickel (Ni) electrode. While the Zn-CuO@GO nanocomposite demonstrated high affinity to *E. Coli* bacteria with a high bacterial capture efficiency of 70-80%, the burr-like structure was able to lyse bacteria by piercing the bacterial cell wall. This led to leakage of the cytoplasmic and intracellular components provide improved conductivity at the electrode. This sensor demonstrated a low LOD down to 10 CFU/mL which was attributed to the hierarchical burr like

structure which reduced the molecular transport barrier as well as the enhanced signal caused by the release of abundant cytoplasmic content from the bacteria.[53] Another case in point is the paper by Pandey *et al*. in which the ability of cysteine to form hexagonal shaped, flower-like structures with large surface areas in the presence of copper (II) oxide (CuO) as well as the benefits associated with graphene was further exploited. The CuO modified cysteine molecules were immobilised on a reduced graphene oxide (rGO) sheet. This was then grafted on the surface of a gold electrode to form an impedance immunosensing platform (rGO-CysCu). Antibodies were immobilised on the rGO-CysCu surface *via* covalent bonding of the amino-terminated antibodies with the -COOH group of cysteine to provide *E. Coli* O157: H7 specificity to the device.[54] The Nyquist plots obtained from EIS measurements demonstrated the linear variation of the impedance response with the bacterial concentration. In this work, a detection limit of 3.8 CFU/mL was reported and the sensitivity was found to arise from the hydrophilic and three-dimensional nature of the rGO-CysCu which ensured a better adhesion between the antibody and substrate. Furthermore, the biocompatible cysteine imparted improved water stability and stable activity of the antibodies. In comparison to the design by Moakhar *et al*, this design exhibited improved sensitivity and provided a more effective electron transfer rate from the rGO-CysCu as well as a highly specific antigen−antibody immune reaction owing to the localised antibody access provided to the bacteria.[54]

Sandwich assays whereby the target bacteria are trapped between two bioactive layers have also gained popularity in the design of highly sensitive biosensors. Santos and coworkers designed a system capable of detecting bacteria up to 2 CFU/mL with this sensitivity being attributed to their highly specific functionalisation protocol and high affinity between the bacteria and antibody used.[55] This impedance-based system consisted of a gold electrode surface coated with anti-*E. Coli* antibodies. Once *E. Coli* O157:H7 were injected on the surface of the gold electrode and incubated for 45 min, a PDMS microarray with secondary FITC-conjugated anti-*E. Coli* polyclonal antibodies was added, hence trapping the bacteria between the two antibody layers. This ensured that all bacteria were immobilised by both the PDMS microarray and the gold electrode. In this case, EIS was carried

out in real time using a three-electrode electrochemical cell. A linear correlation between the change in impedance and the *E. Coli* concentration was observed. More recently, Hillman and colleagues developed a new monoclonal antibody, mAb-EspB-B7 that can target the EspB protein – the characteristic of Gram-negative bacteria. They exploited the specificity of this antibody by incorporating it in an electrochemical sensor to detect *E. Coli.* Similar to the publication by Santos *et al.*, a very low detection limit of µg/mL scale, was reported.[56] Aside from antibodies, the use of DNA aptamers specific to the target bacteria have been shown to provide the best sensitivity for impedimetric detection platforms.[19] To illustrate this, a nanoporous gold (NPG) surface was functionalised with a thiolated version of the *S. Typhi* specific DNA aptamer, 5'-SH-TAT GGC GGC GTC ACC CGA CGGGGA CTT GAC ATT ATG ACA-G-3' for the detection of *S. Typhi*.[57] EIS was carried out after 40 min incubation of bacteria; it was found that there was a rise in the charge transfer resistance, as the bacterial concentration was increased owing to the bacterial accumulation at the redox probe-electrode interface. While being highly selective to *S. Typhi*, this system had an LOD of 1 CFU/mL which is the lowest LOD reported so far with impedance immunosensors and was credited to the high binding efficiency of the bacteria to the DNA aptamer.[57]

3.1.2. Capacitance-Based Biosensors

Capacitive biosensors belong to a class of impedance biosensors that are non-faradaic in that they do not require the application of an electric potential or reference electrode.[16, 58] In general, capacitive biosensing is based on the electric double layer phenomenon arising from the immersion of two polarised electrodes in an electrolyte which cause migration and accumulation of ions to the surface in response to the analyte.[59] Two main types of capacitive biosensors were described in the review by Berggren *et al.*. In the first type, the recognition element is positioned between two metal conducting electrodes placed close to each other. The subsequent change in capacitance between the two electrodes as the target analyte binds to the recognition element is then registered. The other method involves measuring the capacitance at the electrode-solution interface with the recognition element placed on the surface of the working electrode.[60] This allows direct binding of the target

analyte to the sensing layer bound to the electrode surface for subsequent signal amplification and conversion.

A simple microcapacitive array biosensor with an LOD of 10^3 CFU/mL was described by Mannoor *et al*. In this design, the naturally occurring antimicrobial peptide (AMP), magainin I was immobilised on the surface of interdigitated gold microelectrode arrays *via* covalent bonding using a C-terminal cysteine residue.[61] When the device was incubated with different concentrations of *E. Coli* O157:H7 bacteria, the bacteria interacted with the AMP, which then led to changes in the dielectric properties of the electrode. A similar sensitivity was observed in the capacitive matrix by Piekarz and coworkers. Built on a thick Gallium arsenide substrate, the matrix consisted of transmission lines arranged in five rows and five columns, creating 25 capacitors on their junctions.[62] This matrix was then biofunctionalised with polyclonal anti-*E. Coli* antibody. Upon exposure of the bacterial sample to this matrix, the capacitance of this matrix changed and the presence of bacteria was determined by calculating the mean value of the change in capacitance which was, in turn, obtained by measuring the scattering transmission parameters in the microwave frequency range (1-3 GHz). With this design, an LOD of 10^3 CFU/mL was obtained, which was attributed to the use of 25 capacitors instead of a single one. This allowed for a higher probability of the bacteria being detected.[62]

In an effort to improve the sensitivity of capacitive biosensors, materials such as graphene or polymers are often included in the design of these biosensors. For example, a graphene-based capacitive biosensor was investigated by Pandey *et al*. who earlier proposed the rGO-CysCu impedimetric biosensor which made use of the structure and layered structures of graphene to lower the LOD.[63] In this design, graphene nanostructures were functionalised with *E. Coli* O157:H7 specific antibodies and were directly immobilised on a silicon dioxide surface. Two different types of graphene nanostructures, namely monolayered graphene (MG) and graphene nano pellets (GNPs) were coupled on the substrates. These were then patterned on the surface of gold interdigitated microelectrodes. Upon contact with the device, the bacteria were trapped by the antibodies and the

resulting change in bacterial surface charge and hence, the change in carrier hole density in graphene triggered a change in its capacitance. The capacitance response was found to increase with increasing bacterial concentrations. An LOD of 100 bacterial cells/mL was reported when only GNP was included in the design. It was further improved to 10 bacterial cells/mL by the inclusion of the defect-free MG.[63] This performance was credited to the strong antibody-bacterial interactions as well as the efficient charge redistribution and recombination within these conductive networks of MG-interfaced chips. Aside from graphene, polymer-based capacitive sensors have been widely reported, for instance, in the publication by Mugo and colleagues. Their design made use of pathogen microcontact imprinted polymer (PIP), which involves polymerising specific monomers with pathogen template such that upon removal of the pathogen, the polymer possesses grooves characteristic of the size and shape of the pathogen template. A PIP was constructed by a layer-by-layer assembly process using multiwalled carbon nanotubes (CNT) and cellulose nanocrystal (CNC) nanoporous film coated with polyaniline (PANI) doped with phenylboronic acid (PBA). Furthermore, a polyvinyl acetate sheet was used as the *E. Coli* stamp while poly(methacrylic acid) was deposited on the surface of the layer-by-layer assembly and was used as the PIP sensing layer for *E. Coli* K-12 to yield a final sensing platform denoted as PIP@PBA/PANI@CNT/CNC. *E. Coli* bacteria were initially captured by the PBA via interaction of the liposaccharide – structure characteristic of Gram-negative bacterial cell walls – and boronic acid groups as well as the rod-shaped cavities created by the PIP on the sensor. The capacitance signals upon bacterial binding were found to vary linearly with the *E. Coli* concentration. A low LOD of 8.7 ± 0.5 CFU/mL was reported with the good performance attributed to the efficient bacterial capture mechanism offered by the PIP.[64]

Taking advantage of the high sensitivity associated with DNA technology, DNA probes or aptamers can be functionalised on the surface of the biosensing platforms. Deshmukh and his team designed an indium tin oxide (ITO) chip which was biofunctionalised with an aminated DNA probe that can target the z3276 gene in *E. Coli* (ZEC).[65] The basic function of this sensor relied on hybridisation of a complementary DNA target (the z3276 gene in this case) with the DNA probe. The

change in capacitance before and after hybridisation of the bacterial gene with the DNA probe was then registered and this signal was used to indicate the presence of *E. Coli*. The superior specificity of the sensor chip to the z3276 genetic marker accounted for the extremely low LOD (1.4 CFU/mL).[65]

3.1.3. Potentiometric and Amperometric Biosensors

Unlike impedimetric biosensors, potentiometric and amperometric biosensors are direct current (DC) – based biosensors.[35] As defined by Labib and colleagues, a simple potentiometric biosensor records the potential of an electrochemical cell. The latter is usually made of two reference electrodes which can detect the potential difference across an ion-selective membrane which interacts with the target analyte.[39] Conversely, amperometric biosensors involves applying a constant potential at the working electrode relative to the reference electrode and measuring the resulting current upon analyte binding.[66] Voltammetry is an improvement on these two separate modes and allows simultaneous measurement of current, potential, charge, and time to yield a more versatile and sensitive analytical method to characterise the electron transfer process in redox reactions.[39, 66] Thus, the current ─ arising from an electrochemical reduction or oxidation process at the working electrode─ can be measured while the potential is being increased at a specified rate.[39] These biosensors encompass a range of techniques with cyclic, differential pulse, and square wave voltammetry being the most common. In cyclic voltammetry (CV), the potential applied is varied in both the positive and negative directions (triangular pattern in Figure 4A) over a number of cycles at a constant rate. In a plot of current against potential, the redox peak current usually varies linearly with the bacterial concentration. On the other hand, differential pulse voltammetry (DPV) involves the application of a series of pulses with a fixed potential and scans over a defined potential window and thus, removes the charging current.[16] In most cases, the current is recorded just before and after the pulse and the subsequent difference is plotted against the voltage. Square wave voltammetry (SWV) operates in a similar manner to DPV except a square wave pulse is used in conjunction with a staircase potential variation. The net current is characterised by the difference between the forward and reverse current

steps about the redox potential.[16] The height of the peak is indicative of the bacterial concentration in the case of DPV and SWV. Figures 4A (i)-(iii) below summarise the input (left) and output (right) peak representations for these three types of voltammetric measurements.

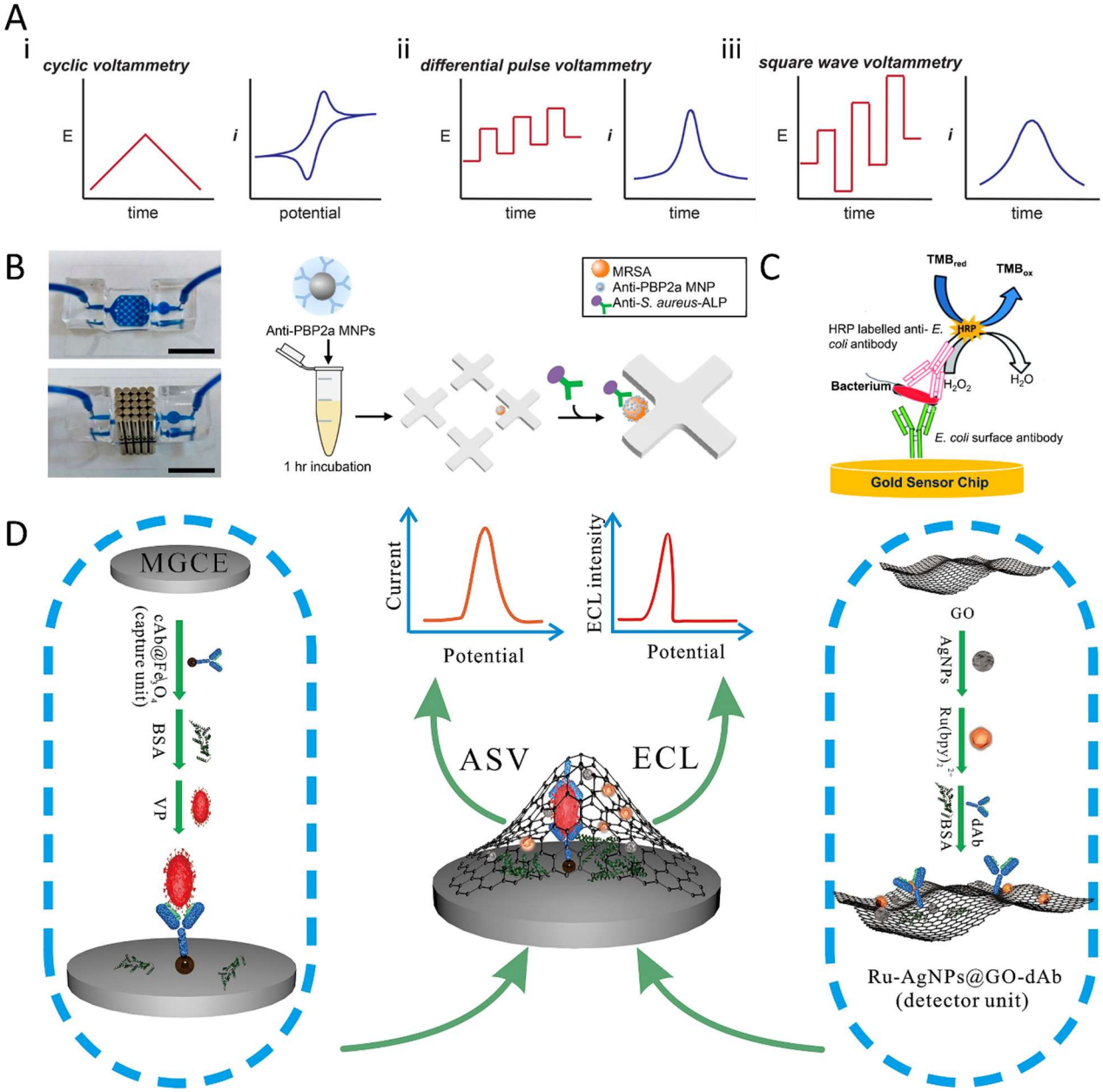

Figure 4: A. Input and output Traces for (i) cyclic voltammetry, (ii) differential pulse voltammetry, (iii) and square wave voltammetry.[16] (Reproduced from reference [16] with permission. Copyright 2019 ACS); B. Design of the nanoparticle-bacteria system.[67] (Reproduced from reference [67] with permission. Copyright 2019 ACS); C. Immunosensor chip designed by Altintas *et al*.[68] (Reproduced from reference [68] with permission. Copyright 2018 Elsevier); D. Schematic diagram showing the Faraday cage design.[69] (Reproduced from reference [69] with permission. Copyright 2019 Elsevier).

Similar to impedimetric biosensors, the use of antibodies and nanomaterials greatly enhance the sensitivity and specificity of these biosensors. A highly resistant strain of *S. Aureus*, *Methicillin Resistant Staphylococcus Aureus (MRSA)* ─ the prime source of infections in hospitals ─ was recently detected by an amperometric-based microfluidic detection system. The system was constructed using PDMS as the base with an inlet and outlet tubing and photolithography was used to create the unique criss-cross pattern on its surface as detailed in Figure 4B. This system was capable of directly analysing swabs from patients without any processing of the collected samples. First, the bacterial samples were incubated with magnetic NPs functionalised with anti-PBP2a (a protein uniquely expressed by *MRSA* which causes β-lactam antibiotic resistance). Then, alkaline phosphatase (ALP) functionalised anti-*S. Aureus* antibodies were immobilised on the bacterial surface to confer bacterial strain selectivity to the detection system.[67] Capture of the bacteria was achieved by placing magnets on either side of the microfluidic platform as shown in Figure 4B. These bacteria were then incubated with p-aminophenyl phosphate (p-APP) monosodium salt which was subsequently converted to electrochemically active p-aminophenol (p-AP) by the ALP. This was finally detected by DPV with current values being indicative of the concentration of *MRSA*. Nemr *et al*. reported an average LOD of 845 CFU/mL with this device. This value was found to vary depending on the nasal swabs which was in line with published data on clinical *MRSA* swabs. Furthermore, the sampling conditions were found to influence the sensitivity of this system in comparison to previously described biosensing platforms.[67]

The sandwich-based detection assay was also employed by Altintas and coworkers to improve the sensitivity of amperometric immunosensors. They developed a microfluidic chip incorporating an immunoassay detection platform which was capable of providing real-time amperometric measurements.[68] *E. Coli* bacteria were sandwiched between two antibodies, namely a polyclonal rabbit anti-*E. Coli* antibody immobilised on a gold sensor chip and a horse radish peroxidase (HRP)-labelled detection antibody, in a similar way to the impedimetric sensor design proposed by Santos *et al*. (Figure 4C) After incubation of the bacteria for 8 min, tetramethylbenzidine (HRP) substrate

was then injected into the system before amperometric measurements. As the concentration of *E. Coli* increased in the presence of a HRP substrate (TMB reagent), the amount of (HRP)-labelled antibody being detected increased and eventually contributed to a more significant measured response. The same system was further modified to include gold NPs which were immobilised on the HRP labelled detector antibody. This led to an improvement in the detection specificity and thus, the sensitivity with a low detection limit of 50 CFU/mL.[68]

Furthermore, combining different sensing modalities and exploiting their individual benefits in a single system have been shown to provide improved bacterial detection accuracy at low sample concentrations. To detect the presence of *Vibrio parahaemolyticus (V. Parahaemolyticus)* – a type of bacteria responsible for a range of health-related issues including vomiting, diarrhoea, and headache – Wang *et al*. developed a Faraday cage immunosensor consisting of a capture and detector unit making use of anodic stripping voltammetry and electrochemiluminescence (ECL), respectively. The surface of a magnetic glassy carbon electrode was decorated with anti-*V. Parahaemolyticus* molecules to form the capture unit (Figure 4D). After addition of the bacteria, the detector unit comprising of a graphene oxide sheet decorated with Ruthenium and anti-*V. Parahaemolyticus* detector antibodies was injected on the electrode.[69] The synergistic action of both sensing elements allowed a detection limit as low as 33 CFU/mL to be observed. This behaviour was found to be the result of less inhibition of electron transfer owing to the Faraday cage detector unit, as well as the ability to load on signal units on the large surface area graphene oxide sheet.[70] A close detection limit was obtained in a simple electrochemical sensing device built by Ishiki *et al*. who made use of 3-(4,5-dimethylthiazol-2-yl)-2,5-diphenyl tetrazolium bromide (MTT) for the detection of the *E. Coli K-12* strain. The MTT was first incubated with the bacteria to allow its penetration into the bacterial cells. The bacteria then converted the MTT to formazan (FORMH) by enzyme catalysed redox reduction. These bacteria were then deposited on an indium tin oxide coated glass strip and lysed. This process led to the adsorption of the microbially-formed formazan on the electrode surface. Voltammetric measurements were carried out at an optimum MTT concentration of 0.5 M and after

1 h incubation at 37℃. The intensity of the oxidation peak currents was found to be directly proportional to the bacterial concentration. From their results, the detection limit for viable bacteria was estimated at 28 CFU/mL.[71] The insolubility of formazan was credited for the high sensitivity obtained in this study, because a high concentration of the FORMH could be concentrated through desiccation and adsorption as well as immobilised on the surface without the risk of diffusion in solution during voltammetric readings, thereby leading to a strong adsorption intensity peak.[71]

Besides the detection of *MRSA*, *V. Parahaemolyticus* , and *E. Coli*, the non-resistant strains of *S. Aureus* also contributes to a wide spectrum of diseases, ranging from skin infections to pneumonia, meningitis and sepsis, hence reaffirming the need for its early detection and therapy.[72] Compared to other bacterial species, the detection of *S. Aureus* is more tricky owing to the thick polysaccharide layer and the limited number of externally exposed surface antigens.[73] As exemplified earlier, the use of highly ordered nanomaterials with specific and large surface areas can promote high sensitivity. In line with this and the need to develop sensing devices capable of detecting *S. Aureus* bacteria from biological samples at low concentrations, Wang *et al*. proposed an immunosensor device consisting of antibody (Ab)-conjugated hierarchical mesoporous silica NPs (HMS) deposited on a glassy carbon electrode. The HMS in this case conferred a large surface area and high porosity to the detection platform owing to its butterfly wing-like microstructure. Subsequent attachment of *S. Aureus* to the anti-*S. Aureus*-loaded MSNs led to changes in peak currents which were registered using a potentiostat. As the concentration of bacteria increased, the current was found to be higher because of the reduction in electrode resistance. This was, in turn, attributed to the increase in electrode surface conductivity arising from changes in the bacterial cell structure and antigen-antibody complex formation. The sensor was able to detect *S. Aureus* as low as 11 CFU/mL owing to the strong affinity of the Ab-HMS to the *S. Aureus*.[74] Taking advantage of the role played by rGO in the design of sensitive biosensors as discussed in Section 3.1.1 and 3.1.3, Jijie *et al*. deposited active layers of reduced graphene oxide/polyethyleneimine (rGO/PEI) on the surface of gold electrodes. The -NH_2 group of the PEI/graphene oxide was then functionalised with anti-fimbiral *E. Coli* UT189 antibodies

as well as poly(ethylene glycol) (PEG) modified pyrene units, thereby allowing highly specific *E. Coli* UT189 binding and thwarting electron transfer to the transducer.[75] The subsequent variation in peak current of the potassium ferrocyanide redox probe was found to be directly proportional to the bacterial concentration. A very low detection limit of 10 CFU/mL was obtained and was attributed to the highly specific binding to the antibodies.[75]

More recently, bacteriophages have become popular in the design of biosensors for bacterial detection down to very low concentrations. Bacteriophages are viruses that are able to infect and proliferate within bacteria.[76] Bacteriophage-based biosensors possess advantages such as extremely high specificity for hosting the relevant bacteria, high capability to reproduce within the host bacteria, stability in adverse pH and temperature conditions, ability to distinguish between live and dead cells and cheap, and simple large-scale production capacities.[77] Farooq *et al*. proposed a bacterial cellulose/carboxylated multi-walled carbon nanotubes composite functionalised with *S. Aureus*-specific lytic phage, the first in the field of bacteriophage-based sensors. Upon capture of *S. Aureus*, bacteria were lysed by the immobilised phages which led to the release of their intracellular components and a resulting rise in the conductivity of the medium. Progeny phages were also simultaneously released and contributed to the capture and infection of surrounding *S. Aureus* cells. The subsequent release of more intracellular components further increased the electron transfer at the solution-electrode interface, thereby producing an increase in the intensity of the current signal which was obtained by DPV. A linear correlation was observed between the current response and bacterial concentration with an impressive detection limit of 3 and 5 CFU/mL obtained in PBS and milk, respectively.[77]

The lowest reported detection limit of 1 CFU/mL for *S. Aureus* was achieved by a potentiometric biosensor as documented in the publication by Hernández *et al*. In their publication, a layer of graphene was deposited on the surface of a glassy carbon rod and then functionalised with *S. Aureus*-responsive DNA aptamers.[73] Two different approaches, namely covalent and non-covalent bonding were trialled and preferential bacterial binding was demonstrated in both cases. The superior

sensitivity of 1 CFU/mL was achieved by the non-covalent approach where the graphene oxide was first reduced before the pyrene-modified aptamer was added, hence resulting in a relatively flat distribution on the surface and more effective $\pi - \pi$ stacking. Another reason provided for this performance was the lower number of defects found in reduced graphene oxide in comparison to those in the graphene oxide used for the covalent binding of aptamers.[73] Aside from *S. Aureus*, *E. Coli* has also been detected down to 1 CFU/mL using voltammetry and was reported by Pankratov *et al*.[78] Their design used magnetic beads (MBs) modified with *E. Coli* specific antibodies or aptamers to trap the bacteria, forming a complex. Free *E. Coli* specific antibodies or aptamers bound to cellulase via streptavidin−biotin linkage were then incubated with the bacteria-MB complex, yielding a sandwich structure. This was then applied to a nitrocellulose-modified electrode surface where the nitrocellulose was digested by the cellulase, thereby triggering a change in the electrochemical properties. This change was recorded by cyclic voltammetry and the low LOD was found to be the result of signal amplification. This was attributed to the ability of several aptamer reporter sequences to simultaneously bind to the *E. Coli* surface as up to three cellulase labels can be accommodated on a single streptavidin bridge at any one time.[78] A multiprobe biosensor capable of detecting the 16S rRNA gene inherent to 5 different bacterial strains, namely *S. Aureus*, *Enterococcus Faecalis* (*E. Faecalis*)*, E. Coli, P. Aeruginosa and Citrobacter Freundii* (*C. Freundii*) was designed by Wang *et al.* The different polyA DNA probes consisted of a polyA tail which covalently binds to the gold electrode surface and a recognition part which was able to capture the specific targeted sequence *via* DNA hybridisation. An enhanced current signal was observed only when the specific DNA target was recognised. An excellent detection limit was observed at a low bacterial concentration of 10 fM. It was attributed to the use of multiprobes which led to improved signal reporting and hybridisation efficiency due to DNA base-stacking forces.[79]

3.1.4. Field Effect Transistor (FET) Biosensors

Field effect transistors (FETs) biosensors are devices that can detect changes in their source-drain ‘channel conductivity’ in response to their external electric field environment , which is subject to

constant change as the target analyte binds to a biological or chemical recognition element as shown in Figure 5A (Left).[80, 81]. A simple FET consists of three electrodes, namely the source, drain and gate. The electric potential is applied at the gate electrode which, in turn, controls the conductivity of the channel between the source and drain electrodes.[9] A change in the source–drain voltage–current (V_{DS}–I_D) characteristics can provide information on the carrier density, which is, in turn, inversely proportional to the electrical resistance. [81] As further evidenced in Figure 5A (Right), the change in electrical field occurs in a direction normal to the gate surface, thereby indicating that the carrier density can be influenced by the polarity and charge density on the surface.

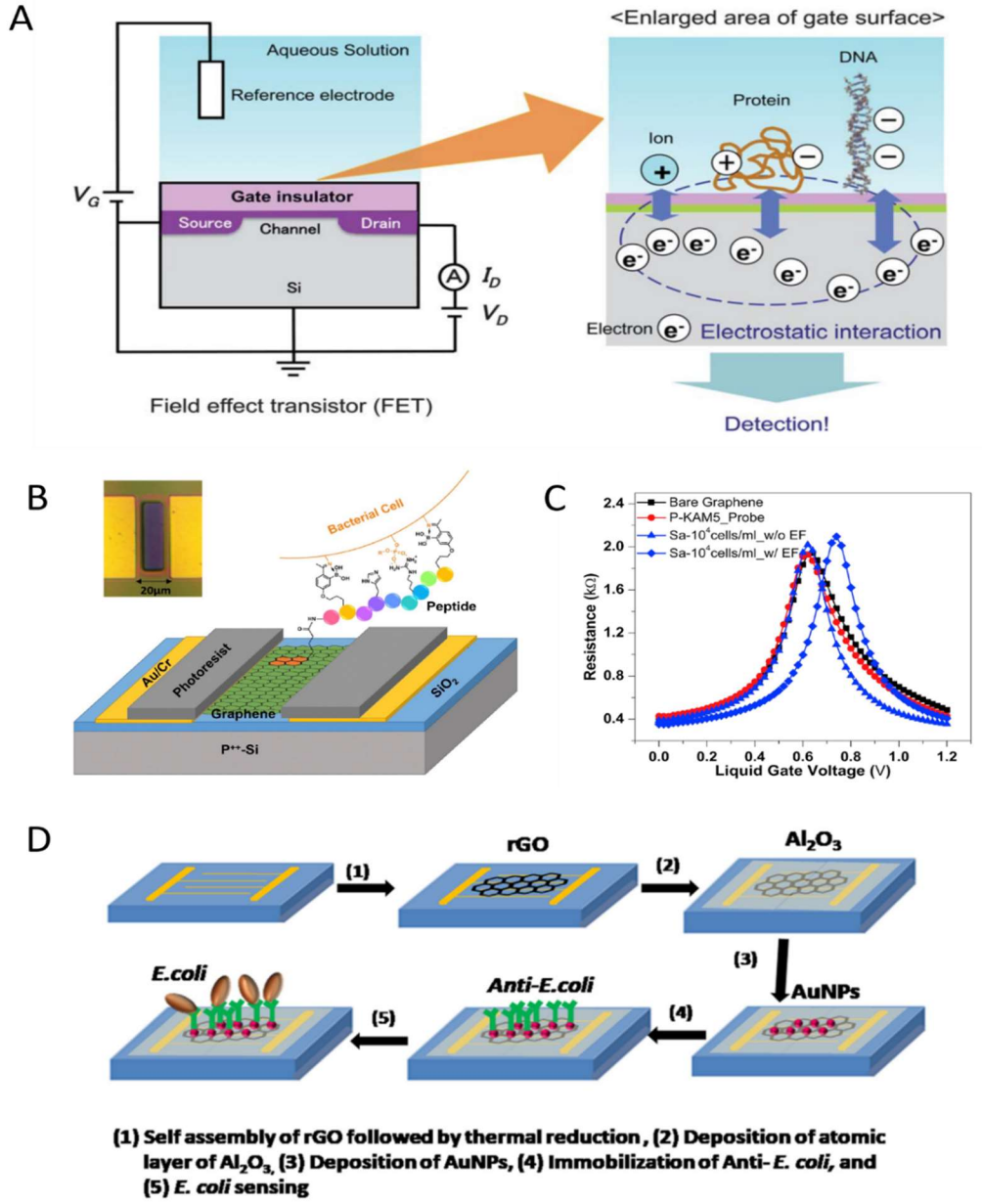

Figure 5: A. Basic Design and Operation of a FET-based sensor.[81] (Reproduced from reference [81] with permission. Copyright 2013 RSC); B. Design of the G-FET proposed by Kumar and associates;

C. Distinct change in variation of resistance with liquid gate voltage with the G-FET and 10^4 *SA* cells/mL.[82] (Reproduced from reference [82] with permission. Copyright 2020 Elsevier); D. Schematic showing the design of the FET sensor proposed by Thakur et al.[84] (Reproduced from reference [84] with permission. Copyright 2018 Elsevier)

There are a range of different substrates used in the design of field effect transistors with graphene being one of the most popular choice for use as biosensors. An innovative take on conventional graphene field effect transistors (G-FET) was very recently described by Kumar *et al*. Their compact and low-cost device incorporated synthetic peptides and electric field- assisted bacterial binding capabilities for specific capture and detection. The graphene on the G-FET was functionalised with peptide-pyrene conjugates responsive to only *S. Aureus*. As the concentration of bacteria on the surface of the graphene increased, an increase in the Dirac voltage was recorded, thereby showing binding of the bacteria to the peptide-pyrene conjugates (Figure 5B).[82] Bacterial binding was further assisted by application of an electric field which caused the bacteria to accumulate on the graphene surface more effectively. This biosensor system was able to detect *S. Aureus* at a concentration of 10^4 CFU/mL which is usually the baseline concentration for detection of urinary tract infections (Figure 5C).[82] The sensitivity was further improved to 10^3 CFU/mL by the application of more incubation and voltage cycles, which would force the charged bacteria to better accumulate on the surface. This LOD was also obtained in the publication by Dey *et al* where an organic-inorganic hybrid trilayer dielectric transistor made of aluminium oxide, titanium oxide, and poly(methyl methacrylate) was devised. The top layer was then coated with N,N-dioctyl-3,4,9,10-perylenedicarboximide (PDI-C8) which acted as the active sensing layer. In the presence of Gram-positive bacteria, an increase in the drain current was registered as the negatively charged teichoic acid in the cell walls of gram-positive bacteria created an additional channel on the PDI-C8 coated top layer. In contrast, the presence of gram-negative bacteria decreased the amount of output current because its cell wall established a more resistive channel.[83] In another example, a FET-based platform incorporating *E. Coli* specific antibodies was designed by Thakur *et al*..[84] First, thermally reduced rGO was deposited on the surface of interdigitated gold electrodes immobilised on a silicon dioxide (SiO_2) surface. Next, a thin layer of aluminium oxide (Al_2O_3) was deposited followed by

glutathione functionalised AuNPs. Last, polyclonal *E. Coli* antibodies was conjugated to the AuNPs to yield the FET sensor (Figure 5D). As *E. Coli* bacteria bonded to the antibodies, more negative charge was developed, thereby reducing the current flow from the source to drain. Increasing the concentration of *E. Coli* led to a decrease in the current flow. An LOD of 10^3 CFU/mL, similar to the publications by Kumar *et al*. and Dey *et al*., was also reported in this paper. However, it was stipulated that this was the result of using a very small sample volume of 1 μL. Thus, with larger volumes and the use of a filtration setup, it was possible to detect down to 1 bacterial cell/mL with this sensor.[84]

In the publication by Moudgil and coworkers, irrespective of the sample volume as in the paper by Thakur *et al*., a very LOD of 50 CFU/mL was reported.[85] A highly sensitive Vancomycin (Van) functionalised molybdenum disulphide/titanium dioxide (MoS_2/TiO_2) FET sensor was developed. The TiO_2 was sputter coated on a thin film of MoS_2 to form a hybrid nano heterostructure; this was then deposited onto a Si/SiO_2 substrate. Channel contact metal pads (Cr/Au) were then deposited followed by the addition of SU-8 photoresist, which was used as a passivation layer to immobilise the Van probe on the channel. When *S. Aureus* was exposed to this sensor, the binding and the capture of *S. Aureus* led to a decrease in the drain current, which was found to vary inversely with an increase in bacterial concentration. This reduction in current was due to the overall negative charge on bacterial membrane and Van complex, which in turn depleted the carriers in the n-type channel of the MoS_2/TiO_2 FET sensor. The high sensitivity of the sensor was attributed to the high binding affinity of the Van to the *S. Aureus*.[85]

3.2. Optical Biosensors

Optical biosensors are usually used to detect changes in optical properties of the sensing element such as luminescence, fluorescence, reflectance, scattering or absorbance properties in the ultraviolet, visible, and near-infrared region upon direct binding of the target analyte.[86] These biosensors are often based on optical phenomena such as surface plasmon resonance (SPR), Förster resonance energy transfer (FRET), Surface enhanced Raman scattering (SERS), interferometric reflectance and

Fourier transform infrared spectroscopy (FTIR) amongst others.[30] In this section, the common types of optical biosensor platforms are summarised and the technological improvements which eventually led to their increase in sensitivity are detailed.

3.2.1 Interferometric reflectance-based biosensors

Interferometric reflectance-based biosensors have been explored in the detection of bacteria using the reflection ability of light. Most of these biosensors use porous silicon(pSi), characterised by the presence of air-filled pores with diameters less than 150 nm embedded within a silicon matrix, as a substrate for binding of the target analyte.[87] It has been extensively exploited since the early 2000s as an optical sensor owing to the material's large surface area, ease of synthesis and functionalisation in addition to being conductive to optical and electrochemical transducing elements.[87, 88] The principle underlying interferometric reflectance and the subsequent design of pSi biosensors is based on the binding of the analyte to the pSi surface. This leads to a change in the refractive index of the medium, which is then detected by a shift in the interference pattern as well as a reduction in the intensity of reflected light. This pattern is usually characteristic of white light reflection through the pSi surface and is related to the effective optical thickness parameter. This was illustrated in a publication by Urmann and coworkers who devised a simple Hemag1P aptamer-functionalised pSi optical biosensor for the capture and detection of the probiotic, *Lactobacillus acidophilus* (*L. acidophilus*) by reflective interferometric FTIR with an LOD of 10^6 CFU/mL.[89] Furthermore, Massad-Ivanir *et al*. immobilised *E. Coli* monoclonal antibodies on the surface of pSi for direct capture of the corresponding bacteria. By monitoring the changes in intensity of the optical interference signal at different bacterial concentrations, the lowest concentration found capable of producing a significant change was 10^4 CFU/mL.[90] The lowest reported LOD using this technique was in the publication by Dey and colleagues who conceptualised a system based on optical interferometry – the technique commonly used with porous silicon based optical sensors – and the use of nanomaterials to target and detect *E. Coli* bacteria. A gold nanohole substrate was decorated with bioprinted microarrays functionalised with recombinant protein G for attachment of *E. Coli*

specific antibodies; this system was then interfaced with a lens-free interferometric microscopy device. Variations in the optical path difference were monitored to determine the binding efficiency of the *E. Coli* to the antibody. A very high sensitivity of 1 bacterial cell/mL was obtained directly from blood plasma and this was found to vary depending on the sample volume used which was 150 μL in this case.[91]

3.2.2 Fluorescence-Based Biosensors

Fluorescence-based biosensing platforms have also found widespread use in bacterial detection as the fluorescence intensity can be used as a measure of the bacterial concentration. Huang *et al.* proposed a fluorescence-based optical system which combined the benefits of stimuli-responsive biosensors as well as the use of antibodies for increased specificity. They synthesised a hybrid nanoparticle system consisting of 500 nm spherical mesoporous silica-curcumin NPs functionalised with 6 nm sized spherical zinc oxide NPs (MCZ NPs) which were then modified with polyclonal antibodies (pAbs) against *S. Typhi*. Meanwhile, MNPs were also modified with monoclonal antibodies (mAbs) against *S. Typhi*.[92] The three inlets of the microfluidic device were filled and mixing was carried out by the Koch fractal micromixer to yield MNP-bacteria-MCZP complexes, which were then captured by an external magnetic field. To trigger the release and capture of the curcumin signal reporter, acetic acid was introduced from inlet 4 as the carboxylate ions in acetic acid were able to convert hydrophobic curcumin to hydrophilic curcumin, thereby imparting allochroic and fluorescent properties to the curcumin; this was then collected and magnetic separation was used to obtain the released curcumin. The corresponding absorbance and fluorescence intensity were then measured. As the concentration of bacteria was increased, a more noticeable change in colour was observed in addition to a higher fluorescence intensity and absorbance. An LOD of 63 CFU/mL and 40 CFU/mL for absorbance and fluorescence measurements was obtained, respectively. This improved sensitivity was made possible by the use of curcumin and its ability to generate strong optical signals even at low concentrations. This method in fact combined both optical and colourimetric biosensing, which is further illustrated in Section 3.2.3. A ‘turn-on fluorescence’ biosensing platform was invented by Guo and coworkers

which made use of a fluorescence resonance energy transfer (FRET) system comprising citrate-functionalised copper clusters (Ca-CuNCs) and dopamine stabilised AuNPs (DA-AuNPs) electrostatically bound to the surface of a 1H,1H,2H,2H-perfluorooctyltriethoxysilane (POTS) modified bacteria-imprinted PDMS film. In this system, the DA-AuNPs acted as the fluorescence energy acceptor while the negatively charged CA-CuNCs were used as the fluorescence energy donors. Owing to the reduction in distance between these two components as a result of the charge interaction as well as the overlapping in the fluorescence emission spectrum of CA-CuNCs and the absorption spectrum of DA-AuNPs, led to quenching of the CA-CuNCs. In the detection procedure, *S. Aureus* bacteria was captured by the device and since they possess a negative charge, they competed with the Ca-CuNCs and eventually bound to the DA-AuNPs, leading to an enhancement of the fluorescence associated with Ca-CuNCs. Very low detection limits of 11.12 CFU/mL were reported in this paper.[93]

As evidenced earlier, sandwich-based assay can provide very high sensitivity levels and this design feature has also been successfully incorporated in fluorescence-based optical sensors. A sandwich composite system made of immunomagnetic NPs was devised by Wang *et al*.[94] Three different bacteria-recognising peptides were attached on the surface of magnetic NPs; three different quantum dot probes were functionalised with bacteria-specific aptamers. In the presence of the specific bacteria, the bacteria bound to the peptides and consequently the quantum dots (QDs) bound to the bacteria due to the aptamer coating. Then the magnetic NPs-peptide-bacteria-QDS complex was removed by magnetic separation. After magnetic separation of the bacteria bound to the fluorescent magnetic probe system, the fluorescence of the supernatant was used to determine the concentration of the bacteria. In general, a greater reduction in fluorescence was characteristic of a high bacterial concentration as more and more QDs bound to the bacteria. With this sandwich-based system, impressive limits of detection were obtained, namely 2.46, 5.41 and 3.77 CFU/mL for *E. Coli* O157:H7, *S. Aureus*, and *V. Parahaemolyticus*, respectively.[94] Another example by Zeinhom *et al*. who developed a smartphone-based fluorescence device for the detection of *E. Coli* O157:H7 *via* a

sandwich assay. Their setup involved a field-portable fluorescent imager consisting of an excitation light source, sample loading chamber and a long-pass filter and focusing lens for signal collection mounted on a cell phone.[95] A sandwich assay was developed whereby magnetic beads labelled with mono anti-*E. Coli* O157:H7 were used to identify and capture the bacteria from the sample mixture using an external magnet. FITC labelled poly- anti-*E. Coli* O157:H7 formed the other component of the sandwich structure which were capable of binding to the bacteria and producing fluorescence images. This was then captured by the phone and converted into fluorescence intensity measurements which was found to vary linearly with the bacterial concentration. This system was found to possess a high sensitivity of 1 CFU/mL with a very low background noise, which was the result of the relatively low and unspecific mutual absorption of the two types of antibodies used. This performance was also attributed to the high specificity and binding affinity to *E. Coli* as well as the high entrapment efficiency of the affinity- purified antibodies labelled magnetic beads.[95] An almost identical design using magnetic NPs to capture and concentrate bacteria was explored by Lee and coworkers. Their 'count on cartridge' system involved detecting *S. Aureus* using fluorescent carboxylate quantum dot-labelled NPs capable of binding to the cell membrane of the bacteria. In this system, anti-*S. Aureus*-functionalised, protein A (a surface protein commonly found on the *S. Aureus* bacterial cell wall) -coated and fluorescently labelled magnetic NPs were mixed with *S. Aureus* culture and a cartridge was used to separate, capture, and concentrate the bacteria to a small volume. The cartridge was then placed into the cartridge loading slot in a fluorescent image reader, a modified version of the system, which counts the fluorescent bacterial cells held by a hard magnet within the field of view on the cartridge. Owing to the guidance from magnetic NPs and identification by fluorescent markers alike, the reported assay had a very impressive LOD of 1 CFU/mL, similar to the system developed by Zeinhom and coworkers.[96]

In a very recent publication by Shen *et al.*, a stimuli-responsive ratiometric fluorescent nanoprobe with an excellent LOD of 1 CFU/mL was reported. In their design, Vancomycin and *S. Aureus* specific aptamer dual-functionalised near-infrared (NIR) fluorescent N-acetyl-L-Cysteine cadmium

telluride (NAC-CdTe) QDs were bound to the surface of unreported blue fluorescent π-rich electronic carbon NPs (CNPs) by noncovalent π−π stacking interactions (Apt-Van-QDs@CNPs).[97] With this design the blue CNPs acted as the energy donors while the NIR Apt-Van-QDs acted as the energy acceptors; as they were close enough, the phenomenon of FRET was made possible, thereby leading to a blue fluorescence quenching and a clear NIR fluorescence enhancement. Upon incubation with *S. Aureus* bacteria, this process was hindered, consequently exhibiting a ratiometric fluorescent response characterised by a large Stokes shift of ~260 nm. The high sensitivity of this sensing platform was due to the efficient targeting of the bacteria with the dual-functionalised QDs.[97] Finally, DNA technology has been incorporated in the design of optical biosensors as they are able to provide better sensitivity than nanomaterial or antibody-based transducing elements. Thus, Chang *et al*. designed a graphdiyne-based fluorescent biosensing platform for the detection of *Mycobacterium tuberculosis* (*M. tuberculosis*). Very thin 0.9 nm graphdiyne nanosheets that were able to adsorb single stranded DNA (ssDNA) on their surface and subsequently quench the ssDNA fluorescence were synthesised. Consequently, a corresponding target sequence, isolated from the bacteria was added, which restored the lost fluorescence as double stranded DNA (dsDNA) was formed.[98] As the target bacterial probe concentration was increased, there was a rise in the fluorescence intensity. A superior selectivity owing to its ability to recognise DNA mismatches as well as a sensitivity of 25 pM was observed using this platform, which was also capable of multiplexed bacterial detection.[98]

3.2.3 Plasmonic Biosensors

Plasmonic biosensors have attracted great interest for highly sensitive real-time and label-free biosensing applications. The popularity of nanoplasmonic sensors with a focus on noble NPs such as gold and silver and their inherent localised surface plasmon resonance (LSPR) properties has been widely studied.[99] As shown in Figure 6A, a typical gold nanoplasmonic sensing platform comprises a light source directly above the sensor chip and is linked to a spectrophotometer. The sensor chip can be further functionalised with gold nanostructures of different shapes and sizes to optimise their

performance.[100] For example, a gold-based SPR biosensor was developed to detect *S. Aureus* in the publication by Khated and colleagues. The hole mask colloidal lithography (HMCL) technique was used to generate nanostructured gold disks (two different diameters: 200 and 100 nm) as plasmonic nanostructures on glass slides. The surface of these gold nanodisks was then biofunctionalised with DNA aptamers that specifically bind to *S. Aureus*.[101] The changes in extinction spectra produced by subsequent binding of the bacteria was monitored. The performance of 200 and 100 nm gold disks was also compared and the larger diameter disk displayed a significantly larger extinction spectra and produced a more heightened shift in the spectra. The improved sensitivity of this sensor was attributed to the bulk refractive index and the extent to which the local field emanates out from the sensor. This sensor was able to detect bacteria down to 10^3 CFU/mL within 120 s.[101] To increase the sensitivity of SPR-based sensors, a chip incorporating the azimuthally-controlled grating-coupling technology (GC-SPR) was designed to detect *Legionella pneumophila* (*L. Pneumophila*) bacteria. Plasmonic gold substrates were pegylated and then biofunctionalised with the Virostat IgG α-*L. Pneumophila* polyclonal antibodies (#6051) and Abnova IgG α- *L. Pneumophila* rabbit polyclonal antibodies (#PAB13999) to specifically detect this type of bacteria. Moreover, the antibodies were labelled with Alexa fluor 647 to endow fluorescence signal detection capabilities to the biosensor. Changes in the plasmonic reflectivity were used to determine the concentration of bound bacteria. The fluorescence signal further validated the presence of bacteria in the test sample. This sensor was able to detect down to 10 CFU of bacteria.[102] A similar sensor design with increased specificity and sensitivity was reported by Yoo and coworkers as illustrated in Figure 6B. This platform was able to successfully identify three different bacterial strains in multiplexed mode. It was biofunctionalised with three different aptamers, each able to bind specifically to *Lactobacillus Acidophilus* (*L. Acidophilus*), *S. Typhi* and *Pseudomonas Aeruginosa* (*P. Aeruginosa*), respectively. This sensor was capable of detecting 30 CFU per assay in a sample volume of 3 μL.[103]

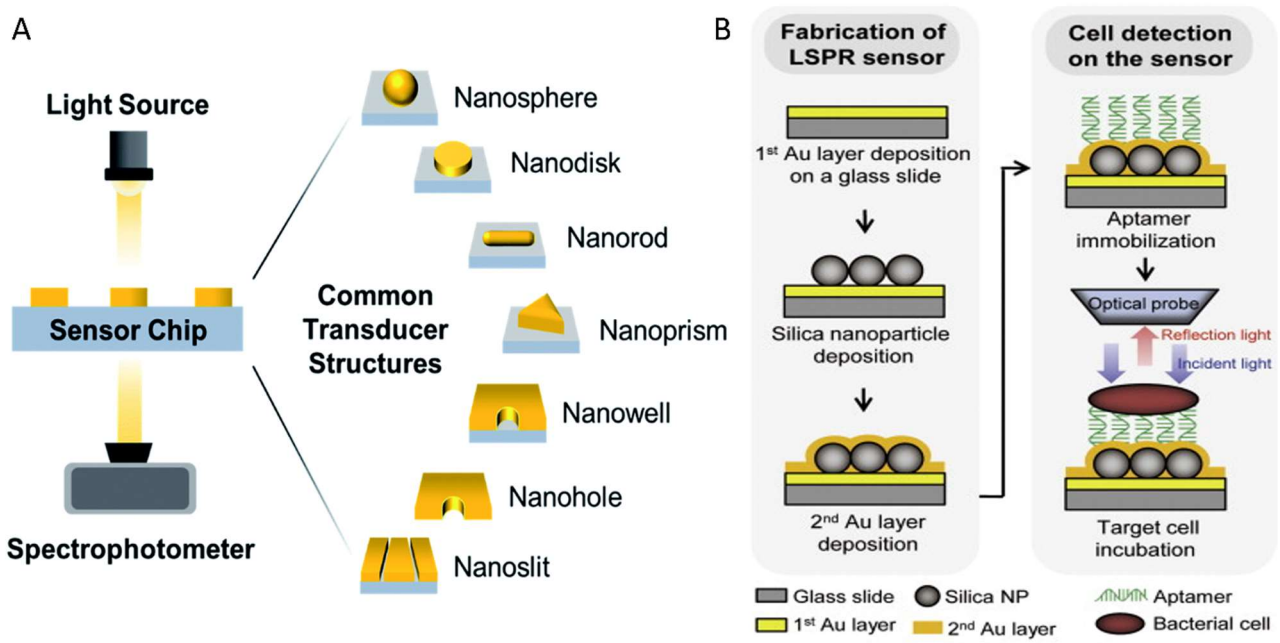

Figure 6: A. Schematic showing a simple plasmonic sensor system with different gold-based surface functionalisation.[100] (Reproduced from reference [100] with permission. Copyright 2020 RSC); B. Schematic showing the design of the platform by Yoo *et al*.[103] (Reproduced from reference [103] with permission. Copyright 2015 Elsevier)

Aside from LSPR-based biosensors, these gold nanostructures have been employed in SERS-based optical biosensors as illustrated by Whang and colleagues. In their design, plasmonic gold NPs were first assembled on Gram-negative bacteria *E. Coli* or *P. Aeruginosa* – found to cause nosocomial infections such as pneumonia, urinary tract infections (UTIs), and bacteremia – and then deposited on a gold-coated porous polycarbonate nanoporous membrane. The hydrodynamic trapping allowed these plasmonic bacteria to be enriched near the gold nanopores. Thus, focused light by constructive interference between incident light and its diffraction *via* the nanopore, self-assembled nanoplasmonic antennas on the bacterial surface, and plasmonic mirrors all contributed to a strong intensity Raman signal. After passing the bacteria through a microfluidic channel and analysis of the detection capabilities of the system, a low detection limit of 100 CFU/mL was obtained.[104] This was made possible by the dense assembly of the gold NPs on the bacterial surface which, in turn, led to amplification of the optical signal. As the bacterial concentration was increased, a shift towards higher intensity values were observed while identical peaks in the Raman spectra corresponding to the bacteria were obtained. Gao and coworkers also reported a similar SERS-based system with gold

nano islands deposited on the surface of a chip which could capture and detect *S. Aureus* and *E. Coli* bacteria. A detection sensitivity of 100 CFU/mL comparable to the one reported by Whang *et al*. was obtained, thereby showing the reliability of SERS to detect bacteria at low concentrations.[105]

In virtue of the enhanced sensitivity benefits associated with the use of aptamers, a gold nanoparticle-based SERS aptasensor was developed by Zhang *et al*. for the detection of *S. Aureus* and *S. Typhi*, thereby endowing the platform with the highly prized functionality of simultaneous detection of different bacterial species. Two different types of signal probe solutions were fabricated; Mercaptobenzoic acid (MBA) and 5,5′-Dithiobis(2-nitrobenzoic acid) (DNTB) were each grafted on the surface of gold NPs (GNPs) which were then further functionalised with aptamers for selective capture of *S. Typhi* and *S. Aureus*.[106] The capture probe consisted of magnetic-gold NPs (MGNPs) functionalised with aptamers to attract the relevant bacteria, which in turn adhered to the signal probe, giving rise to a sandwich structure. The bacteria concentrations were monitored by their Raman intensities at 1333 cm^{-1} from DNTB and 1582 cm^{-1} from MBA, respectively. The reduction in the Raman intensity with decreasing bacterial concentration was found to be linear. This biosensor design gave rise to an LOD of 35 and 15 CFU/mL for *S. Aureus* and *S. Typhi*, respectively. [106]

3.2.4 Colourimetric Biosensors

A major part of optical biosensors are colourimetric biosensors which have recently become popular as a diagnostic tool owing to their simplicity, visual nature of the results, low cost, and ease of use. Colourimetric biosensors usually take advantage of the inherent colour change properties of materials in response to chemical or biological reactions. As described by Song *et al*., the detection events are converted into colour changes by the naked eye.[107] Very often, these events are redox and enzyme-catalysed reactions. A case in point is the redox-responsive biosensor reported by Sun *et al*. which combined the benefits of colourimetric analysis and electrochemical sensing. This design used a redox compound *p*-benzoquinone which was reduced in response to the enzymatic reaction of bacterial respiration to form hydroquinone. Reaction of this reduction product with the rest of the *p*-benzoquinone yielded quinhydrone which produced a distinct red colour. This was then used to detect

bacterial concentration up to 10^4 CFU/mL.[108] The system further exploited the electric current which was generated from the remaining *p*-benzoquinone on the surface of the working electrode and was able to improve the *E.Coli* detection limit to 10^3 CFU/mL. Despite the relatively high detection limit, this system was capable of sorting *E.Coli* from other types of bacteria as well as antibiotic-resistant strains of *E.Coli* and provided a qualitative and visual approach to bacterial detection.[108]

Interactions of smart materials with their external environment can also cause conformational transformations and hence, intense colour changes under specific conditions.[109] Nanomaterials have been extensively explored for this application with a strong focus on AuNPs colourimetric biosensing.[107] This is often attributed to the ability of AuNPs to shift their surface plasmon resonance in response to different aggregation states which in turn triggers a visible change in colour.[110] Verma *et al*. also highlighted the benefits of gold such as tuneable size and shape, ease of functionalisation amongst others which can influence their stability and hence, intensity of colour change.[111] Enzyme-catalysed reactions involving AuNPs was explored in the publication by Creran and coworkers who reported an enzyme-nanoparticle sensor patterned on the surface of a paper strip using inkjet printing, which is a low-cost, reliable, and simple technique capable of large-scale manufacture to facilitate their introduction in clinics. The sensor was made of tetraethylene glycol trimethyl ammonium (TTMA) functionalised gold NPs (TTMA-AuNPs). Binding of the anionic β-galactosidase (β-gal) enzyme to the cationic TTMA-AuNPs led to inhibition of the β-gal enzymatic action. Incubation with the (chlorophenol red-β-D-galactopyranoside (CPRG)) substrate did not produce a colour change and the sensor remained pale yellow. However, when the negatively charged *E. Coli* or *Bacillus Subtilis* (*B. Subtilis*) was added, the enzymatic activity was reversed and the substrate turned into a deep purple colour based on the bacterial concentration.[112] This sensor was found to be suitable for bulk detection of bacteria as the most noticeable and measurable change in colour occurred at 10^3 CFU/mL. Moreover, Mou *et al*. designed a colourimetric biosensor based on the click reaction between azide- and alkyne-AuNPs and coupled their system with MNPs for improved bacterial specificity. Since bacteria have been shown to undergo redox reactions in copper-rich environments,

the AuNPs were incubated in a copper chloride solution. Cupric reductase NDH-2 found in bacteria then reduced the Cu^{2+} ions to Cu^{+} ions which then led to aggregation of the NPs and a colour change from red to blue (Figure 7A).[113] This system was interfaced with a smartphone application developed for analysis of the solution colour, hence giving an accurate representation of the concentration (Figure 7B). The sensitivity of the system was further enhanced to increase its responsiveness to *E. Coli*. Iron oxide magnetic NPs functionalised with *E. Coli*-identifiable aptamers were added to the sample and the bacteria were allowed to aggregate on their surface. First using a magnet and then treatment with DNase, the bacteria were separated and released from the NPs to trigger the click reaction. This led to an 85% trapping efficiency of *E. Coli*, release efficiency of 90%. This publication was an improvement to the publication by Sun and coworkers as corroborated by the lower detection limit of 200 CFU/mL. The sensitivity was found to be dependent on the concentration of the functionalised gold NPs used with 5.4 nM being the optimal concentration. [113]

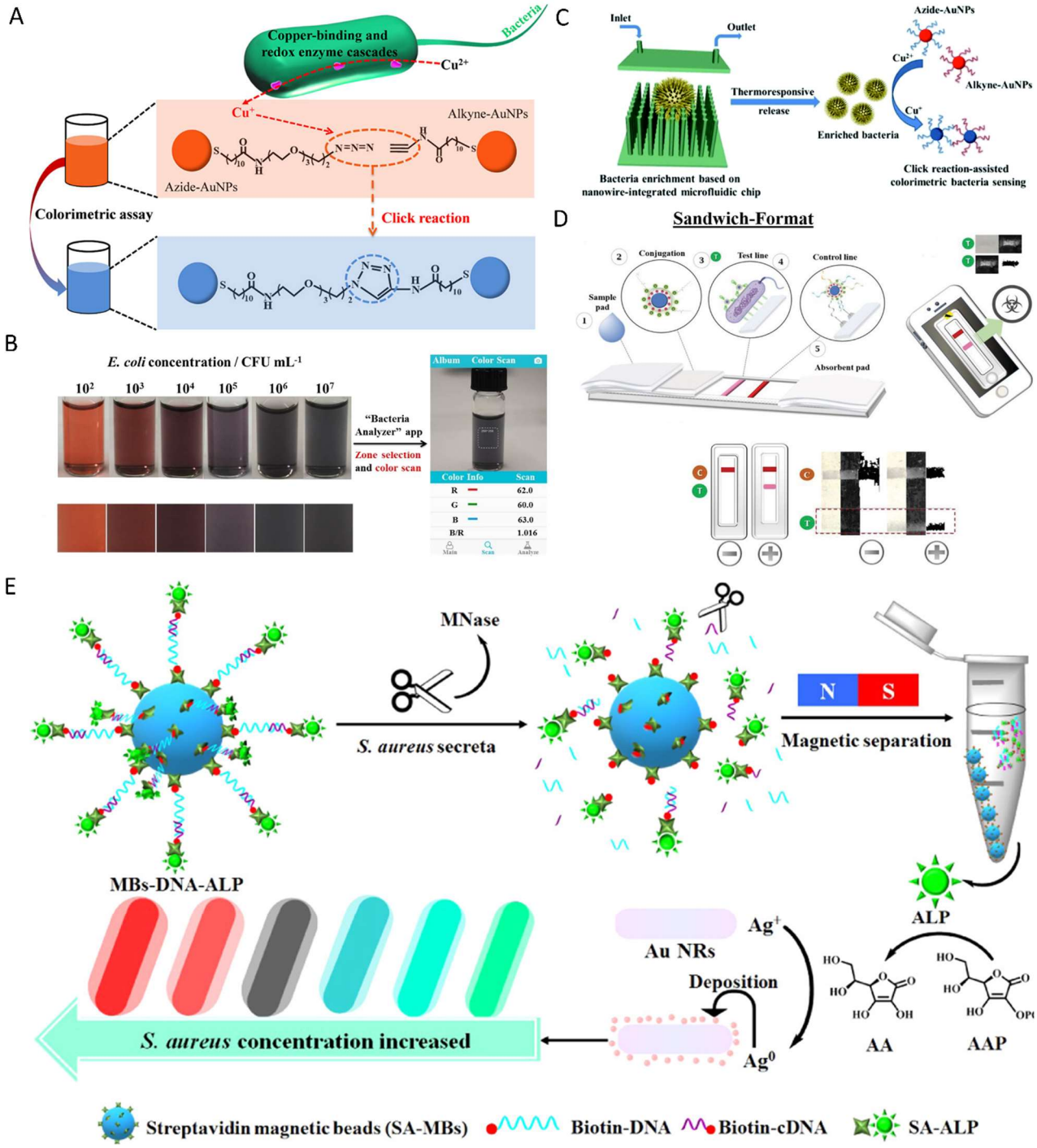

Figure 7: A. Click reaction showing the colour change as a result of the click reaction; B. Variation of 'blue' colour depth based on *E. Coli* concentration.[113] (Reproduced from reference [113] with permission. Copyright 2019 ACS); C. Schematic showing the mode of action of the on-demand detection platform.[114] (Reproduced from reference [114] with permission. Copyright 2019 RSC); D. Test-strip system proposed by Díaz-Amaya *et al.*[115] (Reproduced from reference [115] with permission. Copyright 2019 John Wiley and Sons); E. Schematic illustration of the design proposed by Zhou *et al.*[117] (Reproduced from reference [117] with permission. Copyright 2020 ACS)

Aside from chemically responsive gold NPs, thermoresponsive systems using AuNPs has also been explored. In the publication by Du and colleagues, the click reaction between azide- and alkyne-

AuNPs as well as the benefits of on-demand detection devices were combined and exploited to improve biosensing efficacy. Nanowires grafted with PNIPAAm polymer brushes were integrated on a silicon wafer to produce a thermoresponsive microfluidic chip. The surface of the nanowires was then modified by biotin-streptavidin-biotin-conA coupling to improve bacterial trapping at the physiological temperature of 37 °C.[114] *E. Coli* were then thermoresponsively released at 25°C with a 90 % efficiency in only 30 min as shown in Figure 7C. Bacteria were incubated with a colourimetric system including copper ions and azide- and alkyne-functionalised AuNPs. Following a similar protocol to the publication by Mou *et al*., Cu^{2+} to Cu^{+} ions were then reduced by the released bacteria, thereby initiating the click reaction between the azide- and alkyne-AuNPs and the subsequent colour change. They further demonstrated the ability of selective capture and identification of bacteria on different bacterial species by modifying the biotin conjugation molecules. For example, they employed biotin-*S. Aureus* specific aptamers (biotin-Apt) which showed a binding efficiency of 93% for *S. Aureus*. The lowest limit for visual colour changes as reported by Du *et al*. was 100 CFU/mL. Furthermore, a blood sample containing around 40 CFU/mL *S. Aureus* and 500 CFU/mL *E. Coli* was tested and based on the calibration curve of the pixel value of the blue/red colour ratio versus concentration, an *S. Aureus* concentration of 290 ± 70 CFU/mL was detected after enrichment, release, and analysis.[114]

To lower the LOD of these colourimetric sensors, aptamers were included in their design, as exemplified by the 2019 publication by Díaz-Amaya *et al*. who employed inkjet printing technique in conjunction with aptamers and gold nanoclusters (AuNCs). They designed a paper-based chromatographic nitrocellulose platform decorated with carboxyl-functionalised aptamers by nanocontrolled inkjet printing to detect shiga toxin-producing *E. Coli*, *E. Coli* O157:H7. AuNCs (20 nm) were then immobilised on the surface of polystyrene beads and coated with branched polyethyleneimine.[115] A truncated aptameric DNA sequence (a-aptamer) highly specific to *E. Coli* O157:H7 was then conjugated to the fabricated particles. Upon addition of the bacterial sample, it was recognised and interacted with the inkjet patterned capture aptamer (carboxy/ DNA aptamer)

found on the test and label lines. A positive test was characterised by two coloured lines as shown in Figure 7D below. Similar to the publication by Creran *et al*., the colour intensity of the lines was linearly proportional to the concentration of the bacterial sample. The LOD obtained was 25 and 233 CFU/mL, when tested in PBS and ground beef respectively.[115] Even with a very LOD of 25 CFU/mL, it was established that this may not be as accurate owing to the low concentration and small sample volume of <100μL and high possibility of poor reproducibility. Conversely, at concentrations greater than 100 CFU/mL, a linear correlation between the intensity response and concentration was observed. This behaviour was further confirmed by the detection limit found when tested in a real beef sample. The use of aptamers was also harnessed in the publication by Yu *et al.* where *S. Aureus* specific aptamers were immobilised on the surface of a 96-well plate decorated with capture probes via streptavidin-biotin binding. As the bacteria bonded to the aptamer, the aptamer was released from the capture probe-aptamer complex. The capture probe then underwent hybridisation with a DNA-based detection probe (SYBR Green I) added to the plate surface. 3,3′,5,5′-tetramethylbenzidine (TMB) was used to produce a colourimetric response under photoirradiation as its oxidation could be triggered by the formation of the capture probe-SYBR Green I complex. The colour of the TMB was used as an indicator of the bacterial concentration and an improved LOD of 81 CFU/mL was obtained. This was found to be the result of combining the use of aptamers with the photocatalytic behaviour the complex formed.

Several other research groups also demonstrated the superior sensitivity offered by the use of DNA aptamers or bacteria-specific phage as recognition probes for bacteria. A class of material, nanozymes, has become popular in the design of colourimetric sensors as the colour change exploits the chemical interactions and reactions between enzymes and substrates. In the colourimetric sensor proposed by Zhou and team, dual enzyme mediated gold-silver alloy nanorods (Au-Ag NRs) were developed for the detection of *S. Aureus*. To monitor the bacterial concentration, alkaline phosphatase (ALP)−oligonucleotide-functionalised magnetic beads (MBs− DNA−ALP) were used. As illustrated in Figure 7E, micrococcal nuclease (MNase) released by *S. Aureus* cleaved the oligonucleotides on

the MBs and magnetic separation of ALP from the MBs was carried out. Next, the supernatant containing ALP and *S. Aureus* was introduced into a solution containing L-ascorbic acid 2-phosphotrisodium salt (AAP), silver nitrate, and gold nanorods (AuNRs). The ALP then catalysed the conversion of AAP into ascorbic acid (AA) which, in turn, catalysed the reduction of Ag+ to Ag0. This led to the deposition of a Ag layer on the Au NRs. The newly formed Au−Ag alloy NRs showed significant shifts in their localised surface plasmon resonance and gave rise to rainbow-like colour changes which varied depending on the *S. Aureus* concentration incubated with the sensing solution. A high sensitivity of 25 CFU/mL was obtained and was mainly attributed to the dual enzymatic amplification reaction based on MNase and ALP as well as the superior properties of Au NRs. Another AuNR biosensor based on enzyme-mediated cascade reactions was developed by Zhou and team for the colourimetric detection of *E. Coli* as well as specific detection of β-galactosidase (β-gal), an indicator of the concentration of *E. Coli*. In this design, manganese dioxide (MnO_2) nanosheets – nanozymes with high oxidase mimicking activity – was used to catalyse the conversion of TMB into TMB^{2+} under acidic conditions. These ions then etched the surface of the AuNRs and led to a blue shift in the localised surface plasmon resonance peak of the AuNR, hence triggering a colour change.[118] To determine the *E. Coli* concentration and trigger the cascade reaction, β-gal hydrolysed the paminophenyl β-D-galactopyranoside (PAPG) substrate to p-aminophenol (PAP) which then reduced the MnO_2 nanosheets. As their oxidase activity was thwarted, the resulting formation of TMB^{2+} and AuNR etching was stopped, thereby affecting the intensity of the subsequent colour changes. With this system, an LOD of 22 CFU/mL was obtained and this performance was mainly attributed to the two rounds of catalytic amplification as well as superior optical properties of AuNRs.

Furthermore, in the publication by Zhang and colleagues, DNA aptamers were immobilised on the surface of iron oxide NPs (Fe_3O_4 NPs) – another type of nanozyme – to detect the dental bacteria, *Streptococcus Mutans* (*S. Mutans*), which is known to cause caries and periodontitis. Since these NPs possess inherent peroxidase-like properties, they are able to speed up the oxidation of the

colourless 3,3′,5,5′-tetramethylbenzidine substrate into its corresponding blue colour product in the presence of hydrogen peroxide. Three different DNA immobilisation configurations were tested on the surface of the Fe_3O_4 NPs. The third system was found to be the best owing to the enhanced catalytic activity inhibition and subsequent signal suppression arising from the simultaneous use of a split DNAzyme and a specific-binding aptamer, and a high coupling affinity of DNA molecules.[119] The superior properties of system 3 was confirmed by the sensitivity of only 12 CFU/mL obtained. As the DNA-nanozyme encountered the bacteria, there was a colour change from blue to colourless. The degree at which the blue colouration fade was found to directly correlate to the increase in bacterial concentration. Furthermore, Liu and coworkers designed a bovine serum albumin (BSA)-templated Co_3O_4 nanoflower functionalised by self-assembly with an *S. Aureus* specific fusion major coat protein pVIII which was isolated from the *S. Aureus*-specific phage AQTFLGEQD. This nanocomposite, Co_3O_4 MNE@fusion-pVIII, possessed both magnetic properties and peroxidase-like activity which allowed the magnetic separation of Co_3O_4 MNE@fusion-pVIII@*S. Aureus* complexes from unbound bacteria and nanocomposites alike and generation of a colour change from colour to blue in the presence of the substrate, namely diammonium salt of 2,2′-azino-bis(3-ethylbenzo-thiazoline-6-sulfonic acid) (ABTS). Specific targeting and capture of *S. Aureus* was also made possible *via* the surface phage protein.[120] An impressive LOD of 8 CFU/mL was obtained and this was found to be the result of using sensitive nanozymes in combination with the phage fusion protein which provided enhanced affinity of the nanocomposite to the bacteria.

Even though colourimetric biosensors rely mostly on visual changes, very low detection limits have been reported in 2020, hence showing their increasing reliability as a detection technique. The best detection limit for colour-based detection platform using gold NPs was reported in 2020 by Amin and coworkers and was found to be 4 CFU/mL. Two fiber glass strips were each functionalised with gold nanoclusters (AuNCs) and anti- *E. Coli* O157:H7 conjugated AuNPs (AuNPs-anti- *E.Coli*) and then placed in a polypropylene microtube. Owing to the ability of AuNPs to quench the fluorescence of AuNCs by the FRET mechanism, the latter was used as the sensing photoluminescence probes

(energy donors) while the AuNPs-anti- *E.Coli* was used as the quencher label (energy acceptors) to form an ON/OFF fluorescent signal based on the presence or absence of *E. Coli*, respectively as shown in Figure 8A. Thus, in the presence of the bacteria, the approach of AuNCs was hindered as the antibody functionalised AuNPs bonded to the bacteria, thereby restoring the fluorescence. The colour change was then quantified after the assay using a smartphone under UV-LED; there was an increase in fluorescence as the bacterial concentration was increased as illustrated in Figure 8B. The high sensitivity observed with this platform was attributed to the optimised concentrations of AuNPs, AuNCs, and antibodies used.[121] A better LOD of 2.4 CFU/mL was obtained by Sadsri *et al* using *V. Parahaemolyticus* aptamer-functionalised AuNPs as the signal detector.[122] However, they incorporated *V. Parahaemolyticus* aptamer-functionalised magnetic NPs in their system to create a sandwich assay. This allowed for effective capture of the bacteria and their subsequent magnetic separation, hence triggering fading of the colour of the solution. The use of magnetic NPs and a sandwich design was found to positively influence the sensitivity of the device. A more recent example by Yang *et al*. described a stochastic DNA dual-walker-based colourimetric biosensor for *MRSA* detection.[123] The assay involved mixing thiol-tagged oligonucleotide-functionalised AuNPs, exonuclease III (Exo III) and polymer containing aptamers and walking strands with the bacterial sample (Figure 8C). Upon encountering bacteria, the aptamers (black strands) preferentially bonded to them, simultaneously releasing the red and blue walking strands. These were able to autonomously follow on the AuNP-based 3D track as they were propelled by the Exo III which consumed the thiol-tagged oligonucleotide probes. Aggregation of the probes was then triggered owing to the repeated cycles of hybridisation and digestion of the walking strands with the probes. This process, in turn, produced a colour change from red to blue and was characterised by a decrease in the absorption intensity at 520 nm at the bacterial concentration increased (Figure 8D). An LOD of 1 CFU/mL and a high specificity for *MRSA* was observed.[123]

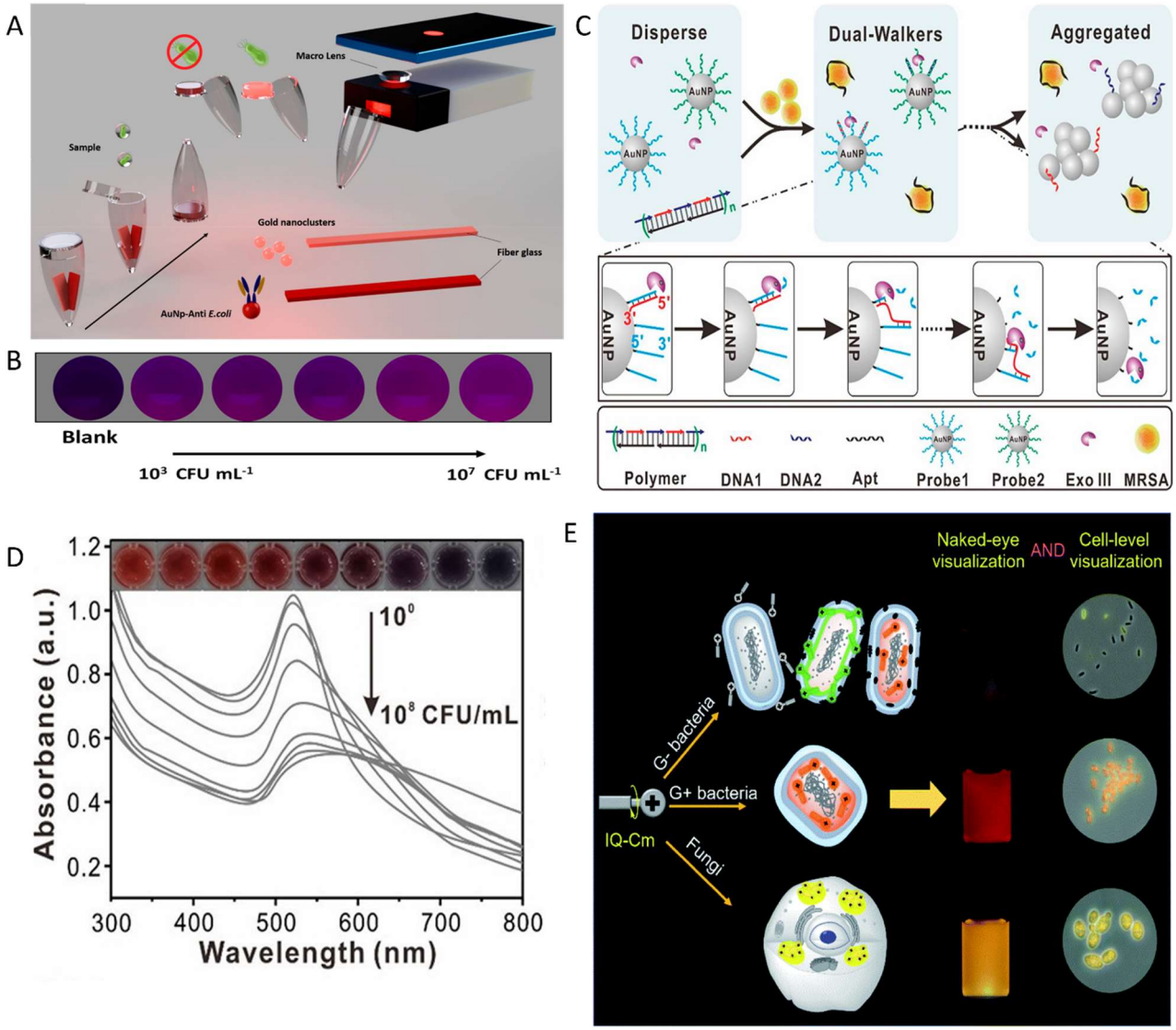

Figure 8: A. Schematic representation of the 'Lab in a tube' design; B. Colour change arising from the increase in bacterial concentration.[121] (Reproduced from reference [121] with permission. Copyright 2020 ACS); C. Schematic diagram showing the stochastic dual walkers for colourimetric bacterial detection; D. Variation in absorbance intensity with bacterial concentrations and the corresponding calibration curve.[123] (Reproduced from reference [123] with permission. Copyright 2020 ACS); E. Schematic diagram showing the ability of the IQ-Cm AIEgen to target three different microorganisms.[124] (Reproduced from reference [124] with permission. Copyright 2020 RSC)

Apart from improved device sensitivity, another application of colourimetric bacterial sensing was presented by Zhou and coworkers whereby three pathogens were simultaneously identified with a microenvironment-sensitive aggregation-induced emission luminogen (AIEgen) called IQ–Cm. The structure of IQ-Cm consisted of a diphenyl isoquinolinium (IQ) unit, a coumarin-derived (Cm) moiety and a phenyl linker, each capable of binding to specific bacterial sites and sensing the surrounding microenvironment. Thus, these bioactive molecules were able to produce different

fluorescence emissions in response to the selective interactions with the microorganisms. From their studies, *E. Coli*, *S. Aureus* and *Candida Albicans* (*C. Albicans*) showed weak pink, bright orange-red and yellow fluorescence, respectively, as illustrated in Figure 8E.[124] This platform boasted several benefits such as ability to differentiate between gram-positive and gram-negative bacteria owing to the different colour changes triggered.

3.3. Mechanical Biosensors

Most of these sensors work by applying a mechanical force to a deformable device, usually a cantilever, which is then converted into a measurable displacement. In mechanical biosensing the cantilever is designed to be highly sensitive to the target analyte.[125] Out of the different types of mechanical biosensors available, surface stress and dynamic mode biosensors are the most common. The former uses the surface stress to cause a deflection of the cantilever.[125] This stress is often caused by electrostatic repulsion or attraction, steric interactions, hydration, and entropic effects which occurs when the target analyte binds to the cantilever. The extent of deflection is then recorded using laser beam reflection or electrical readouts.[126] Dynamic mode biosensors are non-quasistatic and oscillate with a resonant frequency. Upon binding of the analyte, there is a subsequent oscillating frequency change which can be then recorded for analysis.[125, 127]

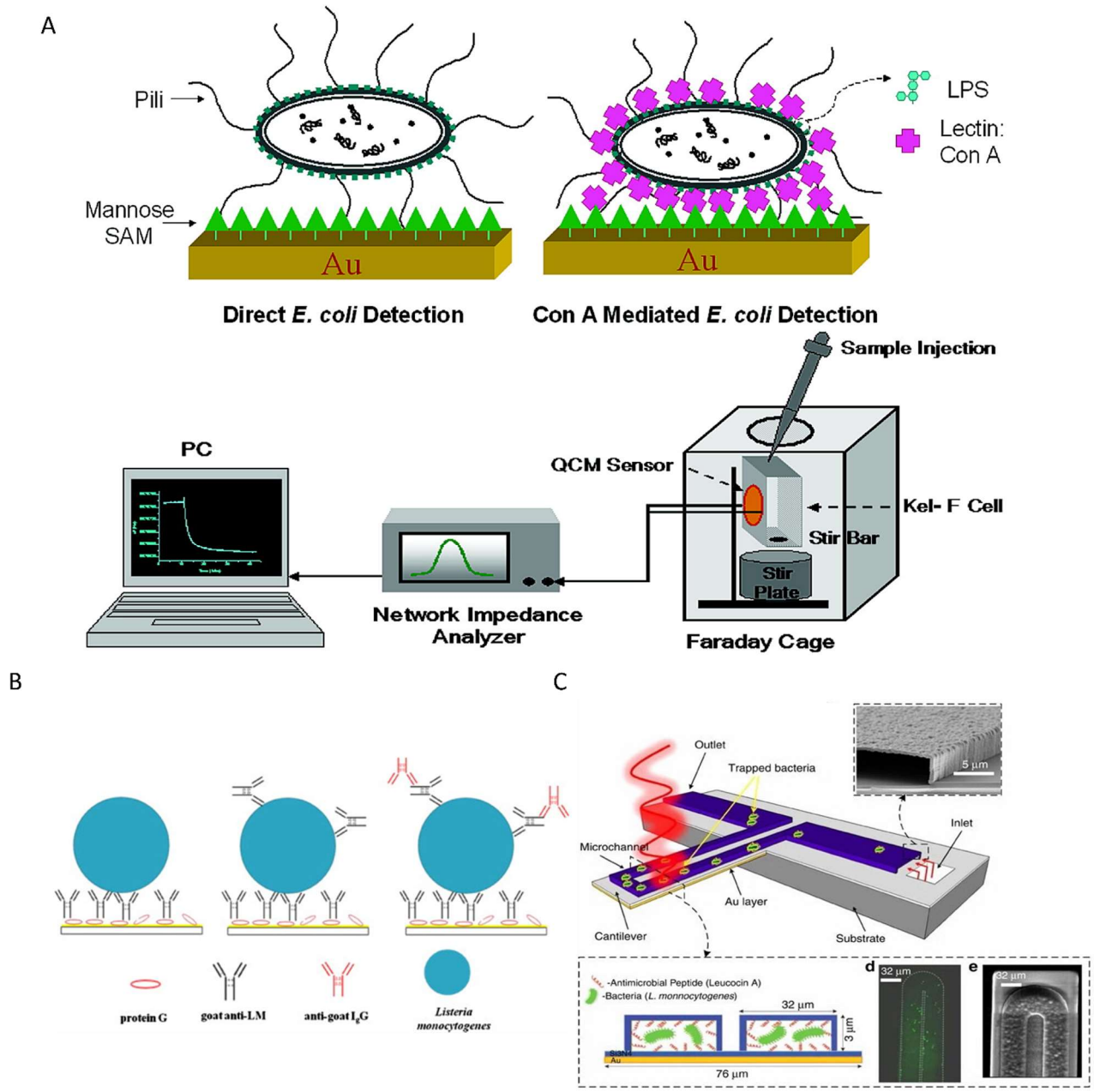

Figure 9: A. Schematic showing the QCM platform designed for *E. Coli* detection.[128] (Reproduced from reference [128] with permission. Copyright 2007 ACS); B. Secondary and tertiary antibody binding design.[129] (Reproduced from reference [129] with permission. Copyright 2013 Elsevier); C. Bimetallic cantilever system proposed by Etayash *et al*.[131] (Reproduced from reference [131] with permission. Copyright 2016 Springer Nature)

In most cases, the surface of the cantilever is functionalised to attract and trap bacteria efficiently. Thus, a dynamic mode gold quartz crystal microbalance (QCM) – a mass balance which can detect very small changes in mass per unit area – sensor system was reported by Shen and coworkers in 2007, where its surface was functionalised with mannose receptors for specific binding of *E. Coli W1485* via the type I fimbriae (Figure 9A).[128] The QCM sensor proposed circumvented

the issues associated with the non-rigid nature of bacterial cells. Thus, the rigid QCM sensor surface was functionalised with mannose receptors. Moreover, concanavalin A (Con A) attached to the surface O-antigen glucose receptor of *E. Coli* was used to increase the binding efficiency of the bacteria to the surface of the mannose decorated sensor and hence, imparted rigidity to the system. Marked improvement in the rigidity of the QCM mass sensor implied that the variation of the mass with the resonant QCM frequency was free of damping action. This modification led to a frequency enhancement from ~100 to ~230 Hz of the electrode connected to the QCM sensor at a concentration 7.5×10^7 CFU/mL with the lowest LOD reaching 7.5×10^2 CFU/mL.[128] A label-free piezoelectric cantilever sensor system was developed by Sharma and Mutharasan to detect *L. Monocytogenes* bacteria which is known to cause febrile gastroenteritis, perinatal and systemic infections. It was made of a lead-zirconate–titanate (PZT) strip which was embedded into epoxy to create an anchor on one side while the other side was free to move. Protein G was first bound to the surface and then coated with polyclonal goat anti- *L. Monocytogenes* (anti-*LM*) which led to adhesion of the bacteria, which resulted in a frequency drop. Upon addition of more anti- *L. Monocytogenes*, a sandwich structure was obtained as they bonded to the exposed surface of the bacteria, thereby leading to a further decrease in frequency from 180 to 83 Hz. The introduction of a tertiary antibody layer of anti- protein G on the secondary anti- *LM* led to further amplification of the signal (Figure 9B). With the use of the third antibody layer, an LOD of 100 CFU/mL was obtained.[129] As the bacterial concentration increased, higher frequencies were recorded during the experiments.

It was stipulated that the sensitivity of QCM sensing platforms can be improved by using crystals with high resonant frequencies or operated at higher harmonics which is in line with the Sauerbrey equation driving QCM technology. Building on the interaction of *E. Coli* with mannose receptors studied by Shen and colleagues, a more recent publication by Ma *et al*. proposed a detection system based on the mechanical properties of a conductive quinone-carbohydrate functionalised polythiophene surface. Analysis of their results revealed a considerably improved and very low LOD of 50 bacterial cells/mL, with a widened logarithmic range of detection for the Con A mediated

mannose binding.[130] An improvement to the basic cantilever design was recently reported by Etayash and colleagues to overcome the drawbacks of conventional cantilever measurements. They designed a gold-coated silicon nitride bimaterial cantilever (BMC) which was interfaced with a microfluidic system as illustrated in Figure 9C.[131] *L. Monocytogenes* bacteria were loaded on the anti-*L. Monocytogenes* or antimicrobial peptide (AMP) decorated BMC and the heat generated as a result of the mismatched coefficients between the silicon nitride and gold led to deflection of the cantilever. Irradiation of the BMC led to further heat production and cantilever deflection. Bending of the functionalised BMC was found to increase with increasing bacterial concentration. A remarkable sensor sensitivity of 1 cell per μL were observed as the semi-selective nature of the AMP from class IIa bacteriocins and the specific properties of mAbs allowed effective capture of the bacteria.[131]

3.4. Microbe-based Biosensors

Microbe-based biosensors have emerged whereby microbial species can be directly immobilised on a surface to form the sensing element and is in contact with the transducer. Thus, they have been integrated with a range of transducing elements for the design of bacteria-based biosensing platforms.[132] A review was published by Park *et al*. where the benefits of incorporating whole cells in detection systems over the use of proteins and antibodies were highlighted. These include low cost, stability, easy culturing with no purification steps required, and good sensitivity.[133] A case in point is the publication by Zurier and colleagues where a phage-based magnetic nanobots were designed to detect *E. Coli* bacteria.[134] A luminescent reporter bacteriophage (T4) was created by amber suppression and then a small outer capsid (SOC) protein was incorporated such that it endowed alkyne functionality to the bacteriophage (T4). Furthermore, azide-functionalised magnetic NPs were conjugated to this bacteriophage. Upon addition to a mixture of different bacteria, the nanobots were able to specifically bind to *E. Coli*. This bacteria-nanobot complex was then collected using a magnet and excess volume removed. These harvested phages were then vacuum filtered to immobilise the luminescent reporter enzyme fusion to the cellulose filter (Nluc cellulose-binding module (Nluc

CBM)). The subsequent luminescence is then measured to detect the presence of *E. Coli* (Figure 10A). A good sensitivity of less than 10 CFU/mL was obtained and was dedicated to the synergistic use of the different components, including the bacteriophage, SOC and magnetic NPs.

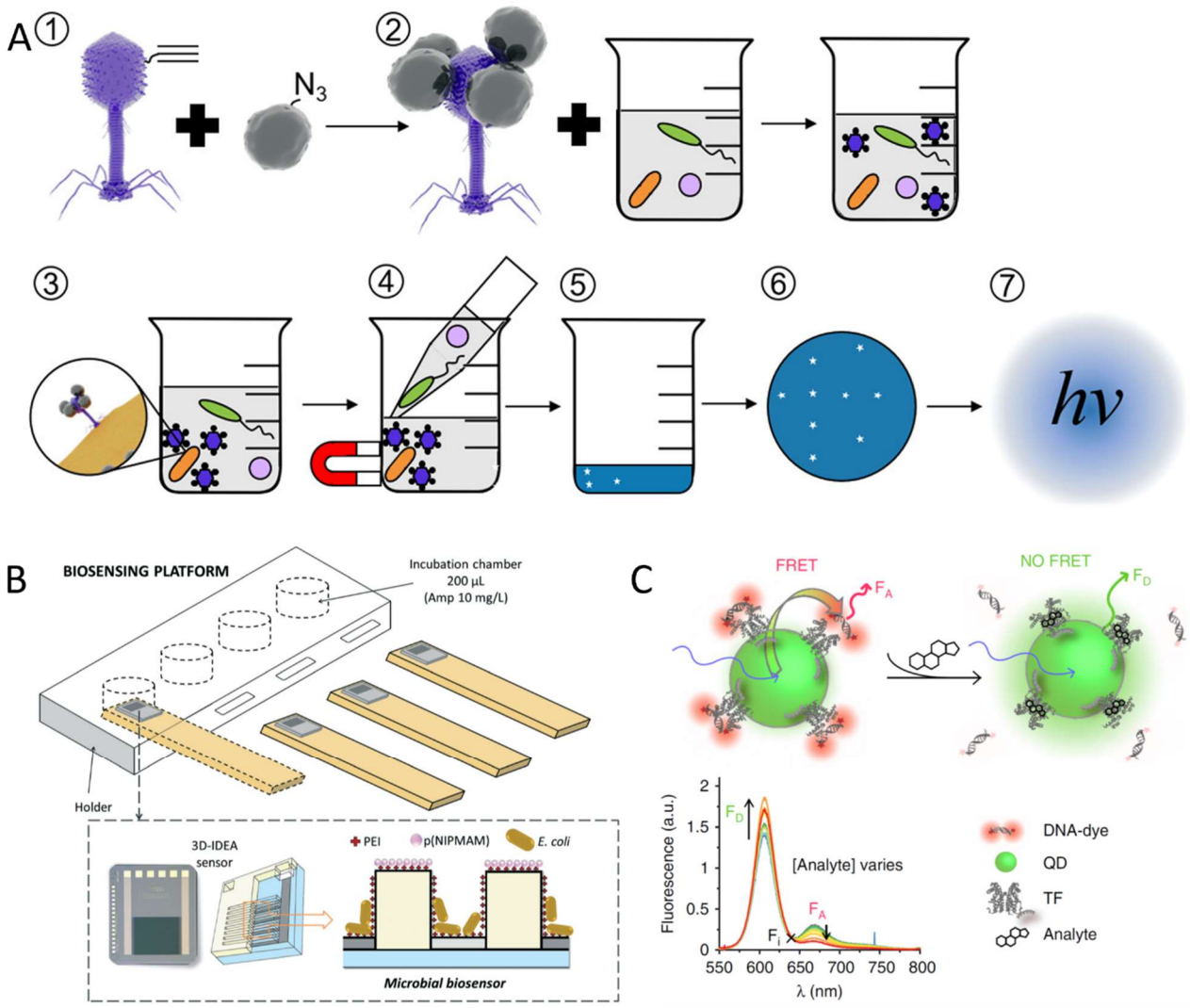

Figure 10: A. Schematic representation of E. Coli detection via T4 phage (1) Conjugation of alkynylated T4 Nluc CBM phage to the azide coated MNP (2) Resulting magnetic phage-based nanobot added to a mixture of bacteria (3) magnetic phage-based nanobot binds to E. Coli (orange) (4) beads containing phage and E. Coli are collected by magnet (5) Infection cycle of T4 phages is completed and Nluc CBM released into the solution (6) sample is filtered on cellulose (7) luminescence arising from T4 phage is measured.[134] (Reproduced from reference [134] with permission. Copyright 2020 ACS); B. Impedance sensing platform by Brosel-Oliu and coworkers.[138] (Reproduced from reference [138] with permission. Copyright 2019 RSC); C. FRET process in the detection of progesterone.[139] (Reproduced from reference [139] with permission. Copyright 2020 Springer Nature)

While detection of bacteria remains a priority, their subsequent response to antibiotics and mechanism of resistance development is also crucial. As described in the publication by Leonard *et*

al, the detection of bacteria is followed by prescription of antibiotics which is, in turn, determined by antimicrobial susceptibility testing (AST). This helps calculate the minimum inhibitory concentration (MIC) of the antibiotic against the detected bacterial species. Current commercially available AST techniques include agar dilution, broth microdilution, disk diffusion, live/dead staining, PCR, matrix-assisted laser desorption/ionisation-time-of-flight mass spectrometry (MALDI-TOF MS), VITEK 2, PhenoTest BC Kit amongst others. While being effective, they still suffer from long turnaround times ranging from 2 – 18 h.[136] In line with this, a range of electrochemical and optical microbe-based sensors have been introduced for application in AST as well as the detection of biomarkers characteristic of other diseases as summarised by Su and coworkers.[137] An instance is the impedimetric microbe-based sensor proposed by Brosel-Oliu and coworkers, which was capable of detecting the antibiotic, ampicillin. The system was made of a three-dimensional interdigitated electrode arrays (3D-IDEA) on a silicon wafer which was functionalised by polyethyleneimine. A poly(N-isopropylmethacrylamide) (p(NIPMAM)) microgel was then deposited on the surface by microcontact printing and finally functionalised with *E. Coli* as illustrated in Figure 10B. An optimum *E. Coli* concentration of 10^7 CFU/mL in potassium chloride (KCl) solution and 20 min incubation time was chosen for the study. The bacterial sample was placed in the incubation chamber and changes in the *E. Coli* cell structure in response to addition of the antibiotic, ampicillin were measured by the 3D sensors that were inserted into the holder chamber prior to bacterial loading.[138] Contact of the ampicillin with *E. Coli* led to a disruption and release of the conductive contents of the cells into the surrounding KCl solution. This, in turn led to an increase in the solution's conductivity and decrease in resistance which was recorded by the sensor. However, when a resistant strain of *E. Coli.* was used, no obvious change in impedance was observed. In a 2020 publication by Grazon *et al*., an optical microbe-based biosensor which makes use of a microbial allosteric transcription factor (aTF) – a regulatory protein capable of changing their affinity for specific DNA sequences upon binding to specific molecules and thus, causing environmental changes in bacterial gene expression – to detect progesterone was unveiled.[139, 140] An aTF was functionalised on the surface of

CdSe/CdS/ZnS QDs to yield a (QD-aTF-FRET) biosensing platform (Figure 10C).The aTF used in this case was capable of affinity recognition and could undergo reversible analyte binding to their cognate DNA sites. FRET was used to obtain a fluorescence signal upon formation of the aTF-DNA complex. The QD FRET donors were functionalised with TFs and a DNA oligonucleotide (SRTF1) while the TF binding site was bound to a FRET acceptor (Cyanine, Cy5 dye). Since the binding of the TF to the hormone progesterone changed the TF-DNA binding, there was a change in the fluorescence. Thus, the acceptor emission intensity was triggered as the aTFs were bound to the DNA probe, leading to a close proximity of FRET donors and acceptors.[139] As shown in Figure 10C, there was a dose-dependent decrease in the sensor response as the progesterone concentration was increased. By reducing the TFs to QD ratio to 1:1 while maintaining an oligonucleotides to QD-TF ratio of 18:1, the LOD was improved down to a progesterone concentration of 15 nM.

3.5. Biosensors for the Detection of Bacterial Biomarkers

Aside from the detection of whole bacterial species and the use of bacteria for the detection of antibiotics or biological hormones, identifying biomarkers such as bacterial cell components, enzymes, or bacteriophages that are specifically expressed by bacteria can be useful in further confirming the presence of bacteria and informing therapeutic decisions. A review of literature revealed that electrochemical and optical biosensing mechanisms underpin the majority of these biosensors with a strong focus on surface functionalisation and capture of target molecules due to their excellent sensitivity and specificity levels as described earlier. Taking advantage of substrates like AAO and pSi, which were discussed in Sections 3.1 and 3.2, a number of publications over the last 5 years have further demonstrated their versatility in biosensor design for the detection of bacterial biomarkers. A case in point is the optical biosensor in the publication by Krismastuti *et al.* They developed a porous anodised AAO coated with poly(sodium-4-styrenesulfonate) (PSS) and poly-L-lysine (PLL) using a layer-by-layer technique. In the presence of proteinase K, a surrogate of *P. Aeruginosa*, the peptide bonds in the PLL are cleaved, thereby disrupting the LBL coating.[141] This disruption was quantified by the reduction in refractive index of the coating and finally correlated

to the concentration of proteinase K. The system expressed an LOD down to 0.1 mg/mL proteinase K. The popularity of pSi for this biosensing application was evident from the most recent publications. For example, in a paper, a synthetic antimicrobial peptide known as K-$[C_{12}K]_7$ or K-$7\alpha_{12}$ with specific binding ability to *E. Coli* cell components was used to functionalise the surface of a pSi film. The subsequent changes in reflectivity upon capture of bacterial fragments were monitored. This optical behaviour was found to vary linearly with the bacterial lysate concentration and the authors reported an LOD of 10^3 CFU/mL. Thus, this system allowed detection of *E. Coli* via detection of the bacterial cell lysis by-products.[142] Other pSi-based biosensing platforms reported are summarised in Table 1 below. In all these cases, the pSi membrane surface was functionalised with molecules that have affinities to the target biomarkers expressed by the specific bacteria.

Table 1: Functionalised pSi films for the detection of bacteria-specific biomarkers

Publication	**Biosensing technique**	**pSi surface functionalisation**	**Targeted biomarker**	**Limit of detection (LOD)**
Reta *et al*., 2016[143]	Electrochemical - DPV	Anti- MS2 bacteriophage (monoclonal antibody)	MS2 bacteriophage specific to *E. Coli*	6 plaque-forming unit (pfu)/mL
Krismastuti *et al.,* 2016[144]	Optical - FRET	Sortase A (SrtA) fluorogenic peptide substrate	SrtA - bacterial enzyme present in cell membrane protein of *S. Aureus*	(8×10^{-14}) M
Tücking *et al*., 2018[145]	Electrochemical - DPV	Enzyme-responsive hyaluronic acid methacrylate/ polyethylene glycol diacrylate polymer coating	Enzyme hyaluronidase (hyal) secreted by *S. Aureus*	0.1mg/mL
Reta *et al*., 2019[146]	Electrochemical - DPV	Antimicrobial peptide, polymyxin B	Lipopolysaccharides (LPS) found on two Gram-negative bacteria, *E. Coli* and *P. Aeruginosa*	LPS: 1.8 ng/mL 1 CFU/mL
Antunez *et al*., 2021[147]	Optical	Thermoresponsive N-isopropylacrylamide (NIPAm) decorated with lactose/ GM1 oligosaccharide recognition motifs	*E. Coli* heat-labile enterotoxin (LTB)	0.135 μM

3.6. Discussion

In the above sections, we have described the mechanisms and applications of a range of different types of biosensors for bacterial detection. Each approach has its merit and disadvantages and each is suitable for certain applications. In this section, we will discuss in more detail about the advantages and limitations of these different types of biosensors. Without doubt, impedimetric sensors and their derivatives (conductometric and capacitive biosensors) are highly versatile and sensitive bacterial detection systems as evidenced by the low detection limits reported earlier. Also, since they are passive detection methods, they do not suffer from interference and have relative low signal to noise ratio as detailed by Zhang and coworkers.[148] Another benefit is their low turnaround time with a maximum of 2 h which was reported by Tan *et al* and Zhang *et al*. Even lower detection times of 45, 40, 30, 10, and 5 min were also demonstrated by the other sensing platforms.[47, 52, 55, 57, 149] The ability of impedance-based biosensors to target specific bacteria also makes them ideal candidates for bacterial detection, for instance, there was an impedance change caused by high specificity to *E. Coli*; no noticeable change in the impedance was observed when *S. Aureus* was incubated on the anti-*E. Coli* membrane in the paper by Tan *et al*. Similarly, Pal *et al*. and Santos *et al*. also demonstrated the specificity of their system to *S. Typhi* and *E. Coli*. Finally, most impedance sensors as well as conductometric and capacitive sensors are label free – do not require prior labelling of bacterial test samples or any additional probes – and thus can be directly added to the detection device for analysis.[54, 55]

Besides impedimetric sensing, a benefit enjoyed by capacitive biosensors in particular is their ability to run non-stop for hours until the target analyte is added or recognised.[150] Furthermore, several design features have been progressively improved over the years to optimise the performance of these sensors as outlined in the publications discussed in Section 3.1. An example is switching to nanoporous alumina surfaces from conventional nanoporous membranes which are usually formed on silicon surfaces and thus, suffer from instability and low binding efficiency of antibodies to the membrane.[151] In the publication by Tan *et al*., the membrane fabrication process was simplified and

a nanoporous alumina surface was used which conferred improved stability and attachment of antibodies.[43] In a paper by Rajeev and coworkers, the benefits associated with the use of nanoporous alumina-based biosensors were further highlighted, for instance, high surface-to-volume ratio, biocompatibility, ease of biofunctionalisation, unique optical and electrochemical properties, and simple and cheap fabrication by electrochemical anodisation.[152] Also, instead of using an unstable and less specific monolayer detection system, sandwich-based assays have been shown to provide exceptional sensitivity as they ensure proper immobilisation of bacteria for more accurate and stable electrical impedance measurements.[55]

Like most systems, there are some issues associated with the use of impedimetric sensors despite their high sensitivity. Factors such as electrical properties of the buffer, layout of the patterned electrodes, choice of different parameters such as voltage and frequency applied and output signals have been found to influence the detection abilities of sensors. While the use of redox probes as mediators for EIS impedimetric measurements can improve the proximity of the bacteria to the sensing platform, there is a trade-off with sensitivity as it is limited by the mass transfer rate of the probe.[37] Thus, a considerable effort has to be initially applied to identify the optimum conditions for operating the device.[47] Furthermore, the impedance-based detection of bacteria in complex media comprising two or more strains is still a challenge with label-free detection platforms, thereby limiting their applications.[52, 153] For those sensors using nanoporous membranes, the capture efficiency of bacteria by antibodies may be hindered owing to size differences between the bacteria and the nanopores. Furthermore, the binding efficiency of bacteria to antibodies can be affected by many factors such as random orientation, and binding affinity. This can eventually lead to random capture and inefficient bacterial coverage. As evidenced by Tan *et al*., the fluorescence images of the FITC-labelled antibodies showed that bacteria did not completely cover the alumina-PDMS surface (some antibodies did not capture bacteria) and hence, reduced the capture efficiency.[43] Bacterial aggregation at the electrode when using high concentrations could be another reason for the reduced efficiency. Reproducibility at low bacterial concentrations is another issue plaguing the successful

operation of these devices. Pal *et al*., for instance, were able to detect bacteria down to 10 CFU/mL with their sensor. However, the impedance measurements were unstable and could not be repeated, hence justifying the threshold of 100 CFU/mL that was reported in their publication.

While being low cost, easy to fabricate and rapid, potentiometric and amperometric sensors can also feature high sensitivity and low detection times as further illustrated in Table 2 below.[35] The high sensitivity of these sensors at low sample volumes is often attributed to the dependence of the output signals on the logarithm of bacterial concentration, rather than the actual concentration as well as the small surface areas provided by the small sized electrodes.[154, 155] Furthermore, the use of a constant potential ensures that the charging current –current required to attain that constant potential value– is nearly negligible and thus, reduces any background signal during measurements.[37]

Table 2: Summary of the bacterial potentiometric and amperometric biosensor performances reported in this review

Reference	**Bacterial Species**	**Limit of Detection (LOD) / (CFU/mL)**	**Detection Time /min**
Hernández *et al*., 2014[73]	*S. Aureus*	1	1-2
Ishiki *et al*., 2018[71]	*E. Coli K-12 strain*	28	60
Altintas *et al*., 2018[68]	*E. Coli*	50	35
Jijie *et al*., 2018[75]	*E. Coli*	10	30
Wang *et al*., 2019[69]	*V. Parahaemolyticus*	33	60
Wang *et al*., 2019[74]	*E. Coli* *L. Monocytogenes* *S. Typhi*	11	20
Nemr *et al*., 2019[67]	*MRSA*	845	240
Farooq *et al*., 2020[77]	*S. Aureus*	3 (PBS) 5 (Milk)	30
Pankratov et al., 2020[78]	*E. Coli*	1 cell/mL	60-90

Yet, there are some drawbacks potentially limiting the successful clinical application of these electrochemical biosensors, for instance, a reduction in signal variability at low concentrations and further optimisation of the sensitivity of these sensors may require additional device design

modifications, thereby raising the manufacturing costs. A case in point is the G-FET sensor designed by Kumar *et al.* whose design, PDMS well size, and the electric-field application process may need to be altered at higher costs and time scales. Another case in point is the dependence of the current on temperature in voltammetric biosensing, which consequently requires constant monitoring of the temperature associated with the detection system for more reliable results.[37] Impedimetric, potentiometric, and amperometric biosensors all use electrical currents as input signals with the only difference being the nature (DC or AC) of the current applied.[35, 59] In comparison to potentiometric sensors, amperometric sensors are not very selective as the faradaic current originating from the components in the sample solution have a standard potential which is often lower than the operating potential of the sensor.[154] Thus, they are often used in conjunction with other biological recognition elements to confer increased bacterial detection specificity to the system. AC-based biosensors have been found to be more effective and useful over DC-based ones for use in clinics. This is because voltammetric sensors are less specific as they can respond to false positives from other consituents of the sample having identical redox properties.[35] Also, the use of DC currents could possibly damage the recognition elements usually immobilised on biosensor surfaces, thereby truncating the measured output signal.[59]

Similar to the detection performance of electrochemical biosensors, optical biosensors are able to exhibit high sensitivities even down to 1 bacterial cell/mL as well as rapid testing times, ranging from less than 1 min to a maximum of 2 h.[98] Furthermore, the use of smartphones for fluorescence-based detection is a highly promising strategy for the development of more simple, cheap, and robust POC bacterial biosensing systems. Also, the use of highly fluorescent biorecognition elements, for instance, the use of curcumin in the acid-responsive sensor system proposed by Huang *et al*. is exceptionally useful, easier to work with and cheaper than most fluorescent dyes. In addition to curcumin having a strong inherent absorbance and fluorescence intensity at concentration as low as 1 μM, the use of curcumin in acetic acid greatly improved the stability of the system.[92]. The use of DNA technology with optical sensors has also been shown to

demonstrate unrivalled sensitivity down to the pM scale and high specificity. However, optical sensors using fluorescent labels often suffer from increased costs associated with developing the sensor platform on top of the fabrication process which, in turn, requires more complex synthesis protocols. The analytical instruments used to measure and quantify optical signals in some applications may introduce further costs to the system design.[95] Another drawback of these sensors is potential interference from the bacterial media which may lead to erroneous signal detection. Signal emission overlap is also a problem in cases where multiple bacteria have to be detected and thus, are often unsuitable for identification of different bacteria in a single sample.[156] Furthermore, despite the very high sensitivity, the SERS technique for bacterial quantitative analysis is limiting, because SERS substrates are often unstable, non-uniform, and difficult to produce high reproducibility of SERS measurements. The primary advantage of colourimetric sensors is their simplicity, inexpensive nature and ease of detection without the need for trained professionals and complex equipment.[157] It was estimated to be one quarter to one third of the total cost incurred by other diagnostic methods per colourimetric test.[158] In addition, the testing time is very quick, up to a maximum of 1 h for most of the above-described colourimetric biosensors. While they are mostly used to provide a visual and quantitative representation of the bacterial concentration, colourimetric sensors can be combined with other electrochemical detection methods to increase the sensitivity of the system as confirmed by the low detection limits reported, ranging from 1 to a maximum of 300 CFU/mL which is a highly prized quality for detection devices. Aside from the obvious direct detection offered by colourimetric biosensors, they are associated with low sensitivity compared to other types of biosensors and even traditional detection methods unless they are used in combination with other techniques or heavily modified with biorecognition elements. Owing to their inherent low sensitivity, these sensors often require large sample volumes to be able to produce a reliable readout which may not be always possible in some cases.[158] Moreover, since the perception of colour by users are arbitrary and unique to each individual, results from these sensors may not be entirely reproducible. Thus, there is a need to use colour analysis software such as the smartphone app designed by Mou *et al*. to produce an

accurate and quantifiable representation of the colour change, which may increase the operating costs.[113]

Mechanical biosensors possess similar properties to impedimetric biosensors. They exhibit high sensitivity and selectivity, quick turnaround times while being label-free.[125] This was confirmed by the low detection limits observed in Section 3.4 with detection times being approximately 1- 2 h. Furthermore, the new improved cantilever (BMC) design by Etayash *et al*. allowed multimodal real-time detection of liquid-phase analytes with enhanced response time, selectivity, sensitivity, and increased reliability, which could be the future of mechanical biosensing of bacteria. Another benefit of the BMC is its low cost and potential for large-scale production, hence making them highly suited for biosensor applications. Yet, the use of cantilevers for detection is often associated with liquid damping. As a result, accurate measurement of the change in frequency shift in a liquid environment is hampered. Furthermore, the signal-to-noise ratio increases as the laminar liquid flow inhibits the efficient capture of target bacteria and thus, disturbs the response of the cantilever. These limitations were mitigated by the BMC which allowed measurements of three orthogonal signals —adsorbed mass, adsorption stress and mid-infrared spectroscopy— of the adsorbates as described by Etayash *et al*..[127] Finally, most cantilever-based systems are operated in air, rather than physiological media and thus, may not provide accurate sensing.[159]

Microbe-based sensors possess fairly good sensitivity and selectivity which can be further improved by concentrating bacteria on the electrode surface as well as combination with biomaterials such as microgels as demonstrated in Section 3.5.[138] [160] The fact that changes in structural and functional integrity of specific bacterial cells in response to the analyte can be exploited imparts versatility to these biosensing platforms.[161] Thus, different types of bacteria may be used to detect a diverse range of target analytes. Nevertheless, the design of microbe-based sensors requires high level microbiology and genetic engineering to screen a range of bacterial species to identify and develop an appropriate bacterial strain for the desired sensing application. In cases where bacteria are immobilised on the surface of biomaterials such as hydrogels, it is crucial that their properties such

as protein expression are not altered which would otherwise require extra expertise and additional time and cost. This further hampers their mass production ability.[132, 137] Bacteria, as any other biological organism, require specific conditions such as pH and temperature to survive which could limit their application in biosensing. Hence, selecting the bacteria capable of withstanding the experimental conditions is essential to successful microbe-based biosensor design. [132] Finally, batch-to-batch variation in bacterial cell populations may limit the sensitivity.[162]

There is no doubt that each type of biosensing platform has its benefits as well as drawbacks as evidenced earlier in this section. Based on a range of representative research publications, it was demonstrated that increased sensitivity could be achieved by supplementing the design features of these platforms. A prime example is the use of nanomaterials that was found to greatly help in lowering the detection limits while providing bacterial recognition specificity. Further sensitivity was found to be characteristic of biosensors using DNA technology with detection limits down to 1 bacterial cell. Thus, through different technologies or a combination of these techniques, biosensing platform design could be optimised for desired detection applications. The effects of improving the technology used in bacterial detection on the number of viable CFU as summarised in this report is illustrated in Figure 11.

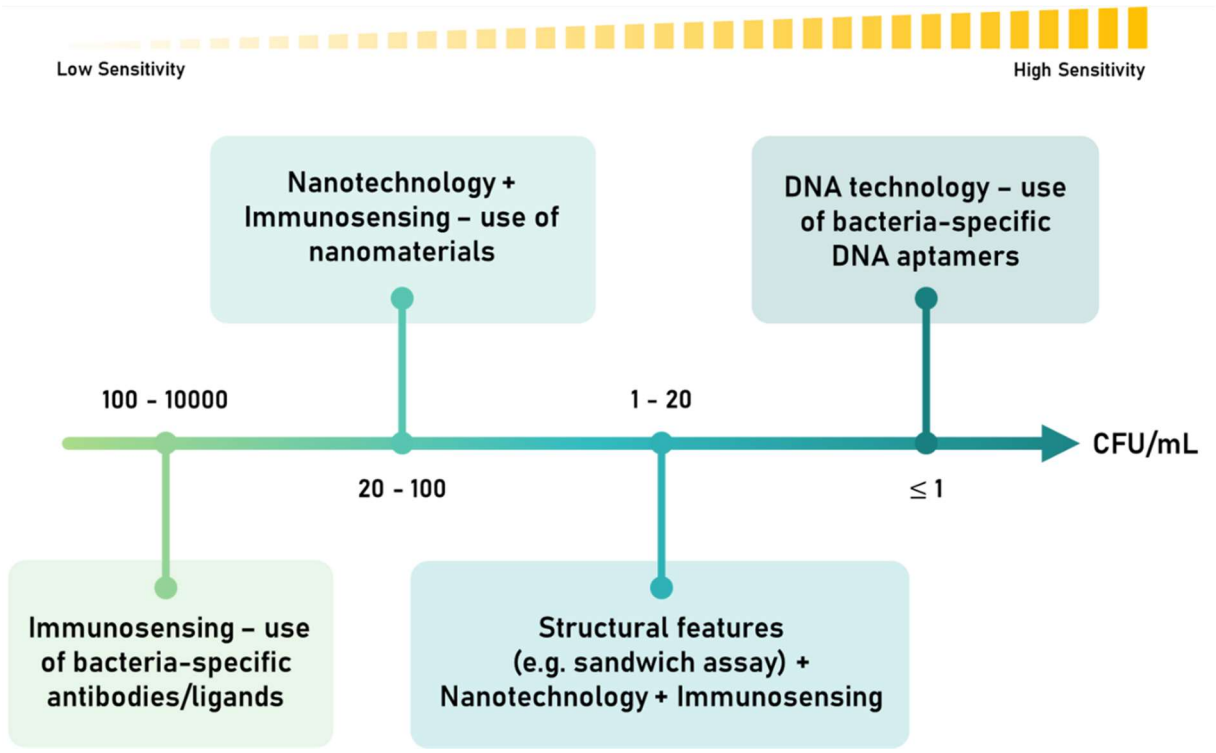

Figure 11: Schematic showing the technological improvements made to bacterial detection platforms for improved sensitivity.

As illustrated, most of these detection platforms demonstrated their ability in differentiating and identifying specific bacteria, some even at low concentrations. Thus, they are highly suited for diagnostic purposes, thereby allowing the correct antibiotic and dosage to be administered to patients. Consequently, the possibility of antibiotic resistance caused by overdose or incorrect therapy could be reduced. However, these platforms do not go further in showing their ability to detect residual bacteria after a course of antibiotics. Even though they may be present at very low or negligible concentrations, it may be useful to further quantify the amount of these bacteria present at infection sites. From an analysis of the publications reported, those biosensing platforms that are capable to detect bacteria between 1 – 100 CFU/mL may be suitable for this application. Results from these detection experiments could be used to further optimise administration of antibiotics to further tackle the recurring issue of antibiotic resistance.

4. Point-of-Care (POC) Detection Systems

4.1. Introduction to Commercially Available POC Devices

One of the great ways of applying the above discussed various types of sensors to applications is to establish POC devices. POC testing is fundamental to the detection and treatment of diseases and its use is fast becoming a staple in most healthcare settings. These systems provide rapid and 'on-site' diagnostic information to healthcare workers for more accurate decision-making in the administration of therapeutics to patients.[163] Thus, they are designed to be fully operational at the site of patient care including hospitals, doctors' offices and even patients' homes.[164, 165] In accordance with a 2003 publication by the World Health organisation, an ideal POC system should follow the 'ASSURED' criteria which translates into the following properties, affordability, sensitivity, specificity, user-friendly, rapid and robust, equipment-free, and deliverable to end-users (Figure 12).[166, 167] Beyond these properties, we believe that POC systems also have to be eco-friendly.

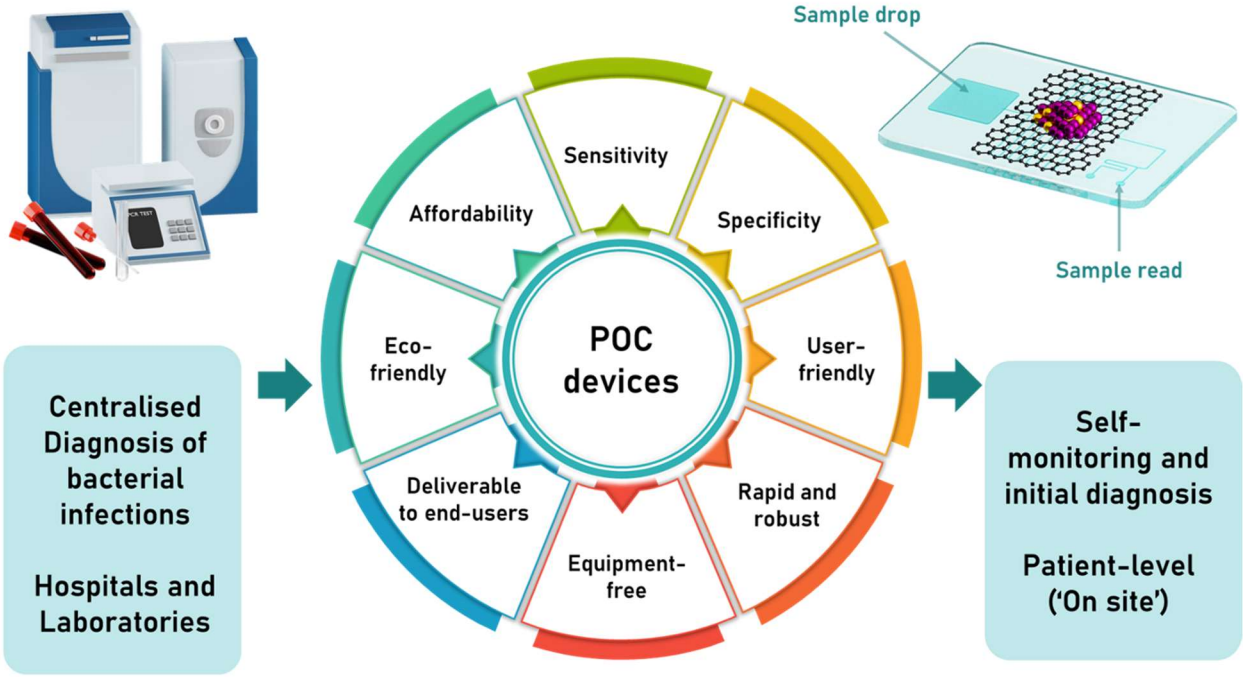

Figure 12: Schematic showing the criteria required for creating the ideal POC device.

The pressing need to curb antibiotic misuse and overdose has led to the development of POC bacterial detection systems for the diagnosis of infection diseases, hence allowing prescription of the correct and most effective antimicrobial therapy to patients. POC testing kits have been devised to detect a diverse range of bacteria responsible for medical conditions such as diarrhoea, meningitis, pneumonia amongst others by using stool, blood, urine, nasal swabs, and sputum from patients.[168]

POC testing kits can be classified into different categories depending on the bacterial screening mechanism involved in their design. A survey of literature revealed that most of the currently commercially available POCs for bacterial detection use nucleic acid amplification technology (NAAT). This technique detects nucleic acid sequences that are specific to certain pathogens and enhances the genetic material in a low sample volume to improve the detection sensitivity.[169] Polymerase chain reaction (PCR) is one of the conventional laboratory-based detection methods that uses NAAT. Thus, these POCs have been devised to achieve similar functions to PCR, but with added benefits such as low LOD, rapidity, and ease of use. A case in point is the cobas® Liat® PCR System developed by Roche Diagnostics which completely automates the PCR process with a 'lab-in-a-tube' design. Its variants include the *Streptococcus Pyogenes* (Group A β-hemolytic Streptococcus, *Strep A*) and *Clostridium Difficile* (*C. Difficile*) nucleic acid tests for detection the onset of pharyngitis and *C. Difficile* infection (CDI), respectively. This design boasts of a 20 min turnover around time and > 90% sensitivity with LOD of 5 – 20 CFU/mL and 90 CFU/swab for *Strep A* and *C. Difficile*, respectively.[170] In addition, Cepheid fabricated the Xpert® MTB/RIF NAAT system for the detection of *M. Tuberculosis* and rifampicin resistance, which is an indicator of the presence of the resistant strains of *M. Tuberculosis*.[171] The effectiveness, low cost and fast detection time (maximum of 2 h) of this design over traditional methods were highlighted in the publication by Lawn and coworkers. Another instance is the AmpliVue™ *C. Difficile* assay —a nucleic acid amplification test to detect diarrhoea— developed by Quidel Corporation which can detect the *C. Difficile* Toxin A gene (tcdA) in stool samples with a reported LOD of 4.2 CFU/assay.[172] Mixing of helicase-dependent amplification (HDA) reagents, with a heat lysed stool sample leads to competitive amplification of the highly conserved fragment of the tcdA DNA sequence. The reaction tube is then placed in a detection tube and the results are displayed as test and the control lines. Based on an evaluation on 200 samples carried out by Deak *et al*., this POC demonstrated a selectivity of 100% and sensitivity of 96% with a total assay time of 73 min.[173] One of the highlighted benefits of AmpliVue™ was its ability to process 24 different samples at the same

time. In a 2020 publication, a highly promising disposable and extremely cheap (0.35 USD) silicon-based all-in-one micro-qPCR POC (Point-of-Need transducer (TriSilix)) was developed by Nunez-Bajo and coworkers for the real-time detection of the bacterial species, *Mycobacterium avium subspecies paratuberculosis* (*M. a. subsp. paratuberculosis*). This detection platform boasted of a detection limit down to a single bacterium within 30 min.[174] Other POCs for the detection of *C. Difficile* described by Deak and colleagues included the Illumigene™ assay which uses a loop-mediated isothermal DNA amplification (LAMP) technology to target a partial DNA fragment of the tcdA in stool samples as well as the Simplexa™ Universal Direct real-time PCR assay which employs fluorescent probes to amplify a conserved region of the toxin B gene (tcdB).[173] Assay times were 68 and 91 min for Illumigene™ and Simplexa™, respectively. The highest sensitivity of 98% was obtained with Simplexa™. In addition to their molecular-based identification principle, the kits exemplified above for *C. Difficile* use a modified version of lateral flow immunoassay (LFIA) for visual detection of the bacteria, similar to the one used in pregnancy tests. In general, this technique makes use of biorecognition elements immobilised on the surface of a substrate, usually a nitrocellulose membrane. The sample to be tested is added to the sample pad and then moves towards the conjugate pad under capillary force. Interaction and binding of the targeted biological species with the biorecognition elements are then qualitatively detected through the reaction membrane which consists of a test and a control line. Building on the success of LFIA owing to their simplicity and fast-action, a protocol for nanoparticle-based LFIA was recently published by Parolo *et al.* which further illustrated their versatility in diagnostic applications.[175] In the above-described cases, the detectors were able to qualitatively indicate the presence or absence of *C. Difficile* after reaction with the testing probes.

Sepsis is another pathogen-associated disease which has ravaged the healthcare industry. It arises from a dysregulation of the immune system response to bacterial infections and is estimated to cause 19.4 million deaths worldwide every year.[176] Thus, early detection of sepsis is crucial to ensure that appropriate treatment are administered to patients on time to prevent fatal organ failure and loss

of life.[177] In the 2018 review published by Reddy Jr., several commercial POCs were explored for the management of sepsis through identification of rogue pathogens. An example is the LightCycler SeptiFast[g] Test MGRADE from Roche diagnostics, which is a real-time PCR test and can detect and identify a wide range of bacterial and fungal DNA simultaneously with an LOD of 30 CFU/mL and a turnaround time of 6 h.[178] Other similar examples include SepsiTest (Molzym Molecular Diagnostics) and IRIDICA BAC BSI (Abbott Diagnostics) which exhibited LOD of 10 – 80 and 39 CFU/mL with a turnaround time of 3 – 4 and 6 h, respectively.[178] Apart from traditional detection techniques, owing to its superior analytical properties such as specificity and sensitivity, nanotechnology has also found its use in the diagnosis of sepsis and bacterial detection in general.[179] Some examples of commercially available sepsis detection nanoplatforms highlighted in the extensive revies by Papafilippou and coworkers include Verigene test (Nanosphere Inc.), TAK-242 (Takeda Global Research & Development Center, Inc) and so on.[177] Yet, it was stressed that the widespread use of nanotechnology in this case is hindered by a number of factors such as feasibility of scale up, long term safety and efficacy of nanomaterials, which necessitates further product testing and development of the sepsis 'nanotools' pipeline.

Another category of bacterial POC systems is based on antigen-antibody interactions. The presence of specific infectious biomarkers in patients can be detected by using the corresponding antibodies.[180, 181] The Afinion™ C-reactive protein (CRP) analyser designed by US-based healthcare company Abbott is a compact and fully automated system which is capable of determining the level of CRP for the rapid diagnosis of lower respiratory tract bacterial infection.[182] It comprises a membrane decorated with anti-human CRP antibodies which reacts to the CRP obtained from a fingerstick sample. The analyser then measures the colour intensity of the sample which is proportional to the amount of CRP. It requires only 1.5 μL of blood sample and has a highly impressive 3-4 min 'drop-to-result' time.[183] Even with an average selectivity of 86%, this device showed a low sensitivity up to a maximum of 55% owing to its colourimetry-based detection.

The success enjoyed by commercial bacterial detection POCs is often attributed to their performance relative to traditional detection methods, but they are still far from being the ideal POC device for the diagnosis of infectious bacteria. A major drawback, as discussed by Shanmugakani and coworkers, is that they are optimised for use on pure cultured bacterial samples, rather than actual samples from patients which might contain a range of different microorganisms.[184] While the DNA amplification techniques described provide high sensitivity, some of these exhibited quite high processing times as evidenced by the POC devices used for sepsis detection. Furthermore, expensive, and complex DNA-based precursor materials are often used during manufacture of the devices, thereby raising their initial procurement costs. The use of some POCs, as in the antigen-antibody ones, is often associated with low clinical sensitivity as they can, at best, provide an accurate qualitative test result.[180]

4.2. Biosensors as POCs for Bacterial Detection

Biosensors integrating nanotechnology, microfluidics and the use of smartphones have been found to possess superior qualities and have caught the interest of clinical scientists and engineers in the last decade with a common ambitious aim to design a near-perfect POC system.[185] In the latest study by Park and coworkers, several user-friendly microfluidic systems were highlighted, for instance, self-operated ones which rely on capillary force, vacuum-driven pressure, or gas-generating chemical reactions for pressure application into the microchannels. Hand-operated microfluidic devices were also described, as they use simple equipment, such as syringes, pipettes or even human power through finger actuation.[186] Thus, these techniques were found to further simplify the multistep sample preparation and injection processes which are currently required for some POC bacterial detection platforms. Other benefits of microfluidics was described by Chen and colleagues which included low sample volumes, automation, and miniaturisation.[187] Aside from using simple microfluidic systems, the use of nanomaterials opens up a wide spectrum of design opportunities owing to their variable size, shape and properties as detailed in the review by Quesada-González and Merkoçi.[188] Alafeef and coworkers also highlighted other benefits of using nanomaterials, for instance, their conductivity,

large surface area to volume ratio, uniformity, and ability of accelerating signal transduction amongst others.[189] The synergistic use of these technologies could result into innovative POCs with unparalleled functional and detection properties. Thus, this novel class of POC biosensors could offer better control of spatial and temporal factors, thereby improving their reliability while being safe, inexpensive, compact, and easy to operate.[166] The proposed and improved designs featuring nanotechnology and microfluidics alike are highly promising as they are more likely to fulfil a crucial property - to provide similar or even better sensitivity and selectivity as conventional laboratory diagnostic techniques.[158]

More recently, there has been a shift in the design of POCs for bacterial detection with the benefits of NAATs being harnessed while integrating them with microfluidic systems, thereby considerably enhancing their sensitivity and decision time, all while requiring a very small sample volume. An example is the "sample-in-multiplex-digital-answer-out" polydimethylsiloxane (PDMS) chip designed by Yin and colleagues which was integrated with multiplex digital recombinase polymerase amplification (ImdRPA). This design could detect 3 different bacterial species within 45 min as shown in Figure 13A while using a circumventing the use of complex pumping equipment.[190] To aid the diagnosis of sepsis, a microfluidic assay capable of measuring changes in the motility and phenotype of native neutrophils from a fingerstick blood sample was constructed by Ellet *et al*. Based on a study carried out on 42 patients, this assay was able to identify those who were suffering from sepsis with a 97% sensitivity and 98% specificity.[191] Another microfluidic-based NAAT platform for the detection of the sepsis-causing bacteria such as *E. Coli*, *S. Epidermidis, and Staphylococcus Saprophyticus (S. Saprophyticus*) was described by Fang *et al.* with detection limits down to 5 CFU/mL.[192]

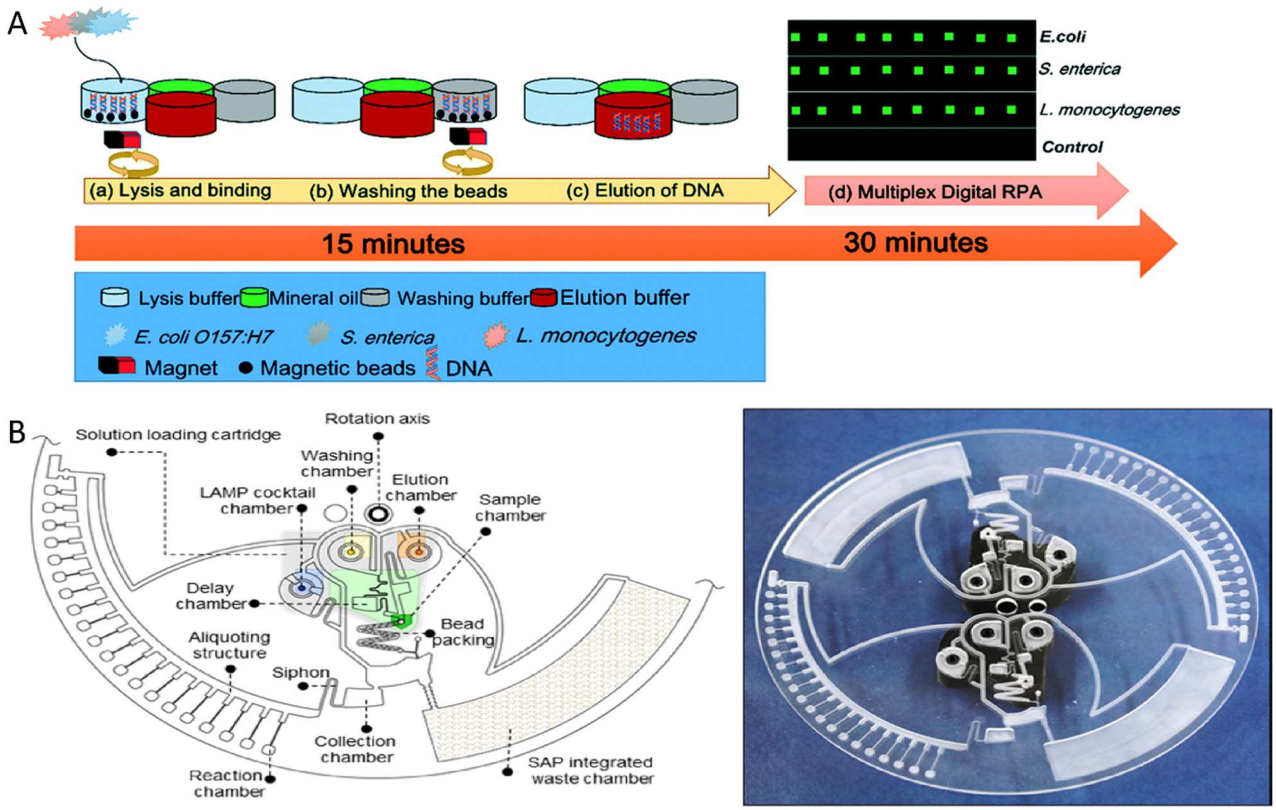

Figure 13: A. Experimental workflow of the sample-in-multiplex-digital-answer-out design by Yin *et al.*[190] (Reproduced from reference [190] with permission. Copyright 2020 RSC); B. Schematic illustration of the integrated centrifugal disc and a digital image of the disc.[196] (Reproduced from reference [196] with permission. Copyright 2019 Elsevier).

Beyond the use of NAATs for POC detection, few research groups have forayed into the design of POCs based on colourimetric bacterial sensing. The metabolic activity of bacteria was employed in the design of a colourimetric biosensor for potential POC applications. Wu *et al*. took advantage of the ability of electrochromic and naturally oxidised poly(3,4-propylenedioxythiophen-alt-3,4-ethylenedioxythiophene) copolymer (PPE) to produce a colour change upon contact with by-products of bacterial metabolism, namely cysteine and glutathione. A detection limit of 10^4 CFU/mL was reported and the detection time was a mere 0.5 h.[193] The colourimetric detection of *E. Coli* causing urinary tract infections (UTIs) was explored in the publication by Iseri *et al*. Their simple digital dipstick involves directly immersing the polymethyl methacrylate-based stick which houses chromogenic agar into the urine samples. Based on enzymatic reactions of the strip with the growing bacterial culture, the solution turns blue. They reported detection limits ranging from 10^2–10^5 CFU/mL with an 89% sensitivity.[194] Another POC device, which is inexpensive, palm-sized, simple

in design, robust and easy to operate for the detection of UTIs was developed by Michael and coworkers. Designed to operate in a similar fashion to fidget spinners, the device is hand-operated and uses the centrifugal force arising from spinning the device to concentrate the sample on a nitrocellulose membrane. The detection solution is then added by spinning which then reacts with the bacteria on the membrane to produce a colour change after 45 min.[195] This device was able to carry out bacterial analysis on urine samples 39 patients with UTIs within 50 min with a detection limit down to 10^3 CFU/mL.[195] Another POC 'sample to answer' device based on loop-mediated isothermal amplification (LAMP) was reported by Nguyen *et al*. LAMP is a technique used to amplify the specific target DNA sequences at a constant temperature and was used in this case. The system consisted of two modules, namely an integrated centrifugal microdevice and a portable genetic analyser. The centrifugal microdevice was made of a microfluidic disc and a 3D printed cartridge for loading the solution and was capable of carry out a range of operations including bead-based DNA extraction, isothermal amplification *via* LAMP rection and amplicon detection by UV/vis detector (Figure 13B). The portable genetic analyser was added as an additional accessory and performed chip rotation for the mixing of solutions, controlling temperature, UV-Visible light measurements of the reaction chamber, and data reporting. Three different foodborne bacteria *E. Coli* O157:H7, *S. Typhi*, and *V. Parahaemolyticus* were tested and their presence were confirmed when the Abs_{640nm}/Abs_{570nm} was ≥ 1.0. This design demonstrated a low LOD of 100 CFU/mL with the whole process taking an hour to complete.[196] A similar LOD was obtained with the fuchsin dye-based colourimetric LAMP device by Trinh and colleagues. This design was also fully integrated in that it consisted of a sample zone, reaction zone, and detection zone while boasting of a total turnaround time of 65 min.[197] In a 2021 publication, Celik *et al.* proposed a simple smartphone-assisted colourimetric POC system based on bacteria-induced chemical reaction for the detection of *Helicobacter Pylori (H. Pylori)*. Upon secretion of urease by these bacteria, urea is hydrolysed into ammonia. The alkaline environment produced led to a colour change when incubated with anthocyanin-rich red cabbage

(*Brassica oleracea*) extract (RCE) which was used as a natural pH indicator. This system was capable of detecting 10 CFU/mL in 20 min and down to 1 CFU/mL in 3 h.[198]

Taking advantage of the portability of mobile phones, a smartphone-based 'sample-to-answer' device combining NAAT and colourimetric sensing built on a passive, self-driven microfluidic device was developed by Ma *et al*. As the LAMP polymerisation reaction was complete, a colour change from purple to blue was observed, indicating the presence of the bacterial species. Properties associated with this system included the ability to detect both viral and bacterial samples, ease of use owing to the punching-press mechanism driving the liquid flow, automation, and quantification of the colourimetric assays using a smartphone. With a total analytic time of 40 min, an LOD of 30 CFU/mL for *MRSA* was obtained.[199] A similar 'sample-in-result-out' device which uses LAMP and smartphone monitoring in a single microfluidic-based device was proposed by Wang and colleagues. Their design involved incubating magnetic NPs coated with anti-*S. Typhi* capture antibodies in propidium monoazide (PMA) with the bacteria under exposure to 470 nm blue light.[200] While the PMA hindered the amplification of the DNA of dead bacteria, the viable target *S. Typhi* bacteria was captured by the magnetic NPs. After separation of the PMA-treated dead bacteria by the application of a magnetic field, the viable bacteria's DNA was amplified using LAMP in the detection chamber. This device demonstrated an improved sensitivity of 14 CFU/mL with a detection time of 1.5 h and was mainly attributed to the highly effective mixing process and separation of the dead bacteria from the viable ones.[200] Finally, the lowest LOD reported using microfluidic systems is 3 CFU/mL, which was detailed by Schulz and associates.[201] They designed a centrifugal-based microfluidic device which allowed storage of reagents, loading of *MRSA* bacteria from nasal swabs of patients, and distribution of the sample into droplets. Two chemical processes, namely enzymatic lysis, and recombinase polymerase amplification, were also carried out within the device, which in turn triggered a change in fluorescence.[201] This design boasted of a very high sensitivity and a processing time of 55 min while being fully automated, thereby increasing their suitability as a POC device in hospital settings where the occurrence and spreading of *MRSA* is highly probable. Similar detection

mechanisms based on colourimetric NAAT biosensing were reported by Suea-Ngam and colleagues with a detection ability down to one copy of the *MRSA* bacterium within 30 min.[165] The same detection limit was obtained using the fluorometric paper-based, LAMP biosensor devised by Choopara *et al*. for the POC detection of *MRSA*.[202] More recently and with advances in healthcare technology, wearable biosensors have been found to be highly promising for non-invasive, continuous, and real time monitoring of patient's health. Hence, it allows for efficient management of chronic diseases and can detect any abnormalities which require medical attention in real-time.[10] A range of wearable biosensors have been devised by researchers and proved to be effective in monitoring and detection devices in a laboratory setting. These biosensors, for instance the smart contact lens, eyeglasses, nanomaterial-based patch or iontophoretic patch, have been mostly made for monitoring glucose levels in diabetic patients. Aside from diabetes and monitoring of biological functions such as body temperature, pH and sweat and tear production, an important application of wearable POC sensors is seizure detection. In the review by Mondal *et al.*, a wide range of commercially available seizure detection wearables were discussed, for instance, the Smart Sleep Mask by Neuro:On, Emfit Seizure Monitor by Emfit or even Epilepsy Seizure Monitoring System by Holst Centre/IMEC Hobo Heeze BV amongst others.[203] The field of bacterial detection and growth monitoring using wearables is still in its infancy with very few wearable bacterial biosensors reported, most of them being proof-of-concept designs. Out of those, a popular example is the graphene-based tooth sensor which could detect bacteria present in saliva down to a single cell developed by Mannoor *et al*. This device was widely discussed in the review by Kim and colleagues and the most recent 2021 publication by Sharma *et al.*[204] However, the designs can be referenced to convert a laboratory designed POC biosensor into a commercially available medical equipment. Most of these wearable biosensors are electrochemical based in that they offer a wide range of benefits as highlighted in the review by Yoon *et al*. These include rapid response, high sensitivity and selectivity, inherent miniaturisation, convenient operation, and portability.[205] Even though the design of these electrochemical-based wearable biosensors require further optimisation in terms of their substrate

composition and electrochemical properties as well as fabrication techniques, they are still highly sought for the design of personalised POC healthcare devices.

5. Conclusions and future perspectives

In a time where the world is reeling from the aftermath of a global pandemic, there is no doubt that biosensors are becoming ubiquitous in the fight against both bacterial and viral infections. Effective diagnosis and treatment is primarily hinged on accurate identification of the infection-causing species. As discussed, the sensitivity of bacterial biosensors is highly dependent on their biorecognition elements. While the use of nanomaterials and sandwich-based assays were found to improve the LOD, DNA technology was found to yield the best sensitivity across all the types of biosensors explored. As evidenced by the biosensors described earlier in Section 3, the current research pipeline is in constant flux with highly promising technologies which have demonstrated their ability for rapid, cheap, and sensitive bacterial detection. Out of the different types of biosensors, it is apparent that optical sensing have the most potential for use as POC. Optical sensing platforms in combination with smartphone technology can greatly enhance their ease of use, inexpensive nature, and portability, making them highly suited as POC devices for bacterial detection.

Driven by the need to translate these biosensor designs into highly efficient POC devices, researchers are currently endeavouring to optimise their functional properties and performance. However, their development for commercial use has been thwarted by several implementation issues that must be addressed, for instance, the lack of robust and realistic evaluations to show effectiveness in patients. Most of the reported systems are proof-of-concept studies and demonstrated good efficacy and low detection limits when carried out in growth media or other types of controlled environment. Yet, only a few publications showed evidence of promising results in actual patient samples. Furthermore, commercialisation of wearable biosensors is challenging as the accuracy and specificity of the measurements may be influenced by biofouling at the body-sensor interface, inefficient transport of sample over the sensor, limited stability of many bioreceptors as well as issues posed by calibration for on-body biosensors. In addition, relaying the data collected by the biosensor is critical

for effective patient monitoring which, in turn requires power and wireless communication connection systems integrated within the device. Troubleshooting these problems need additional design optimisation and thus, incur additional costs. Finally, before these biosensing platforms can be used as POC, international guidelines must be devised to ensure operational safety and subsequent disposal. Therefore, the process of patenting the design and approval of these POC biosensors for clinical use may take a long time to come to fruition.

Acknowledgement

The research was supported by the Global Challenges Research Fund from the Scottish Funding Council.

References

[1] R. Sugden, R. Kelly, S. Davies, *Nat. Micro* **2016**, *1*, 16187; J. O'Neill, *Tackling Drug-Resistant Infections Globally: Final Report and Recommendations*, Wellcome Trust & HM Government, London, UK **2016**.
[2] D. Şen Karaman, U. K. Ercan, E. Bakay, N. Topaloğlu, J. M. Rosenholm, *Adv. Funct. Mat* **2020**, 30, 1908783; B. D. Brooks, A. E. Brooks, *Adv. Drug. Delivery. Rev* **2014**, *78*, 14.
[3] WHO, *Antibacterial agents in clinical development: an analysis of the antibacterial clinical development pipeline*, Geneva **2019**.
[4] L. Váradi, J. L. Luo, D. E. Hibbs, J. D. Perry, R. J. Anderson, S. Orenga, P. W. Groundwater, *Chem. Soc. Rev* **2017**, *46*, 4818.
[5] P.-E. Fournier, M. Drancourt, P. Colson, J.-M. Rolain, B. L. Scola, D. Raoult, *Nat. Rev. Microbiol* **2013**, *11*, 574.
[6] C. Zhang, D. Paria, S. Semancik, I. Barman, *Small* **2019**, *15*, 1901165.
[7] M. Mayer, A. J. Baeumner, *Chem. Rev* **2019**, *119*, 7996.
[8] B. R. Eggins, *Chemical Sensors and Biosensors*, John Wiley & Sons, West Sussex, UK **2002**.
[9] D. Grieshaber, R. MacKenzie, J. Vörös, E. Reimhult, *Sensors (Basel, Switzerland)* **2008**, *8*, 1400.
[10] J. Kim, A. S. Campbell, B. E.-F. de Ávila, J. Wang, *Nat. Biotechnol* **2019**, *37*, 389.
[11] L. C. Clark Jr, C. Lyons, *Ann. N. Y. Acad. Sci* **1962**, *102*, 29.
[12] Grand View Research, *Biosensors Market Size, Share & Trends Analysis Report By Application (Medical, Agriculture, Bioreactor) By Technology (Thermal, Electrochemical, Optical), By End Use, By Region, And Segment Forecasts, 2020 - 2027*, California, US **2020**.
[13] O. Lazcka, F. J. D. Campo, F. X. Muñoz, *Biosens. Bioelectron* **2007**, *22*, 1205.
[14] N. Bhalla, P. Jolly, N. Formisano, P. Estrela, *Essays Biochem* **2016**, *60*, 1; A. Chaubey, B. D. Malhotra, *Biosens. Bioelectron* **2002**, *17*, 441.
[15] O. Simoska, K. J. Stevenson, *Analyst* **2019**, *144*, 6461.
[16] A. L. Furst, M. B. Francis, *Chem. Rev* **2019**, *119*, 700.
[17] Y. Wang, J. K. Salazar, *Compr. Rev. Food Sci. Food Saf* **2016**, *15*, 183.
[18] O. Opota, A. Croxatto, G. Prod'hom, G. Greub, *Clin. Microbiol. Infect* **2015**, *21*, 313.
[19] C. Singhal, J. G. Bruno, A. Kaushal, T. K. Sharma, *ACS Appl. Bio. Mater* **2021**, *4,* 5, 3962.
[20] O. G. Brakstad, K. Aasbakk, J. A. Maeland, *J. Clin. Microbiol* **1992**, *30*, 1654.
[21] J. S. Kim, G. G. Lee, J. S. Park, Y. H. Jung, H. S. Kwak, S. B. Kim, Y. S. Nam, S.-T. Kwon, *J. Food. Prot* **2007**, *70*, 1656.
[22] J. Alvarez, M. Sota, A. B. Vivanco, I. Perales, R. Cisterna, A. Rementeria, J. Garaizar, *J. Clin. Microbiol* **2004**, *42*, 1734; M. Vidal, E. Kruger, C. Durán, R. Lagos, M. Levine, V. Prado, C. Toro, R. Vidal, *J. Clin. Microbiol* **2005**, *43*, 5362.
[23] K. S. Gracias, J. L. McKillip, *Can J Microbiol* **2004**, *50*, 883.
[24] S. Aydin, *Peptides* **2015**, *72*, 4.

[25] G. López-Campos, J. V. Martínez-Suárez, M. Aguado-Urda, V. López-Alonso, *Detection, identification, and analysis of foodborne pathogens*, Springer US, New York **2012**.
[26] X. Zhou, Z. Hu, D. Yang, S. Xie, Z. Jiang, R. Niessner, C. Haisch, H. Zhou, P. Sun, *Adv. Sci* **2020**, *7*, 2001739.
[27] A. E. Budding, M. Hoogewerf, C. M. J. E. Vandenbroucke-Grauls, P. H. M. Savelkoul, *J. Clin. Microbiol* **2016**, *54*, 934.
[28] J.-C. Lagier, S. Edouard, I. Pagnier, O. Mediannikov, M. Drancourt, D. Raoult, *Clin. Microbiol. Rev* **2015**, *28*, 208.
[29] E. de Boer, R. R. Beumer, *Int. J. Food Microbiol* **1999**, *50*, 119.
[30] V. Velusamy, K. Arshak, O. Korostynska, K. Oliwa, C. Adley, *Biotechnol. Adv* **2010**, *28*, 232.
[31] R. Stephan, S. Schumacher, M. A. Zychowska, *Int J Food Microbiol* **2003**, *89*, 287; L. Li, N. Mendis, H. Trigui, J. D. Oliver, S. P. Faucher, *Front. Microbiol* **2014**, *5*, 258.
[32] P. Houpikian, D. Raoult, *Emerg. Infect. Dis* **2002**, *8*, 122.
[33] C. A. Batt, *Science* **2007**, *316*, 1579.
[34] H. Kim, S. Lee, H. W. Seo, B. Kang, J. Moon, K. G. Lee, D. Yong, H. Kang, J. Jung, E.-K. Lim, J. Jeong, H. G. Park, C.-M. Ryu, T. Kang, *ACS Nano* **2020**, *14*, 17241.
[35] A. A. Karbelkar, A. L. Furst, *ACS Infect. Dis* **2020**, *6,* 7, 1567.
[36] S. Coyle, V. F. Curto, F. Benito-Lopez, L. Florea, D. Diamond, in *Wearable Sensors*, (Eds: E. Sazonov, M. R. Neuman), Academic Press, Oxford, **2014**, 65.
[37] N. J. Ronkainen, H. B. Halsall, W. R. Heineman, *Chem. Soc. Rev* **2010**, *39*, 1747.
[38] H. Shan, X. Li, L. Liu, D. Song, Z. Wang, *J. Mater. Chem B* **2020**, *8*, 5808.
[39] M. Labib, E. H. Sargent, S. O. Kelley, *Chem. Rev* **2016**, *116*, 9001.
[40] A. L. Furst, A. C. Hoepker, M. B. Francis, *ACS Centr. Sci* **2017**, *3*, 110.
[41] M. J. Russo, M. Han, P. E. Desroches, C. S. Manasa, J. Dennaoui, A. F. Quigley, R. M. I. Kapsa, S. E. Moulton, R. M. Guijt, G. W. Greene, S. M. Silva, *ACS Sensors* **2021**, *6*, 1482.
[42] J. T. Poolman, A. S. Anderson, *Expert Rev. Vaccines* **2018**, *17*, 607.
[43] F. Tan, P. H. M. Leung, Z.-b. Liu, Y. Zhang, L. Xiao, W. Ye, X. Zhang, L. Yi, M. Yang, *Sens. Actuators, B* **2011**, *159*, 328.
[44] C. K. Joung, H. N. Kim, M. C. Lim, T. J. Jeon, H. Y. Kim, Y. R. Kim, *Biosens. Bioelectron* **2013**, *44*, 210.
[45] T. Wen, R. Wang, A. Sotero, Y. Li, *Sensors (Basel, Switzerland)* **2017**, *17*, 1973.
[46] S. Singh, A. Moudgil, N. Mishra, S. Das, P. Mishra, *Biosens. Bioelectron* **2019**, *136*, 23.
[47] N. Pal, S. Sharma, S. Gupta, *Biosens. Bioelectron* **2016**, 77, 270.
[48] V. Biju, *Chem. Soc. Rev* **2014**, *43*, 744.
[49] W. Zhu, Y. Chen, Y. He, W. Fang, Y. Ying, Y. Li, Y. Fu, *Anal. Chem* **2020**, *92*, 1818.
[50] M. Jalali, T. AbdelFatah, S. S. Mahshid, M. Labib, A. Sudalaiyadum Perumal, S. Mahshid, *Small* **2018**, *14*, 1801893.
[51] B. C. Marin, J. Ramírez, S. E. Root, E. Aklile, D. J. Lipomi, *Nanoscale Horiz* **2017**, *2*, 311.
[52] R. S. Moakhar, T. AbdelFatah, A. Sanati, M. Jalali, S. E. Flynn, S. S. Mahshid, S. Mahshid, *ACS Appl. Mater. Interfaces* **2020**, *12,* 20, 23298.
[53] R. Wu, Y. Ma, J. Pan, S.-H. Lee, J. Liu, H. Zhu, R. Gu, K. J. Shea, G. Pan, *Biosens. Bioelectron* **2018**, *101*, 52.
[54] C. M. Pandey, I. Tiwari, V. N. Singh, K. N. Sood, G. Sumana, B. D. Malhotra, *Sens. Actuators, B* **2017**, *238*, 1060.
[55] M. Barreiros dos Santos, J. P. Agusil, B. Prieto-Simón, C. Sporer, V. Teixeira, J. Samitier, *Biosens. Bioelectron* **2013**, *45*, 174.
[56] Y. Hillman, J. Gershberg, D. Lustiger, D. Even, D. Braverman, Y. Dror, I. Ashur, S. Vernick, N. Sal-Man, Y. Wine, *Anal. Chem* **2021**, *93*, 928.
[57] S. Ranjbar, S. Shahrokhian, F. Nurmohammadi, *Sensors and Actuators B: Chemical*. **2018**, *255*, 1536.
[58] G. Ertürk, B. Mattiasson, *Sensors* **2017**, *17*, 22.
[59] J. S. Daniels, N. Pourmand, *Electroanalysis* **2007**, *19*, 1239.
[60] C. Berggren, B. Bjarnason, G. Johansson, *Electroanalysis* **2001**, *13*, 173.
[61] M. S. Mannoor, S. Zhang, A. J. Link, M. C. McAlpine, *Proc. Natl. Acad. Sci* **2010**, *107*, 19207.
[62] I. Piekarz, S. Górska, S. Odrobina, M. Drab, K. Wincza, A. Gamian, S. Gruszczynski, *Biosens. Bioelectron* **2020**, *147*, 111784.
[63] A. Pandey, Y. Gurbuz, V. Ozguz, J. H. Niazi, A. Qureshi, *Biosens. Bioelectron* **2017**, *91*, 225.
[64] S. M. Mugo, W. Lu, D. Dhanjai, *Med. Devices Sens* **2020**, *3*, e10071.

[65] R. Deshmukh, A. K. Prusty, U. Roy, S. Bhand, *Analyst* **2020**, *145*, 2267.
[66] N. Elgrishi, K. J. Rountree, B. D. McCarthy, E. S. Rountree, T. T. Eisenhart, J. L. Dempsey, *J. Chem. Eng. Educ* **2018**, *95*, 197.
[67] C. R. Nemr, S. J. Smith, W. Liu, A. H. Mepham, R. M. Mohamadi, M. Labib, S. O. Kelley, *Anal. Chem* **2019**, *91*, 2847.
[68] Z. Altintas, M. Akgun, G. Kokturk, Y. Uludag, *Biosens. Bioelectron* **2018**, *100*, 541.
[69] T. Wang, X. Song, H. Lin, T. Hao, Y. Hu, S. Wang, X. Su, Z. Guo, *Anal. Chim. Acta* **2019**, *1062*, 124.
[70] P. Kannan, J. Chen, F. Su, Z. Guo, Y. Huang, *Anal. Chem* **2019**, *91*, 14792.
[71] K. Ishiki, D. Q. Nguyen, A. Morishita, H. Shiigi, T. Nagaoka, *Anal. Chem* **2018**, *90*, 10903.
[72] G. A. Zelada-Guillén, J. L. Sebastián-Avila, P. Blondeau, J. Riu, F. X. Rius, *Biosens. Bioelectron* **2012**, *31*, 226.
[73] R. Hernández, C. Vallés, A. M. Benito, W. K. Maser, F. Xavier Rius, J. Riu, *Biosens. Bioelectron* **2014**, *54*, 553.
[74] H. Wang, Y. Xiu, Y. Chen, L. Sun, L. Yang, H. Chen, X. Niu, *RSC Adv* **2019**, *9*, 16278.
[75] R. Jijie, K. Kahlouche, A. Barras, N. Yamakawa, J. Bouckaert, T. Gharbi, S. Szunerits, R. Boukherroub, *Sens. Actuators, B* **2018**, *260*, 255.
[76] I. U. Haq, W. N. Chaudhry, M. N. Akhtar, S. Andleeb, I. Qadri, *Virol. J* **2012**, *9*, 9.
[77] U. Farooq, M. W. Ullah, Q. Yang, A. Aziz, J. Xu, L. Zhou, S. Wang, *Biosens. Bioelectron* **2020**, *157*, 112163.
[78] D. Pankratov, M. Bendixen, S. Shipovskov, U. Gosewinkel, E. E. Ferapontova, *Anal. Chem* **2020**, *92*, 12451.
[79] Q. Wang, Y. Wen, Y. Li, W. Liang, W. Li, Y. Li, J. Wu, H. Zhu, K. Zhao, J. Zhang, N. Jia, W. Deng, G. Liu, *Anal. Chem* **2019**, *91*, 9277.
[80] J. Choi, T. W. Seong, M. Jeun, K. H. Lee, *Adv. Health Mater* **2017**, *6*, 1700796.
[81] A. Matsumoto, Y. Miyahara, *Nanoscale* **2013**, *5*, 10702.
[82] N. Kumar, W. Wang, J. C. Ortiz-Marquez, M. Catalano, M. Gray, N. Biglari, K. Hikari, X. Ling, J. Gao, T. van Opijnen, K. S. Burch, *Biosens. Bioelectron* **2020**, *156*, 112123.
[83] A. Dey, A. Singh, D. Dutta, S. S. Ghosh, P. K. Iyer, *J. Mat. Chem. A* **2019**, *7*, 18330.
[84] B. Thakur, G. Zhou, J. Chang, H. Pu, B. Jin, X. Sui, X. Yuan, C.-H. Yang, M. Magruder, J. Chen, *Biosens. Bioelectron* **2018**, *110*, 16.
[85] A. Moudgil, S. Singh, N. Mishra, P. Mishra, S. Das, *Adv. Mater. Technol* **2020**, *5*, 1900615.
[86] S. M. Borisov, O. S. Wolfbeis, *Chem. Rev* **2008**, *108*, 423; A. Ahmed, J. V. Rushworth, N. A. Hirst, P. A. Millner, *Clin. Microbiol. Rev* **2014**, *27*, 631.
[87] Arshavsky-Graham, N. Massad-Ivanir, E. Segal, S. Weiss, *Anal. Chem* **2019**, *91*, 441.
[88] A. Jane, R. Dronov, A. Hodges, N. H. Voelcker, *Trends Biotechnol* **2009**, *27*, 230.
[89] K. Urmann, S. Arshavsky-Graham, J. G. Walter, T. Scheper, E. Segal, *Analyst* **2016**, *141*, 5432.
[90] N. Massad-Ivanir, G. Shtenberg, A. Tzur, M. A. Krepker, E. Segal, *Anal. Chem* **2011**, *83*, 3282.
[91] P. Dey, N. Fabri-Faja, O. Calvo-Lozano, R. A. Terborg, A. Belushkin, F. Yesilkoy, A. Fàbrega, J. C. Ruiz-Rodriguez, R. Ferrer, J. J. González-López, M. C. Estévez, H. Altug, V. Pruneri, L. M. Lechuga, *ACS Sensors* **2019**, *4*, 52.
[92] F. Huang, R. Guo, L. Xue, G. Cai, S. Wang, Y. Li, M. Liao, M. Wang, J. Lin, *Sensors. Act, B* **2020**, *312*, 127958.
[93] Y. Guo, J. Li, X. Song, K. Xu, J. Wang, C. Zhao, *ACS Appl. Bio Mater* **2021**, *4*, 420.
[94] D. Wang, F. Lian, S. Yao, Y. Liu, J. Wang, X. Song, L. Ge, Y. Wang, Y. Zhao, J. Zhang, C. Zhao, K. Xu, *ACS Omega* **2020**, *5*, 23070.
[95] M. M. A. Zeinhom, Y. Wang, Y. Song, M.-J. Zhu, Y. Lin, D. Du, *Biosens. Bioelectron* **2018**, *99*, 479.
[96] W.-L. Lee, Y. Park, S. Shrivastava, T. Jung, M. Meeseepong, J. Lee, B. Jeon, S. Yang, N.-E. Lee, *Biosens. Bioelectron* **2020**, *152*, 112007.
[97] Y. Shen, T. Wu, Y. Zhang, N. Ling, L. Zheng, S.-L. Zhang, Y. Sun, X. Wang, Y. Ye, *Anal. Chem* **2020**, *92*, 19, 13396–13404.
[98] F. Chang, L. Huang, C. Guo, G. Xie, J. Li, Q. Diao, *ACS Appl. Mater. Interfaces* **2019**, *11*, 35622.
[99] J. N. Anker, W. P. Hall, O. Lyandres, N. C. Shah, J. Zhao, R. P. Van Duyne, *Nat. Mat* **2008**, *7*, 442.
[100] A. R. Ferhan, B. K. Yoon, W. Y. Jeon, N.-J. Cho, *Nanoscale Adv* **2020**, *2*, 3103-3114.
[101] H. Khateb, G. Klös, R. L. Meyer, D. S. Sutherland, *ACS Appl. Bio Mater* **2020**, *3*, 3066.
[102] A. Meneghello, A. Sonato, G. Ruffato, G. Zacco, F. Romanato, *Sensors. Act, B* **2017**, *250*, 351.
[103] S. M. Yoo, D. K. Kim, S. Y. Lee, *Talanta* **2015**, *132*, 112.

[104] K. Whang, J.-H. Lee, Y. Shin, W. Lee, Y. W. Kim, D. Kim, L. P. Lee, T. Kang, *Light: Sci. Appl* **2018**, *7*, 68.
[105] X. Gao, H. Wu, Z. Hao, X. Ji, X. Lin, S. Wang, Y. Liu, *Nanoscale* **2020**, *12*, 6489.
[106] H. Zhang, X. Ma, Y. Liu, N. Duan, S. Wu, Z. Wang, B. Xu, *Biosens. Bioelectron* **2015**, *74*, 872.
[107] Y. Song, W. Wei, X. Qu, *Adv. Mat* **2011**, *23*, 4215.
[108] J. Sun, A. R. Warden, J. Huang, W. Wang, X. Ding, *Anal. Chem* **2019**, *91*, 7524.
[109] E. Mann, S. Kolusheva, R. Yossef, A. Porgador, M. Aviram, R. Jelinek, *Mol. Diagn. Ther* **2015**, *19*, 35; J. Chen, Z. Jiang, J. D. Ackerman, M. Yazdani, S. Hou, S. R. Nugen, V. M. Rotello, *Analyst* **2015**, *140*, 4991.
[110] J.-Y. Kim, J.-S. Lee, *Nano Lett* **2009**, *9*, 4564.
[111] M. S. Verma, J. L. Rogowski, L. Jones, F. X. Gu, Biotechnol. Adv 2015, 33, 666.
[112] B. Creran, X. Li, B. Duncan, C. S. Kim, D. F. Moyano, V. M. Rotello, *ACS Appl. Mater. Interfaces* **2014**, *6*, 19525.
[113] X.-Z. Mou, X.-Y. Chen, J. Wang, Z. Zhang, Y. Yang, Z.-X. Shou, Y.-X. Tu, X. Du, C. Wu, Y. Zhao, L. Qiu, P. Jiang, C. Chen, D.-S. Huang, Y.-Q. Li, *ACS Appl. Mater. Interfaces* **2019**, *11*, 23093.
[114] X. Du, C. Wu, W. Wang, L. Qiu, P. Jiang, J. Wang, Y.-Q. Li, *J. Mater. Chem. B* **2019**, *7*, 7301.
[115] S. Díaz-Amaya, M. Zhao, L.-K. Lin, C. Ostos, J. P. Allebach, G. T. C. Chiu, A. J. Deering, L. A. Stanciu, *Small* **2019**, *15*, 1805342.
[116] T. Yu, H. Xu, Y. Zhao, Y. Han, Y. Zhang, J. Zhang, C. Xu, W. Wang, Q. Guo, J. Ge, *Sci. Rep* **2020**, 10, 9190.
[117] J. Zhou, R. Fu, F. Tian, Y. Yang, B. Jiao, Y. He, *ACS Appl. Bio Mater* **2020**, *3*, 9, 6103–6109.
[118] J. Zhou, F. Tian, R. Fu, Y. Yang, B. Jiao, Y. He, *ACS Appl. Nano Mater* **2020**, *3*, 9016.
[119] L. Zhang, Z. Qi, Y. Zou, J. Zhang, W. Xia, R. Zhang, Z. He, X. Cai, Y. Lin, S.-Z. Duan, J. Li, L. Wang, N. Lu, Z. Tang, *ACS Appl. Mater. Interfaces* **2019**, *11*, 30640.
[120] P. Liu, Y. Wang, L. Han, Y. Cai, H. Ren, T. Ma, X. Li, V. A. Petrenko, A. Liu, *ACS Appl. Mater. Interfaces* **2020**, *12*, 9090.
[121] N. Amin, A. S. Torralba, R. Álvarez-Diduk, A. Afkhami, A. Merkoçi, *Anal. Chem* **2020**, *92*, 4209.
[122] V. Sadsri, T. Trakulsujaritchok, M. Tangwattanachuleeporn, V. P. Hoven, P. Na Nongkhai, *ACS Omega* **2020**, *5*, 21437.
[123] H. Yang, M. Xiao, W. Lai, Y. Wan, L. Li, H. Pei, *Anal. Chem* **2020**, *92*, 4990.
[124] C. Zhou, M. Jiang, J. Du, H. Bai, G. Shan, R. T. K. Kwok, J. H. C. Chau, J. Zhang, J. W. Y. Lam, P. Huang, B. Z. Tang, *Chem. Sci* **2020**, *11*, 4730.
[125] J. L. Arlett, E. B. Myers, M. L. Roukes, *Nat. Nanotechnol* **2011**, *6*, 203.
[126] P. A. Rasmussen, J. Thaysen, O. Hansen, S. C. Eriksen, A. Boisen, *Ultramicroscopy* **2003**, *97*, 371.
[127] H. Etayash, T. Thundat, *Encyclopedia of Nanotechnology*, (Ed: B. Bhushan), Springer, Netherlands **2016**.
[128] Z. Shen, M. Huang, C. Xiao, Y. Zhang, X. Zeng, P. G. Wang, *Anal. Chem* **2007**, *79*, 2312.
[129] H. Sharma, R. Mutharasan, *Biosens. Bioelectron* **2013**, *45*, 158.
[130] F. Ma, A. Rehman, H. Liu, J. Zhang, S. Zhu, X. Zeng, *Anal. Chem* **2015**, *87*, 1560.
[131] H. Etayash, M. F. Khan, K. Kaur, T. Thundat, *Nat. Commun* **2016**, *7*, 12947.
[132] Y. Lei, W. Chen, A. Mulchandani, *Anal. Chim. Acta* **2006**, *568*, 200.
[133] M. Park, S.-L. Tsai, W. Chen, *Sensors (Basel, Switzerland)*. **2013**, *13*, 5777.
[134] H. S. Zurier, M. M. Duong, J. M. Goddard, S. R. Nugen, *ACS Appl. Bio Mater* **2020**, 3, 9, 5824–5831.
[135] H. Leonard, C. Heuer, D. Weizman, N. Massad-Ivanir, S. Halachmi, R. Colodner, E. Segal in *Proc. SPIE 10895, Frontiers in Biological Detection: From Nanosensors to Systems XI* (Eds: A. Danielli, B. L. Miller, S. M. Weiss), California, United States **2019**.
[136] H. Leonard, R. Colodner, S. Halachmi, E. Segal, *ACS Sensors* **2018**, *3*, 2202.
[137] L. Su, W. Jia, C. Hou, Y. Lei, *Biosens. Bioelectron* **2011**, *26*, 1788.
[138] S. Brosel-Oliu, O. Mergel, N. Uria, N. Abramova, P. van Rijn, A. Bratov, *Lab Chip* **2019**, *19*, 1436.
[139] C. Grazon, R. C. Baer, U. Kuzmanović, T. Nguyen, M. Chen, M. Zamani, M. Chern, P. Aquino, X. Zhang, S. Lecommandoux, A. Fan, M. Cabodi, C. Klapperich, M. W. Grinstaff, A. M. Dennis, J. E. Galagan, *Nat. Commun* **2020**, *11*, 1276.
[140] N. D. Taylor, A. S. Garruss, R. Moretti, S. Chan, M. A. Arbing, D. Cascio, J. K. Rogers, F. J. Isaacs, S. Kosuri, D. Baker, S. Fields, G. M. Church, S. Raman, *Nat. Methods* **2016**, *13*, 177.
[141] F. S. H. Krismastuti, H. Bayat, N. H. Voelcker, H. Schönherr, *Anal. Chem* **2015**, *87*, 3856.
[142] E. Tenenbaum, E. Segal, *Analyst* **2015**, 140, 7726.
[143] N. Reta, A. Michelmore, C. Saint, B. Prieto-Simón, N. H. Voelcker, *Biosens. Bioelectron* **2016**, *80*, 47.

[144] F. S. H. Krismastuti, A. Cavallaro, B. Prieto-Simon, N. H. Voelcker, *Adv. Sci* **2016**, *3*, 1500383.
[145] K.-S. Tücking, R. B. Vasani, A. A. Cavallaro, N. H. Voelcker, H. Schönherr, B. Prieto-Simon, *Macromol. Rapid Commun* **2018**, *39*, 1800178.
[146] N. Reta, A. Michelmore, C. P. Saint, B. Prieto-Simon, N. H. Voelcker, *ACS Sensors* **2019**, *4*, 1515.
[147] E. E. Antunez, C. S. Mahon, Z. Tong, N. H. Voelcker, M. Müllner, *Biomacromolecules* **2021**, *22*, 441.
[148] J. Zhang, Y. Li, S. Duan, F. He, *Anal. Chim. Acta* **2020**, *1123*, 9.
[149] L. Zhu, L. Wang, X. Zhang, T. Li, Y. Wang, M. A. Riaz, X. Sui, Z. Yuan, Y. Chen, *Carbon* **2020**, *159*, 185.
[150] M. Labib, M. Hedström, M. Amin, B. Mattiasson, *Anal. Bioanal. Chem* **2008**, *393*, 1539.
[151] J. Yu, Z. Liu, Q. Liu, K. T. Yuen, A. F. T. Mak, M. Yang, P. Leung, *Sens. Actuators, A* **2009**, *154*, 288.
[152] G. Rajeev, B. Prieto Simon, L. F. Marsal, N. H. Voelcker, *Adv. Healthcare Mater* **2018**, *7*, 1700904.
[153] U. Dharmasiri, M. A. Witek, A. A. Adams, J. K. Osiri, M. L. Hupert, T. S. Bianchi, D. L. Roelke, S. A. Soper, *Anal. Chem* **2010**, *82*, 2844.
[154] J. Monzó, I. Insua, F. Fernandez-Trillo, P. Rodriguez, *Analyst* **2015**, *140*, 7116.
[155] S. Farrell, N. J. Ronkainen-Matsuno, H. B. Halsall, W. R. Heineman, *Anal. Bioanal. Chem* **2004**, *379*, 358.
[156] A. D. Dias, D. M. Kingsley, D. T. Corr, *Biosensors* **2014**, *4*, 111.
[157] L. Shen, J. A. Hagen, I. Papautsky, *Lab Chip* **2012**, *12*, 4240.
[158] S. Reali, E. Y. Najib, K. E. Treuerné Balázs, A. Chern Hui Tan, L. Váradi, D. E. Hibbs, P. W. Groundwater, *RSC Adv* **2019**, *9*, 21486.
[159] G. Longo, L. Alonso-Sarduy, L. M. Rio, A. Bizzini, A. Trampuz, J. Notz, G. Dietler, S. Kasas, *Nat. Nanotechnol* **2013**, *8*, 522.
[160] J. W. Lim, D. Ha, J. Lee, S. K. Lee, T. Kim, *Front. Bioeng. Biotechnol* **2015**, *3*, 61.
[161] V. Gaudin, *Biosens. Bioelecton* **2017**, *90*, 363.
[162] N. Gupta, V. Renugopalakrishnan, D. Liepmann, R. Paulmurugan, B. D. Malhotra, *Biosens. Bioelecton* **2019**, *141*, 111435.
[163] H. Chen, K. Liu, Z. Li, P. Wang, *Clin. Chim Act*a **2019**, *493*, 138.
[164] C. P. Price, *BMJ* **2001**, *322*, 1285.
[165] A. Suea-Ngam, L. Bezinge, B. Mateescu, P. D. Howes, A. J. deMello, D. A. Richards, *ACS Sensors* **2020**, *5*, 2701.
[166] A. Tay, A. Pavesi, S. R. Yazdi, C. T. Lim, M. E. Warkiani, *Biotechnol. Adv* **2016**, *34*, 404.
[167] P. K. Drain, E. P. Hyle, F. Noubary, K. A. Freedberg, D. Wilson, W. R. Bishai, W. Rodriguez, I. V. Bassett, *Lancet Infect. Dis* **2014**, *14*, 239.
[168] D. Michel, M.-L. Audrey, B. Sylvie, R. Didier, *Clin. Microbiol. Rev* **2016**, *29*, 19.
[169] C.-H. Shen, in *Diagnostic Molecular Biology*, (Ed: C.-H. Shen), Academic Press, **2019**, 215.
[170] R. Diagnostics, *cobas® Strep A package insert*, Roche Molecular Systems Inc., Pleasanton, CA **2016**; R. Diagnostics, *cobas® Cdiff package insert*, Roche Molecular Systems Inc., Pleasanton, CA **2017**.
[171] C. C. Boehme, M. P. Nicol, P. Nabeta, J. S. Michael, E. Gotuzzo, R. Tahirli, M. T. Gler, R. Blakemore, W. Worodria, C. Gray, L. Huang, T. Caceres, R. Mehdiyev, L. Raymond, A. Whitelaw, K. Sagadevan, H. Alexander, H. Albert, F. Cobelens, H. Cox, D. Alland, M. D. Perkins, *Lancet* **2011**, *377*, 1495.
[172] Q. Corporation, *AmpliVue Clostridium difficile assay package insert*, Quidel Corporation, San Diego, CA **2013**.
[173] E. Deak, S. A. Miller, R. M. Humphries, *J. Clin. Microbiol* **2014**, *52*, 960.
[174] E. Nunez-Bajo, A. Silva Pinto Collins, M. Kasimatis, Y. Cotur, T. Asfour, U. Tanriverdi, M. Grell, M. Kaisti, G. Senesi, K. Stevenson, F. Güder, *Nat. Commun* **2020,** *11*, 6176.
[175] C. Parolo, A. Sena-Torralba, J. F. Bergua, E. Calucho, C. Fuentes-Chust, L. Hu, L. Rivas, R. Álvarez-Diduk, E. P. Nguyen, S. Cinti, D. Quesada-González, A. Merkoçi, *Nat. Protoc* **2020**, *15*, 3788.
[176] B. Reddy, U. Hassan, C. Seymour, D. C. Angus, T. S. Isbell, K. White, W. Weir, L. Yeh, A. Vincent, R. Bashir, *Nat. Biomed. Eng* **2018**, *2*, 640.
[177] L. Papafilippou, A. Claxton, P. Dark, K. Kostarelos, M. Hadjidemetriou, *Adv. Healthcare Mater* **2021**, *10*, 2001378.
[178] National Institute for Health and Care Excellence in *Diagnostics Assessment Programme*, National Institute for Health and Care Excellence (NICE), United Kingdom **2015**.
[179] J. Deng, S. Zhao, Y. Liu, C. Liu, J. Sun, *ACS Appl. Bio Mater* **2020**, *4*, 5, 3863.
[180] T. R. Kozel, A. R. Burnham-Marusich, *J. Clin. Microbiol* **2017**, *55*, 2313.
[181] E. B. Bahadır, M. K. Sezgintürk, *TrAC, Trends Anal. Chem* **2016**, *82*, 286.

[182] Abbott Laboratories, *Afinion^{TM} CRP Make every minute count (Product Information sheet),* Illinois, United States **2018**.
[183] A. M. Carroll, J. Cooke, L. Cross, T. Han, M. Moore in *Medtech innovation briefing MIB81*, National Institute for Health and Care Excellence (NICE), United Kingdom **2016**.
[184] R. K. Shanmugakani, B. Srinivasan, M. J. Glesby, L. F. Westblade, W. B. Cárdenas, T. Raj, D. Erickson, S. Mehta, *Lab Chip* **2020**, *20*, 2607.
[185] S. Arshavsky-Graham, E. Segal, Springer Berlin Heidelberg, Berlin, Heidelberg, 1.
[186] J. Park, D. H. Han, J.-K. Park, *Lab Chip* **2020**, *20*, 1191.
[187] H. Chen, A. Das, L. Bi, N. Choi, J.-I. Moon, Y. Wu, S. Park, J. Choo, *Nanoscale* **2020**, *12*, 21560.
[188] D. Quesada-González, A. Merkoçi, *Chem. Soc. Rev* **2018**, *47*, 4697.
[189] M. Alafeef, P. Moitra, D. Pan, *Biosens. Bioelectron* **2020**, *165*, 112276.
[190] J. Yin, Z. Zou, Z. Hu, S. Zhang, F. Zhang, B. Wang, S. Lv, Y. Mu, *Lab Chip* **2020**, *20*, 979.
[191] F. Ellett, J. Jorgensen, A. L. Marand, Y. M. Liu, M. M. Martinez, V. Sein, K. L. Butler, J. Lee, D. Irimia, *Nat. Biomed. Eng* **2018**, 2, 207.
[192] Y.-L. Fang, C.-H. Wang, Y.-S. Chen, C.-C. Chien, F.-C. Kuo, H.-L. You, M. S. Lee, G.-B. Lee, *Lab Chip* **2021**, *21*, 113.
[193] J. Wu, Y. Zhu, L. You, P.-T. Dong, J. Mei, J.-X. Cheng, *Adv. Funct. Mater* **2020**, *30*, 2005192.
[194] E. Iseri, M. Biggel, H. Goossens, P. Moons, W. van der Wijngaart, *Lab Chip* **2020**, *20*, 4349.
[195] I. Michael, D. Kim, O. Gulenko, S. Kumar, S. Kumar, J. Clara, D. Y. Ki, J. Park, H. Y. Jeong, T. S. Kim, S. Kwon, Y.-K. Cho, *Nat. Biomed. Eng* **2020**, *4*, 591.
[196] H. V. Nguyen, V. D. Nguyen, E. Y. Lee, T. S. Seo, *Biosens. Bioelectron* **2019**, *136*, 132.
[197] T. N. D. Trinh, N. Y. Lee, *Lab Chip* **2019**, *19*, 1397.
[198] C. Celik, G. Can Sezgin, U. G. Kocabas, S. Gursoy, N. Ildiz, W. Tan, I. Ocsoy, *Anal. Chem* **2021**, *93*, 6246.
[199] Y.-D. Ma, K.-H. Li, Y.-H. Chen, Y.-M. Lee, S.-T. Chou, Y.-Y. Lai, P.-C. Huang, H.-P. Ma, G.-B. Lee, *Lab Chip* **2019**, *19*, 3804.
[200] S. Wang, N. Liu, L. Zheng, G. Cai, J. Lin, *Lab Chip* **2020**, *20*, 2296.
[201] M. Schulz, S. Calabrese, F. Hausladen, H. Wurm, D. Drossart, K. Stock, A. M. Sobieraj, F. Eichenseher, M. J. Loessner, M. Schmelcher, A. Gerhardts, U. Goetz, M. Handel, A. Serr, G. Haecker, J. Li, M. Specht, P. Koch, M. Meyer, P. Tepper, R. Rother, M. Jehle, S. Wadle, R. Zengerle, F. von Stetten, N. Paust, N. Borst, *Lab Chip* **2020**, *20*, 2549.
[202] I. Choopara, A. Suea-Ngam, Y. Teethaisong, P. D. Howes, M. Schmelcher, A. Leelahavanichkul, S. Thunyaharn, D. Wongsawaeng, A. J. deMello, D. Dean, N. Somboonna, *ACS Sensors*. **2021**, *6*, 742.
[203] S. Mondal, N. Zehra, A. Choudhury, P. K. Iyer, *ACS Appl. Bio Mater* **2021**, *4*, 47.
[204] M. S. Mannoor, H. Tao, J. D. Clayton, A. Sengupta, D. L. Kaplan, R. R. Naik, N. Verma, F. G. Omenetto, M. C. McAlpine, *Nat. Commun* **2012**, *3*, 763; A. Sharma, M. Badea, S. Tiwari, J. L. Marty, *Molecules* **2021**, *26*.
[205] J. Yoon, H.-Y. Cho, M. Shin, H. K. Choi, T. Lee, J.-W. Choi, *J. Mater. Chem. B* **2020**, 8, 7303.